The Dissertation Committee for Nicole Guckert Harper Certifies that this is the approved version of the following dissertation:

Muscle Function and Coordination of Amputee and Non-Amputee Stair Ascent

Committee:

Richard R. Neptune, Supervisor

Ronald E. Barr

Ashish D. Deshpande

James S. Sulzer

Jason M. Wilken

Muscle Function and Coordination of Amputee and Non-Amputee Stair Ascent

by

Nicole Guckert Harper, B.S.Biomed.E.; M.S.E.

Dissertation

Presented to the Faculty of the Graduate School of

The University of Texas at Austin

in Partial Fulfillment

of the Requirements

for the Degree of

Doctor of Philosophy

The University of Texas at Austin

August 2015

Dedication

This dissertation is dedicated to my loving and supportive husband, Austin, and the family that we are starting together.

Acknowledgements

I would like to thank Dr. Richard Neptune for his continual guidance and support throughout my graduate work. Through his encouragement and constructive feedback, he has helped me to grow as both a researcher and a person. Words cannot describe how grateful I am for everything he has done to help prepare me for my future and it is because of him that I can confidently take the next step.

I am also very grateful for the highly collaborative environment that Dr. Neptune has cultivated in the Neuromuscular Biomechanics Laboratory and for all of the lab members, both past and present, that have helped make it the wonderful environment that it is today. My current lab mates have become some of my nearest and dearest friends and I am grateful to them for their unending encouragement and support.

I would also like to thank our collaborators at the Center for the Intrepid in Fort Sam Houston, TX, specifically Dr. Jason Wilken and Dr. Elizabeth Russell Esposito for their help with subject recruitment and data collection and for sharing their knowledge and expertise. Through this collaboration I have been given the opportunity to develop additional skills and gain experience and I am very grateful.

I am also very appreciative of Dr. Ronald Barr, Dr. Ashish Deshpande, Dr. James Sulzer, and Dr. Jason Wilken for serving on my dissertation committee. The constructive feedback that they have provided throughout my research has been instrumental in the preparation of this dissertation.

I would also like to thank my friends and family for providing wonderful examples of how to lead a good life. They are constant sources of support and motivation for me and I never would have made it to where I am today without them. I am also

appreciative of my two cats, Nox who started this journey through graduate school with me and Oliver who finished it. Above all else, I am particularly grateful to my incredible husband, Austin, for celebrating my successes and helping me overcome my failures. It is through his support and sacrifice that I have been able to pursue my Ph.D. and I am so lucky to have him in my life.

Lastly, I would like to acknowledge the funding support for this work, which included the National Science Foundation Graduate Research Fellowship, Cockrell School of Engineering Fellowship, Graduate Dean's Prestigious Fellowship Supplement and a research grant from the Center for Rehabilitation Sciences Research. The views expressed herein are those of the authors and do not reflect the official policy or position of Brooke Army Medical Center, the U.S. Army Medical Department, the U.S. Army Office of the Surgeon General, the Department of the Army, Department of Defense or the U.S. Government.

Muscle Function and Coordination of Amputee and Non-Amputee Stair Ascent

Nicole Guckert Harper, Ph.D.

The University of Texas at Austin, 2015

Supervisor: Richard R. Neptune

Stair ascent is a common activity of daily living and is necessary for maintaining independence in a variety of community environments. However, it can be a biomechanically challenging task. For example, for transtibial amputees the loss of the ankle plantarflexors coupled with the task demands of stair ascent require amputees to develop compensatory mechanisms that utilize the prosthesis and remaining musculature. The overall goal of this research was to use advanced musculoskeletal modeling and simulation techniques in a series of studies to understand how individual muscles contribute to stair ascent in non-amputees and how unilateral transtibial amputees compensate with the prosthesis and remaining musculature during stair ascent.

In the first study, a simulation of non-amputee stair ascent was developed to elucidate the contributions of individual muscles and the biomechanical mechanisms by which they accomplish stair ascent. The hip abductors, hip extensors, knee extensors and plantarflexors were found to work synergistically to generate, absorb and/or transfer mechanical power to accomplish stair ascent. In the second study, a simulation of transtibial amputee stair ascent was generated to identify functional deficits and compensations necessary for amputees to ascend stairs. The passive prosthesis was able to emulate the role of the uniarticular plantarflexors, but was unable to replicate the role

of the biarticular plantarflexors. As a result, compensations from other muscles were necessary. In the final study, simulations of non-amputee and amputee stair ascent were used to determine the contributions of individual muscles and the prosthesis to dynamic balance control, which was quantified using whole-body angular momentum. The prosthesis was able to replicate the role of the plantarflexors in the regulation of sagittal-plane and, to a lesser extent, transverse-plane angular momentum. However, while the non-amputee plantarflexors contributed minimally to frontal-plane angular momentum, the prosthesis acted to rotate the body towards the contralateral leg, which required additional muscle compensations.

By understanding the role of the individual muscles and prosthesis in achieving stair ascent and identifying the compensations used by amputees, this research provides a foundation for designing refined prostheses and targeted rehabilitation programs that improve an individual's ability to ascend stairs.

Table of Contents

List of Tables

List of Figures

Chapter 1: Introduction

More than 1.6 million individuals in the United States are currently living with the loss of a limb (Ziegler-Graham et al., 2008), 24% of which have unilateral transtibial amputations (Dillingham et al., 2002). The causes of amputation are primarily linked to vascular disease and traumatic injuries. However, due to the aging population and increasingly high rates of vascular disease in older adults (Heidenreich et al., 2011; Wild et al., 2004), the number of amputees is expected to double by the year 2050 (Ziegler-Graham et al., 2008).

As the rate of amputation increases, research is critically needed to improve rehabilitation techniques and prostheses to restore and maintain mobility. A number of studies have investigated the biomechanics of amputee gait to meet these needs. These studies have found that unilateral transtibial amputees have increased energy cost (Genin et al., 2008; Houdijk et al., 2009), altered and asymmetric kinematics and kinetics (for review, see Prinsen et al., 2011), and diminished dynamic balance (Silverman and Neptune, 2011) during level walking compared to non-amputees. Studies have also analyzed amputee gait during stair ambulation (Alimusaj et al., 2009; Powers et al., 1997; Schmalz et al., 2007; Yack et al., 1999), running (Sanderson and Martin, 1996), incline and decline walking (Vrieling et al., 2008a), sit-to-stand tasks (Ozyurek et al., 2013) and obstacle avoidance tasks (Barnett et al., 2013; Hill et al., 1999; Vrieling et al., 2007) and have identified additional asymmetries compared to non-amputees. These studies have improved the understanding of amputee gait and helped facilitate the development of refined rehabilitation techniques (Agrawal et al., 2013a; Kaufman et al., 2014; Nolan, 2012; Vrieling et al., 2009) and prostheses (Agrawal et al., 2014; Delussu et al., 2013;

Herr and Grabowski, 2012; Mancinelli et al., 2011; Segal et al., 2012) aimed at restoring amputee mobility.

However, despite these efforts, challenges with designing improved prostheses and rehabilitation techniques still persist. A principal challenge is our current limited understanding of how the prosthesis and individual muscles contribute to the biomechanical subtasks of amputee gait. To overcome this challenge, it is critical to understand individual muscle function during specific activities in non-amputees and then understand how amputees compensate to achieve the same tasks. One challenge with identifying individual muscle contributions to specific biomechanical subtasks is the inability to directly measure them experimentally. However, musculoskeletal modeling and simulation techniques provide a powerful framework for studying *in vivo* quantities. Muscle-actuated forward dynamics simulations are particularly promising as they mimic the human neuromuscular system and are capable of providing insight into the causal relationships between individual muscle activity and the resulting task performance (for review, see Zajac et al., 2002). Previous studies have used muscle-actuated forward dynamics simulations to investigate the contributions of individual muscles in non-amputees to movement tasks including walking (e.g., Liu et al., 2006; Neptune et al., 2001; Pandy et al., 2010), running (e.g., Hamner et al., 2010; Sasaki and Neptune, 2006), pedaling (e.g., Neptune et al., 2000a) and wheelchair propulsion (Rankin et al., 2011). In addition, studies have used simulations to identify the contributions of the prosthesis and individual muscles needed to perform unilateral transtibial amputee walking (Silverman and Neptune, 2012; Zmitrewicz et al., 2007). Simulations have also been used to improve prosthesis designs by determining the influence of design parameters such as stiffness on the biomechanical subtasks of walking (Fey et al., 2012, 2013). However, despite the benefits of identifying the contributions from the prosthesis and individual muscles in

amputee gait, few studies have investigated these contributions in tasks other than level walking.

Stair ascent is a critical task for mobility independence and can be biomechanically challenging. Stair ascent is a more strenuous activity than stair descent and requires greater muscle activity (Bae et al., 2009; Lyons et al., 1983; McFadyen and Winter, 1988), net joint work (DeVita et al., 2007) and metabolic energy (Teh and Aziz, 2002). In level walking the center-of-mass (COM) is predominantly propelled horizontally, but in stair ascent the COM is simultaneously propelled both horizontally and vertically while leg swing is modulated to avoid contact with the intermediate step (McFadyen and Winter, 1988; Zachazewski et al., 1993). As a result of these increased task requirements, several studies have observed increased energy cost (Ainsworth et al., 2000; Teh and Aziz, 2002) and demands at the hip (Andriacchi et al., 1980; DeVita et al., 2007; Nadeau et al., 2003), knee (Andriacchi et al., 1980; Costigan et al., 2002; DeVita et al., 2007; Hall et al., 2013; McFadyen and Winter, 1988; Nadeau et al., 2003) and ankle (Andriacchi et al., 1980; DeVita et al., 2007; Nadeau et al., 2003) in stair ascent relative to level walking. In addition, previous research has shown that dynamic balance is more difficult to maintain during stair ascent than in level walking (Kendell et al., 2010), particularly in the frontal plane (Pickle et al., 2014; Silverman et al., 2014). This suggests that the biomechanical subtasks of vertical propulsion, anteroposterior propulsion, mediolateral control, leg swing and whole-body dynamic balance during stair ascent likely require altered muscle contributions relative to level walking. However, few studies have investigated the contributions of individual muscles to these subtasks.

In transtibial amputees, the loss of the plantarflexors, which are critical to body support (Liu et al., 2006; Neptune et al., 2001), forward propulsion (Liu et al., 2006; Neptune et al., 2001), mediolateral balance (Allen and Neptune, 2012; Pandy et al.,

2010), leg swing (Neptune et al., 2001) and dynamic balance control (Neptune and McGowan, 2011), affects walking performance and requires compensations from both the residual and intact limbs (for review, see Prinsen et al., 2011). Stair ascent, which requires increased effort to simultaneously propel the COM horizontally and vertically, is often one of the more difficult mobility tasks for amputees to perform as stair ascent is less stable than other mobility tasks (Kendell et al., 2010) and the prosthetic limb is less capable of effectively mimicking the physiologic ankle-foot during stair ascent compared to level walking (Sinitski et al., 2012). The increased demands of stair ascent require amputees to develop additional compensatory mechanisms that utilize the remaining musculature in addition to the prosthesis and result in significant asymmetries between the residual and intact limbs (Alimusaj et al., 2009; Powers et al., 1997; Schmalz et al., 2007; Yack et al., 1999). However, these compensatory mechanisms have not been investigated at the individual muscle level. Identifying the contributions of individual muscles and the prosthesis to the biomechanical subtasks involved in amputee and non-amputee stair ascent could help guide both prosthesis design and the development of targeted rehabilitation programs to improve stair ascent in amputees.

The overall goal of this research was to use a musculoskeletal modeling and simulation framework to understand how individual muscles and the prosthesis contribute to the subtasks of stair ascent (i.e., vertical propulsion, anteroposterior propulsion, mediolateral control, leg swing and dynamic balance) in non-amputees and unilateral transtibial amputees as a foundation for guiding the design of targeted rehabilitation programs and more effective prostheses. This overall goal was addressed through a series of three studies. In the study in Chapter 2, a muscle-driven forward dynamics simulation of non-amputee stair ascent was developed and analyzed to determine the contributions of individual lower-extremity muscles to vertical propulsion, anteroposterior propulsion,

mediolateral control and leg swing in non-amputee stair ascent and the biomechanical mechanisms by which individual muscles work in synergy to perform these subtasks. In the study in Chapter 3, the compensatory mechanisms used by unilateral transtibial amputees were identified by elucidating the role of individual muscles and the prosthesis in generating the necessary vertical propulsion, anteroposterior propulsion, mediolateral control and leg swing during stair ascent by extending the muscle-driven forward dynamics simulation framework developed in Chapter 2 to unilateral transtibial amputees. In the study in Chapter 4, the biomechanical mechanisms by which amputees and non-amputees regulate dynamic balance during stair ascent were determined by quantifying the contributions of individual muscles and the prosthesis to whole-body angular momentum in the frontal, transverse and sagittal planes. Understanding the role of individual muscles and the prosthesis in non-amputee and amputee stair ascent will help identify the compensatory mechanisms used by unilateral transtibial amputees and provide a foundation for designing refined prosthetic devices and targeted rehabilitation programs aimed at improving an individual's ability to ascend stairs while maintaining dynamic balance.

Chapter 2: Muscle Function and Coordination of Non-Amputee Stair Ascent

INTRODUCTION

Stair ascent is a common activity of daily living and necessary for maintaining full independence in a range of community environments. However, stair ascent can be biomechanically challenging. Compared to level walking where the center-of-mass (COM) is predominantly propelled horizontally, stair ascent requires an individual to simultaneously propel the COM both horizontally and vertically (McFadyen and Winter, 1988; Zachazewski et al., 1993) while controlling mediolateral motion and modulating leg swing to avoid contact with the intermediate step (McFadyen and Winter, 1988; Zachazewski et al., 1993). As a result of the task requirements, several studies have observed increased lower-limb joint demands (e.g., Andriacchi et al., 1980; McFadyen and Winter, 1988) as well as increased energy cost (Ainsworth et al., 2000; Teh and Aziz, 2002) and knee contact forces (Costigan et al., 2002) in stair ascent relative to level walking. In addition, previous research has shown that dynamic balance is more difficult to maintain during stair ascent than during level walking (Lee and Chou, 2007). This suggests that the biomechanical subtasks of vertical propulsion, anteroposterior propulsion, mediolateral control and leg swing during stair ascent likely require altered muscle contributions relative to level walking. However, while these contributions have been investigated in level walking (e.g., Liu et al., 2006; Neptune et al., 2001; Pandy et al., 2010), few studies have investigated the contributions of individual muscles to these subtasks during stair ascent.

A number of experimental studies have investigated the contributions of joint moments (Nadeau et al., 2003; Novak and Brouwer, 2011), powers (DeVita et al., 2007;

Nadeau et al., 2003; Wilken et al., 2011) and work (DeVita et al., 2007) to unimpaired stair ascent and have identified the knee extensors (e.g., DeVita et al., 2007; Nadeau et al., 2003; Wilken et al., 2011) and plantarflexors (DeVita et al., 2007; Novak and Brouwer, 2011; Wilken et al., 2011) as important contributors with secondary contributions from the hip abductors (Nadeau et al., 2003; Novak and Brouwer, 2011). However, joint-based studies are unable to differentiate between individual muscles and rely on correlations with other experimental measurements to hypothesize the role of individual muscle groups. As a result, these joint-based analyses were not able to identify the individual muscle contributions to the biomechanical subtasks of stair ascent.

Other studies have investigated muscle function during stair ascent by correlating electromyographic (EMG) data with kinematic and kinetic data (e.g., McFadyen and Winter, 1988) and similarly identified the knee extensors, plantarflexors and hip abductors as primary contributors to stair ascent. However, while these studies were able to identify differences in muscle excitation intensity and timing, they were unable to identify the biomechanical contributions of individual muscles to stair ascent due to the complex nonlinear relationships between muscle excitation, as determined by surface electromyography, and the resulting force (e.g., Zajac, 1989). In addition, a muscle is capable of accelerating all body segments through dynamic coupling (Zajac and Gordon, 1989; Zajac et al., 2002), and can therefore have contributions that are not identifiable through correlations with experimental data alone. As a result, although the plantarflexors, knee extensors and hip abductors have been identified as important contributors to stair ascent, it remains unclear how individual muscles function in synergy to satisfy the biomechanical task demands of stair ascent.

One method for identifying these contributions is to use musculoskeletal modeling and simulation techniques. Previous studies have used muscle-actuated forward

dynamics simulations to investigate the contributions of individual muscles to human movement tasks such as walking (e.g., Liu et al., 2006; Neptune et al., 2001; Pandy et al., 2010), running (e.g., Hamner et al., 2010; Sasaki and Neptune, 2006), pedaling (e.g., Neptune et al., 2000a; Raasch et al., 1997) and wheelchair propulsion (e.g., Rankin et al., 2011) on level ground. Lin et al. (2015) analyzed stair ascent by using a musculoskeletal model and static optimization to determine muscle forces during stance and a pseudo-inverse force decomposition method to determine the contributions of each muscle force to whole-body support, forward propulsion and balance by analyzing whole-body center-of-mass accelerations. However, this study focused on only five muscle groups during stance and did not investigate the specific biomechanical mechanisms by which they contribute to the subtasks of stair ascent (e.g., how muscles generate, absorb or transfer mechanical power between body segments). Others have used forward dynamics simulations to investigate stair ascent at the individual muscle level (Ghafari et al., 2009). However, their analysis focused on the total mechanical power produced by each muscle and did not identify individual muscle contributions to the subtasks of stair ascent. In addition, the model was restricted to the sagittal plane and could not characterize the muscle contributions to non-sagittal plane functions.

The purpose of this study was to develop a three-dimensional muscle-actuated forward dynamics simulation of unimpaired stair ascent to determine the contributions of individual lower-extremity muscles to vertical propulsion, anteroposterior propulsion, mediolateral control and leg swing during unimpaired stair ascent and the mechanisms by which individual muscles work in synergy to perform these subtasks. This study will build upon the work of Lin et al. (2015) to further understand muscle function and coordination in stair ascent and help guide the development of effective, targeted rehabilitation programs aimed at improving an individual's ability to ascend stairs.

METHODS

A three-dimensional muscle-actuated forward dynamics simulation of unimpaired stair ascent was generated to emulate group-averaged experimental joint kinematics and ground reaction forces (GRFs) for 27 unimpaired subjects. To develop this simulation, the musculoskeletal system, foot-ground contact and muscle force generation were modeled and a dynamic optimization algorithm was used to identify the muscle excitation patterns that minimized the difference between the simulated and experimental joint kinematics and GRFs. To identify the contributions of individual muscles to the subtasks of stair ascent, GRF decomposition and segment power analyses were performed. Each of these elements is described below in more detail.

Musculoskeletal model

A previously developed three-dimensional bipedal musculoskeletal model (Peterson et al., 2010) was adapted to simulate stair ascent. The model was developed using SIMM/Dynamics Pipeline (MusculoGraphics, Inc., Santa Rosa, CA) with previously characterized musculoskeletal geometry (Delp et al., 1990) and consisted of 14 rigid body segments representing the head-arms-trunk (HAT), pelvis and bilaterally the thigh, shank, patella, talus, calcaneus and toes. The model consisted of 23 degrees-of-freedom (DOF) with a 6 DOF (3 translations, 3 rotations) joint between the pelvis and ground, a 3 DOF spherical joint between the trunk and pelvis, a 3 DOF spherical joint for each hip, and 1 DOF revolute joints at each knee, ankle, subtalar and metatarsal joint. Passive torques representing the forces applied by passive tissues and structures in the joints, including ligaments, were applied at each joint (Davy and Audu, 1987). The foot-ground contact was modeled using 31 viscoelastic elements with Coulomb friction attached to each foot and evenly distributed across the calcaneus and toes (Neptune et al.,

2000b). In addition, in the foot-ground contact model the height of the ground was modified to represent the surface of the stairs (Rise/Run: 0.1778 m / 0.2794 m). The dynamical equations of motion were generated using SD/FAST (PTC, Needham, MA).

The model was driven by 38 Hill-type musculotendon actuators per leg. Muscle excitations at time *t* (*e(t),* Equation 2.1) for the 38 musculotendon actuators were defined using bimodal excitation patterns and therefore six optimization parameters including the *onset*, *offset* and amplitude (*A*) of each mode (*i*).

$$e(t) = \sum_{i=1}^{2} \begin{cases} \frac{A_i}{2}\left(1 - \cos\left(\frac{2\pi(t-onset_i)}{offset_i - onset_i}\right)\right) & onset_i \le t \le offset_i \\ 0 & t < onset_i \;||\; t > offset_i \end{cases} \quad (2.1)$$

Muscle contraction dynamics were governed by intrinsic force-length-velocity relationships (Zajac, 1989). Muscle activation and deactivation dynamics were modeled using a non-linear first-order differential equation (Raasch et al., 1997) with previously derived activation and deactivation time constants (Appendix A: Table A.1 - Winters and Stark, 1988).

Dynamic optimization

A forward dynamics simulation of stair ascent was generated over a full gait cycle (right foot-strike to right foot-strike) using dynamic optimization (Appendix A: Figure A.1). A simulated annealing optimization algorithm (Goffe et al., 1994) was used to identify the six optimal parameters for each muscle (timing and amplitude) that minimized the following objective function (*J*):

$$J = \sum_{i=1}^{n_{step}} \left(\sum_{j=1}^{n_{vars}} wt_j \frac{\left(Y_{ij} - \hat{Y}_{ij}\right)^2}{SD_{ij}^2} + ws \sum_{k=1}^{n_{musc}} \left(\frac{F_{ik}}{A_k}\right)^2 \right) \quad (2.2)$$

where n_{step} is the number of time steps, n_{vars} is the number of quantities evaluated, including joint angles, pelvis translations and GRFs, n_{musc} is the number of muscles, Y_{ij} is the experimental value at time step i for quantity j, $\hat{Y}_{ij}$ is the simulated value, SD_{ij} is the experimental standard deviation of quantity j at time step i, F_{ik} is the muscle force at time step i for muscle k, A_k is the physiological cross-sectional area of muscle k, wt_j is the weighting for the difference in quantity j and ws is the weighting for muscle stress. The first component of the objective function minimized the differences between simulated and experimental joint kinematics and GRFs while the second component of the objective function minimized total muscle stress in order to minimize unnecessary muscle co-activation. To assess the overall quality of the simulation, the simulated kinematics and GRFs were compared to the experimental kinematics and GRFs using the root-mean-square (RMS) error:

$$RMS\ error = \sqrt{\frac{\sum_{i=1}^{n_{step}} \left(Y_{ij} - \hat{Y}_{ij}\right)^2}{n_{step}}} \quad (2.3)$$

In addition, the simulated muscle excitations were compared with EMG timings for the muscles available in the literature (Bovi et al., 2011; Joseph and Watson, 1967; McFadyen and Winter, 1988; Moffet et al., 1993) to ensure that the simulation excitations were consistent with experimental EMG data.

Simulation analysis

To identify the individual muscle contributions to the biomechanical subtasks of vertical propulsion, anteroposterior propulsion, mediolateral control and leg swing, previously described GRF decomposition and segment power analyses were performed (Neptune et al., 2008; Neptune et al., 2004). The contribution of each muscle to vertical propulsion, anteroposterior propulsion and mediolateral control was quantified by its contribution to the vertical, anteroposterior (AP) and mediolateral (ML) GRF, respectively, during the first (weight acceptance through pull-up, Figure 2.1) and second (forward continuance through push-up, Figure 2.1) halves of stance. Positive (negative) contributions to the AP and ML GRFs indicated that the muscle contributed to forward propulsion (braking) and lateral (medial) control, respectively. Muscle function was further investigated through a segment power analysis by examining the mechanical power generated, absorbed and/or transferred by each muscle to the trunk, ipsilateral leg and contralateral leg during stance in the vertical, AP and ML directions. To quantify each muscle's contribution to leg swing, the power delivered to the leg during swing initiation (push-up, Figure 2.1), early swing (swing - foot clearance, Figure 2.1) and late swing (swing - foot placement, Figure 2.1) was determined. Positive (negative) power generated by a muscle to a segment indicated that the muscle accelerated (decelerated) the segment in the direction of its motion. Muscles with similar function and anatomical classification were combined into 15 muscle groups for the analyses (Table 2.1), with the contributions of the muscles within each group being summed. The contribution of gravity to vertical propulsion, anteroposterior propulsion, mediolateral control and leg swing was also computed since it has been shown to be important in level walking (Anderson and Pandy, 2003; Lin et al., 2011).

Table 2.1: Muscles included in the musculoskeletal model and their corresponding analysis group.

Muscles	Analysis Groups
Iliacus Psoas	IL
Adductor Longus Adductor Brevis Pectineus Quadratus Femoris	AL
Superior Adductor Magnus Middle Adductor Magnus Inferior Adductor Magnus	AM
Sartorius	SAR
Rectus Femoris	RF
Vastus Medialis Vastus Lateralis Vastus Intermedius	VAS
Anterior Gluteus Medius Middle Gluteus Medius Anterior Gluteus Minimus Middle Gluteus Minimus	GMEDA
Posterior Gluteus Medius Posterior Gluteus Minimus Piriformis Gemellus	GMEDP
Tensor Fasciae Latae	TFL
Superior Gluteus Maximus Middle Gluteus Maximus Inferior Gluteus Maximus	GMAX
Semitendinosus Semimembranosus Gracilis Biceps Femoris Long Head	HAM
Biceps Femoris Short Head	BFSH
Medial Gastrocnemius Lateral Gastrocnemius	GAS
Soleus Tibialis Posterior Flexor Digitorum Longus	SOL
Tibialis Anterior Extensor Digitorum Longus	TA

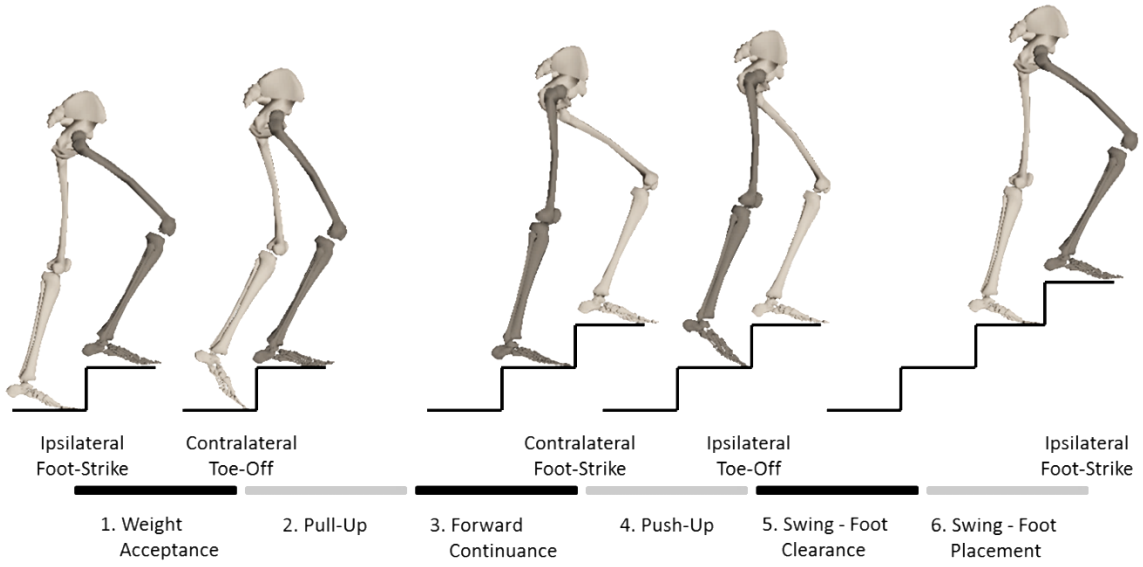

Figure 2.1: The six regions of the gait cycle of the ipsilateral leg (dark shaded leg): 1) weight acceptance (ipsilateral foot-strike to contralateral toe-off), 2) pull-up and 3) forward continuance (contralateral toe-off to contralateral foot-strike divided into two equal sections), 4) push-up (contralateral foot-strike to ipsilateral toe-off), 5) early swing and foot clearance and 6) late swing and foot placement (ipsilateral toe-off to ipsilateral foot-strike divided into two equal sections). The six regions of the gait cycle were adapted from previous studies (McFadyen and Winter, 1988; Wilken et al., 2011).

Experimental data

Twenty-seven unimpaired subjects (15 female; 21.9 ± 4.3 years; 73.0 ± 15.0 kg; 1.7 ± 0.1 m) without pain or history of major lower extremity injury participated in this study, which was approved by the Institutional Review Board at Brooke Army Medical Center (Fort Sam Houston, TX). After obtaining written informed consent, subjects ascended a 16-step instrumented staircase (AMTI, Inc., Watertown, MA) in a step-over-step manner at a fixed cadence (80 steps per minute). GRF data were collected from 2 forceplates (1200 Hz, AMTI, Inc., Watertown, MA) embedded in the staircase. A 26-camera optoelectronic motion capture system (120 Hz, Motion Analysis Corp., Santa

Rosa, CA) and a body segment marker set with 57 reflective markers were used to collect three-dimensional whole-body kinematics (Wilken et al., 2012). In addition, a digitization process was used to identify 20 bilateral anatomical bony landmarks (C-motion, Inc., Germantown, MD). All subject data were collected in the Military Performance Laboratory at the Center for the Intrepid in Fort Sam Houston, TX.

All biomechanical data were processed in Visual3D (C-motion, Inc., Germantown, MD). A 13-segment model was created and scaled to each subject's body mass and height (Dempster, 1955) using the anatomical landmarks to define the joint centers and joint coordinate systems recommended by the International Society of Biomechanics (Grood and Suntay, 1983; Wu and Cavanagh, 1995; Wu et al., 2002). A low-pass, fourth-order Butterworth filter was applied to the marker and GRF data with cut-off frequencies of 6 Hz and 50 Hz, respectively. GRFs were normalized by subject body weight and joint kinematics were computed using Euler angles with pelvis, hip, knee and ankle kinematics defined using the previously determined Cardan rotation sequences (Baker, 2001; Grood and Suntay, 1983; Wu et al., 2002). GRFs as well as three-dimensional joint kinematics corresponding to five complete gait cycles for each limb were time-normalized to 100% of the gait cycle and exported to Matlab (MathWorks, Inc., Natick, MA). In Matlab, the GRFs and joint kinematics were averaged across gait cycles and subjects for each limb.

RESULTS

Simulation quality

The optimization framework identified a set of muscle excitations that successfully emulated the experimental kinematics and GRFs (Appendix A: Figures A.2

and A.3), with most quantities within 2 standard deviations (SDs) of the experimental data. The average RMS error between the simulated and experimental pelvis translations, joint kinematics and GRFs across the gait cycle was 0.023 meters (2 SDs = 0.081 m), 6.30 degrees (2 SDs = 10.05 deg) and 0.063 percent body weight (2 SDs = 0.069 %BW), respectively. In addition, the timing profiles for the optimized muscle excitations compared well with EMG data available in the literature (Appendix A: Figure A.4 - Bovi et al., 2011; Joseph and Watson, 1967; McFadyen and Winter, 1988; Moffet et al., 1993).

Vertical propulsion

During the first half of ipsilateral leg stance (Figure 2.1: weight acceptance through pull-up), VAS was the primary contributor to vertical propulsion of the body COM, with additional contributions from GMAX, SOL, GMEDP and GMEDA (Figure 2.2). Gravity also contributed significantly to the vertical GRF (Figure 2.2). To propel the COM vertically, VAS and SOL both generated vertical power directly to the trunk and ipsilateral leg (Figure 2.3). Concurrently, GMAX generated vertical power to the trunk while it also transferred power from the contralateral leg to the trunk (Figure 2.3). Both GMEDA and GMEDP generated vertical power to the trunk and contralateral leg and transferred power from the ipsilateral leg to the trunk and contralateral leg (Figure 2.3).

During the second half of ipsilateral leg stance (Figure 2.1: forward continuance through push-up), the plantarflexors (SOL and GAS) were the primary contributors to vertical propulsion with additional contributions from VAS while HAM opposed vertical propulsion (Figure 2.2). Gravity was also a critical contributor to the vertical GRF (Figure 2.2). SOL, GAS and VAS all generated vertical power directly to the trunk and ipsilateral leg (Figure 2.3). VAS's contribution decreased to zero around contralateral

foot-strike (~50% ipsilateral gait cycle) after reaching its peak during the first half of stance, whereas SOL and GAS contributed to vertical propulsion throughout the entire second half of stance. Prior to contralateral foot-strike (~50% ipsilateral gait cycle), HAM absorbed vertical power from the legs while also redistributing some of the power from the legs to the trunk (Figure 2.3). Following contralateral foot-strike, HAM began generating vertical power to the trunk, although it continued to redistribute power from the legs to the trunk (Figure 2.3). The power delivered to the trunk was not enough to overcome HAM's power absorption from both legs, causing HAM to ultimately decrease vertical propulsion.

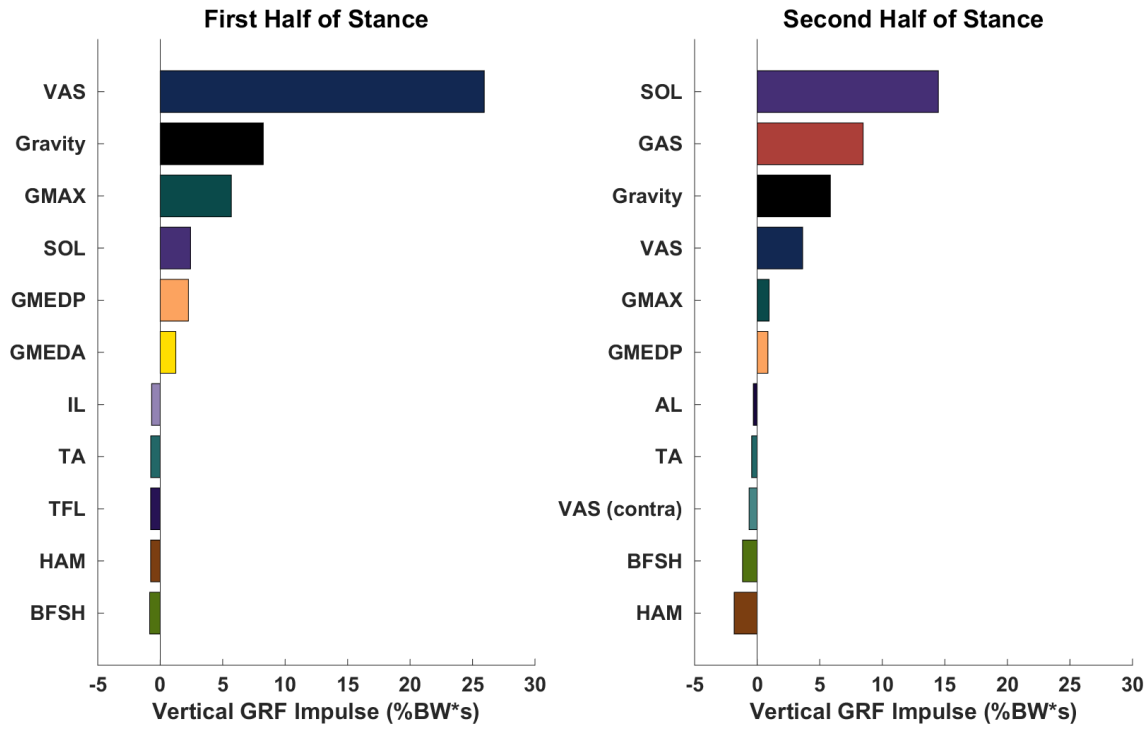

Figure 2.2: Primary positive and negative contributors to vertical propulsion of the body COM (i.e. the vertical ground reaction force (GRF) impulse) during the two halves of ipsilateral stance: 1) weight acceptance through pull-up, and 2) forward continuance through push-up. Each muscle is depicted using a unique, muscle-specific color to enable comparison across figures. Unless otherwise specified, muscles are from the ipsilateral leg. For muscle group abbreviations, please see Table 2.1.

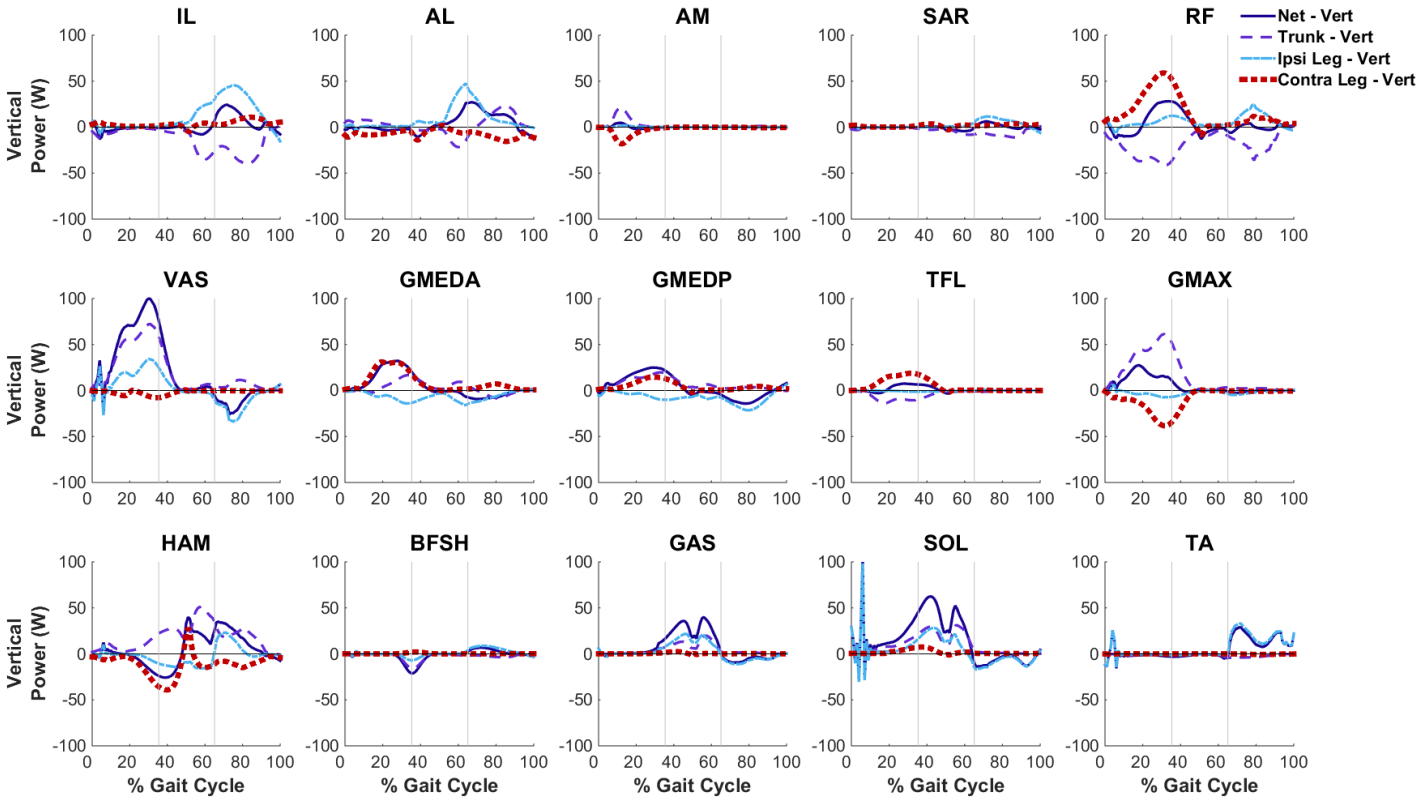

Figure 2.3: Musculotendon mechanical power output from the ipsilateral leg muscles across the ipsilateral gait cycle and distributed to the trunk, ipsilateral (Ipsi) leg and contralateral (Contra) leg in the vertical direction. Positive (negative) net values indicate power generated (absorbed) by the musculotendon actuator. Positive (negative) values for the leg or trunk indicate that power is being generated to (absorbed from) the leg or trunk. The gray lines divide the gait cycle into three regions: 1) weight acceptance through pull-up, 2) forward continuance through push-up, and 3) swing (foot clearance through foot placement). For muscle group abbreviations, please see Table 2.1.

Anteroposterior propulsion

During the first half of ipsilateral leg stance (Figure 2.1: weight acceptance through pull-up), GMAX, gravity, TA, VAS, GMEDP and HAM were the primary contributors to forward propulsion of the body COM while SOL was the primary contributor to braking the body COM with additional contributions from RF, GAS and TFL (Figure 2.4). GMAX, TA, GMEDP and HAM all contributed to forward propulsion by generating or transferring power to one or both legs (Figure 2.5). GMAX and HAM generated power to both legs and transferred power from the trunk to the legs while TA generated power directly to the ipsilateral leg (Figure 2.5). GMEDP absorbed power from the contralateral leg and trunk and redistributed some of this power to the ipsilateral leg (Figure 2.5). Unlike the other primary contributors, GMEDP absorbed net power in the AP direction. However, by transferring a significant amount of power from the trunk to the ipsilateral leg, GMEDP ultimately contributed to forward propulsion (Figure 2.5). Of the primary contributors to forward propulsion, VAS alone contributed to forward propulsion by generating power to the trunk and transferring power from the legs to the trunk (Figure 2.5). The forward propulsion generated by these muscle groups partially counteracted the muscles contributing to braking in the first half of stance (net negative AP GRF). In this region, SOL and GAS absorbed power directly from the ipsilateral leg (Figure 2.5). In addition, RF and TFL absorbed power from both legs, primarily the contralateral leg, and transferred some of this power to the trunk. However, the power transferred to the trunk was not enough to overcome RF and TFL's absorption of power from both legs (Figure 2.5).

During the second half of ipsilateral leg stance (Figure 2.1: forward continuance through push-up), HAM was the primary contributor to forward propulsion while RF and VAS were the primary contributors to braking (Figure 2.4). Gravity also contributed to

braking, but to a lesser extent (Figure 2.4). HAM generated power directly to both the ipsilateral and contralateral legs and transferred a significant amount of power from the trunk to the legs (Figure 2.5). While this decreased the AP power of the trunk, HAM ultimately contributed to forward propulsion by generating greater power to the legs. In addition, while SOL was not a primary contributor to the AP GRF in this region, it played a critical role in redistributing power from the ipsilateral leg to the trunk (Figure 2.5). Similar to the first half of stance, RF continued to absorb power from both legs while transferring power from the legs to the trunk (Figure 2.5). However, contrary to the first half of stance, VAS switched from generating net power to absorbing net power, ultimately absorbing power from the ipsilateral leg while transferring some power from the ipsilateral leg to the trunk (Figure 2.5). As a result, while both RF and VAS redistributed some power to the trunk to propel it forward, it was not enough to overcome their contributions to leg braking.

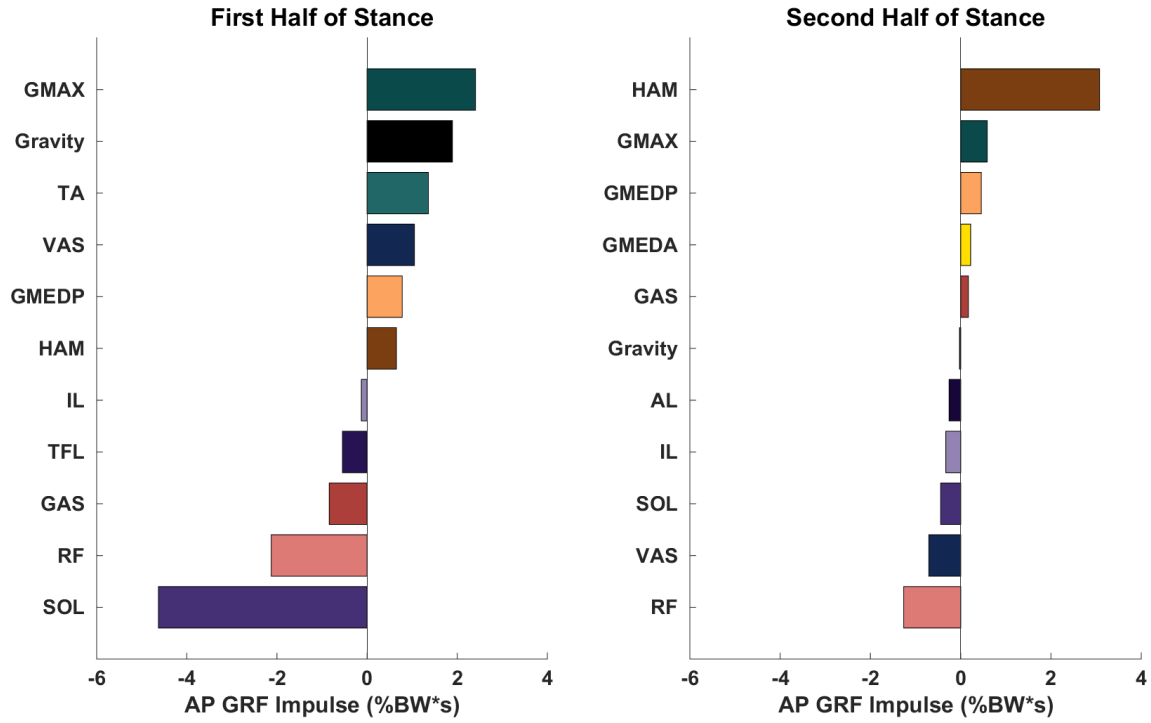

Figure 2.4: Primary positive and negative contributors to anteroposterior (AP) propulsion of the body COM (i.e. the AP ground reaction force (GRF) impulse) during the two halves of ipsilateral stance: 1) weight acceptance through pull-up, and 2) forward continuance through push-up. Positive (negative) GRF impulses indicate contributions to forward propulsion (braking) of the COM. Each muscle is depicted using a unique, muscle-specific color to enable comparison across figures. Muscles are from the ipsilateral leg. For muscle group abbreviations, please see Table 2.1.

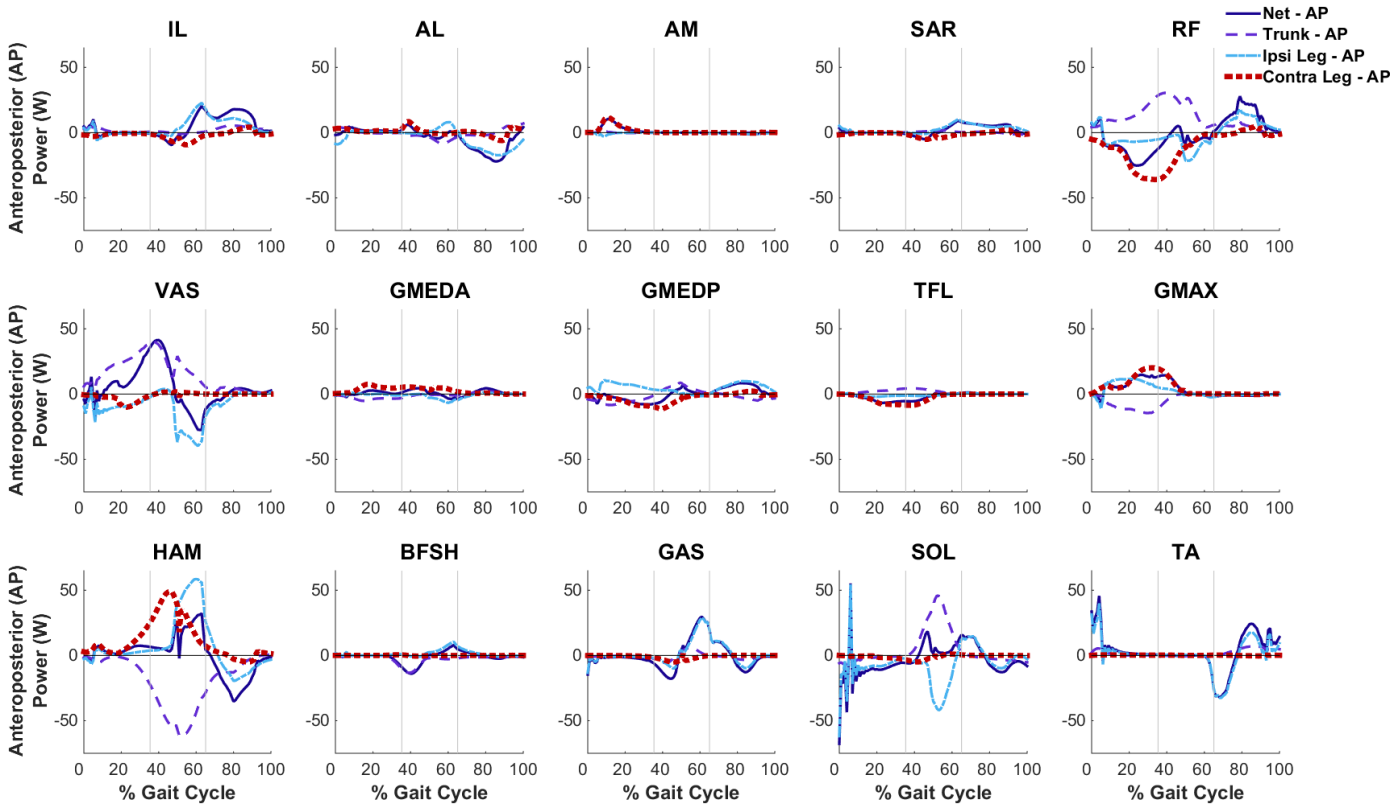

Figure 2.5: Musculotendon mechanical power output from the ipsilateral leg muscles across the ipsilateral gait cycle and distributed to the trunk, ipsilateral (Ipsi) leg and contralateral (Contra) leg in the anteroposterior (AP) direction. Positive (negative) net values indicate power generated (absorbed) by the musculotendon actuator. Positive (negative) values for the leg or trunk indicate that power is being generated to (absorbed from) the leg or trunk. The gray lines divide the gait cycle into three regions: 1) weight acceptance through pull-up, 2) forward continuance through push-up, and 3) swing (foot clearance through foot placement). For muscle group abbreviations, please see Table 2.1.

Mediolateral control

In general, all contributions to mediolateral control were smaller than the contributions to vertical and anteroposterior propulsion. During the first half of ipsilateral leg stance (Figure 2.1: weight acceptance through pull-up), VAS was the primary contributor to lateral (positive) control of the COM while GMEDA was the primary contributor to medial (negative) control with additional contributions from GMEDP (Figure 2.6). In addition, gravity contributed to lateral control (Figure 2.6). VAS absorbed power from the trunk and transferred some power from the trunk to the contralateral leg (Figure 2.7). While this decelerated the trunk's lateral motion, it accelerated the contralateral leg's medial motion which accelerated the overall body laterally. GMEDA generated power to the trunk and initially transferred power from the ipsilateral leg to the trunk prior to generating power to the ipsilateral leg (Figure 2.7). While this accelerated the trunk laterally, it also decelerated and then accelerated the ipsilateral leg's lateral and medial motion, respectively. In contrast, GMEDP absorbed power from the trunk and initially transferred power from the trunk to the ipsilateral leg before absorbing power from the ipsilateral leg (Figure 2.7), decelerating the trunk's lateral motion while also accelerating and then decelerating the ipsilateral leg's lateral and medial motion, respectively.

During the second half of ipsilateral leg stance (Figure 2.1: forward continuance through push-up), HAM was the primary contributor to lateral (positive) control with additional contributions from AL while GMEDP and GMEDA remained primary contributors to medial (negative) control with additional contributions from RF (Figure 2.6). Gravity also contributed to medial control (Figure 2.6). Most of the power generated, absorbed or transferred by the muscles in this region was very small. However, one notable exception was SOL. While SOL was not the major contributor to

medial control, it absorbed and then generated a substantial amount of power to the ipsilateral leg in addition to generating power to the trunk (Figure 2.7). This simultaneously decelerated the ipsilateral leg's medial motion while accelerating the trunk's medial motion and then accelerated both the trunk and the ipsilateral leg's lateral motion.

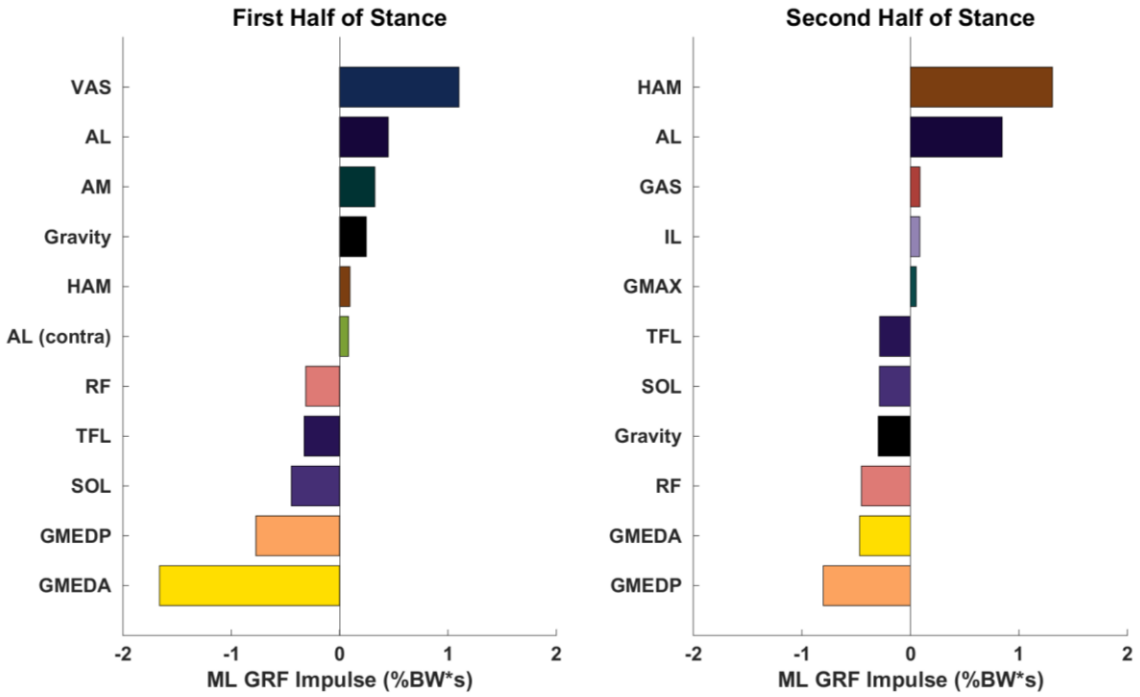

Figure 2.6: Primary positive and negative contributors to mediolateral (ML) control of the body COM (i.e. the ML ground reaction force (GRF) impulse) during the two halves of ipsilateral stance: 1) weight acceptance through pull-up, and 2) forward continuance through push-up. Positive (negative) GRF impulses indicate contributions to lateral (medial) control of the COM. Each muscle is depicted using a unique, muscle-specific color to enable comparison across figures. Unless otherwise specified, muscles are from the ipsilateral leg. For muscle group abbreviations, please see Table 2.1.

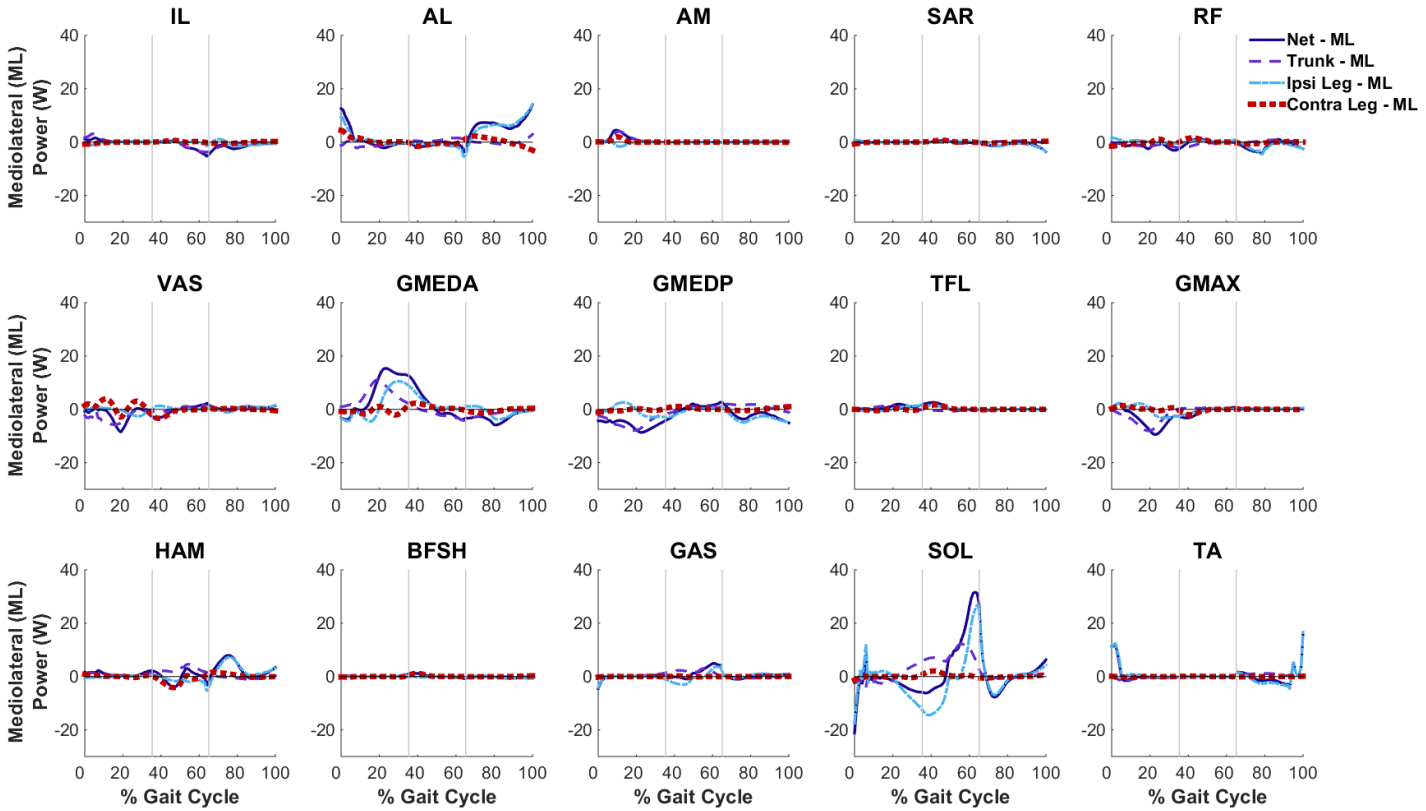

Figure 2.7: Musculotendon mechanical power output from the ipsilateral leg muscles across the ipsilateral gait cycle and distributed to the trunk, ipsilateral (Ipsi) leg and contralateral (Contra) leg in the mediolateral (ML) direction. Positive (negative) net values indicate power generated (absorbed) by the musculotendon actuator. Positive (negative) values for the leg or trunk indicate that power is being generated to (absorbed from) the leg or trunk. The gray lines divide the gait cycle into three regions: 1) weight acceptance through pull-up, 2) forward continuance through push-up, and 3) swing (foot clearance through foot placement). For muscle group abbreviations, please see Table 2.1.

Leg swing

During ipsilateral leg swing initiation (Figure 2.1: push-up), ipsilateral IL, HAM, AL and GAS in addition to contralateral GMEDA were the primary generators of power to the ipsilateral leg (Figure 2.8). Both IL and AL generated power directly to the ipsilateral leg and transferred power from the trunk to the ipsilateral leg while GAS and HAM generated power to the ipsilateral leg and GAS generated power to the trunk as well (Figure 2.9). Contralateral GMEDA also generated power directly to the ipsilateral leg while redistributing power from the contralateral leg to the ipsilateral leg (Figure 2.9: 0-18% gait cycle - contralateral leg is in weight acceptance phase; contralateral and ipsilateral legs are reversed). Gravity as well as ipsilateral VAS were the primary absorbers of power from the ipsilateral leg during swing initiation (Figure 2.8), with VAS absorbing power from the ipsilateral leg and transferring power from the ipsilateral leg to the trunk (Figure 2.9). In early swing (Figure 2.1: swing - foot clearance), ipsilateral IL remained the primary generator of power to the ipsilateral leg while gravity and ipsilateral VAS remained the primary absorbers of power (Figure 2.8). These muscles continued to contribute to leg swing as they had in swing initiation (Figure 2.9).

During late swing (Figure 2.1: swing - foot placement), the primary contributors were partially altered compared to swing initiation and early swing, with ipsilateral IL still generating a large amount of power to the ipsilateral leg but TA and RF also generating a substantial amount of power to the ipsilateral leg (Figure 2.8). IL and RF generated power to the ipsilateral leg and, to a lesser extent, the contralateral leg, while also transferring power from the trunk to the legs (Figure 2.9). Concurrently, TA purely generated power to the ipsilateral leg (Figure 2.9). Gravity as well as the ipsilateral plantarflexors (SOL and GAS) and HAM were the primary contributors to power absorption from the ipsilateral leg in preparation for foot contact (Figure 2.8). All three

muscle groups absorbed power from the ipsilateral leg in preparation for contact with the ground while HAM also transferred power from the legs to the trunk (Figure 2.9).

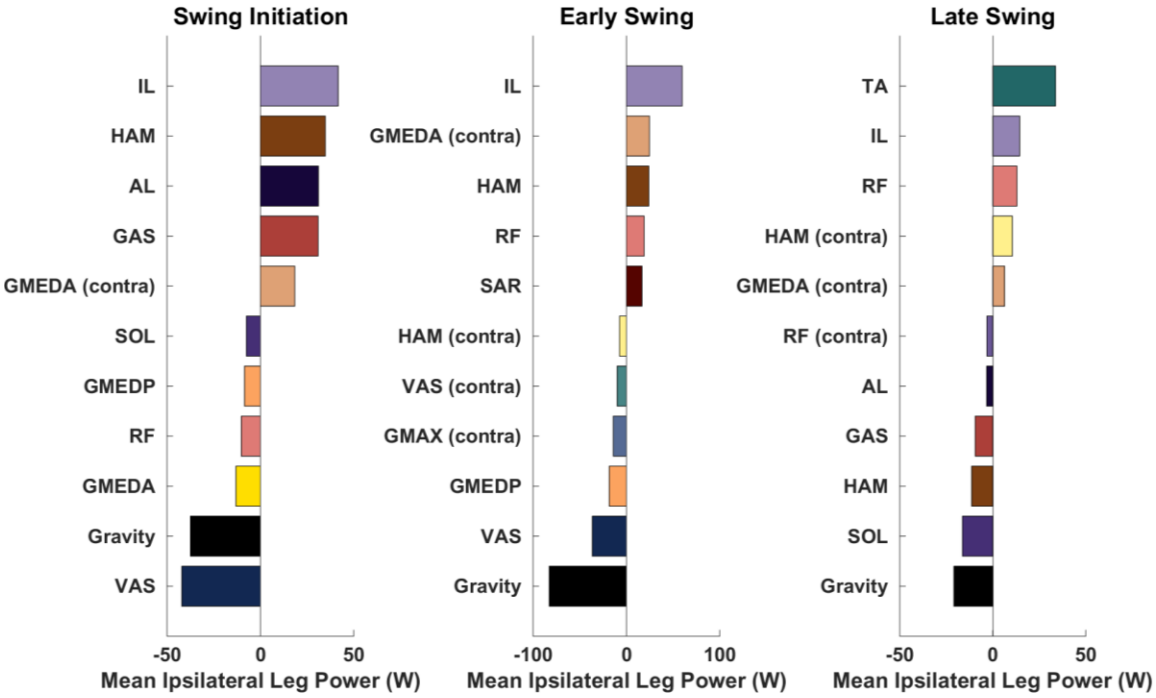

Figure 2.8: Primary contributors to net mean mechanical power generation (positive) to and absorption (negative) from the ipsilateral leg during: 1) swing initiation (push-up), 2) early swing (foot clearance), and 3) late swing (foot placement). Each muscle is depicted using a unique, muscle-specific color to enable comparison across figures. Unless otherwise specified, muscles are on the ipsilateral side. For muscle group abbreviations, please see Table 2.1. Please note the different scale in Early Swing.

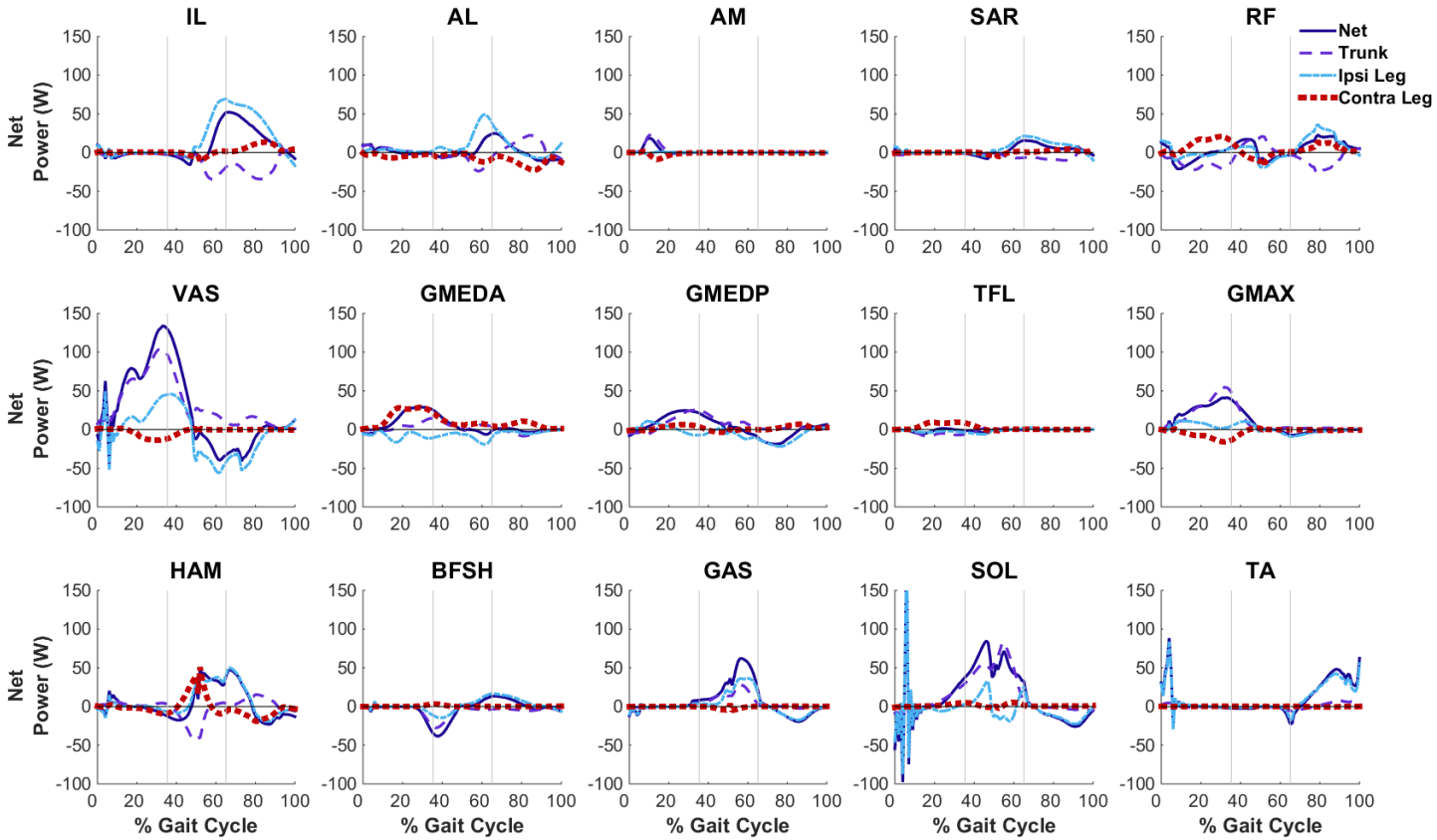

Figure 2.9: Net musculotendon mechanical power output from the ipsilateral leg muscles across the ipsilateral gait cycle and distributed to the trunk, ipsilateral (Ipsi) leg and contralateral (Contra) leg. Positive (negative) net values indicate power generated (absorbed) by the musculotendon actuator. Positive (negative) values for the leg or trunk indicate that power is being generated to (absorbed from) the leg or trunk. The gray lines divide the gait cycle into three regions: 1) weight acceptance through pull-up, 2) forward continuance through push-up, and 3) swing (foot clearance through foot placement). For muscle group abbreviations, please see Table 2.1.

DISCUSSION

Stair ascent and descent are common activities of daily living often required to maintain independence in both the home and community. Compared to stair descent, stair ascent is a more strenuous activity (Protopapadaki et al., 2007) requiring greater muscle activation (Bae et al., 2009; Lyons et al., 1983; McFadyen and Winter, 1988), net joint work (DeVita et al., 2007) and metabolic energy (Teh and Aziz, 2002). As a result of these task demands, individuals with various lower-limb impairments (e.g., Gao et al., 2012; Mandeville et al., 2007; Schmalz et al., 2007) often utilize compensatory mechanisms to ascend stairs. In addition, older or elderly individuals often develop alternate methods for stair ascent to compensate for functional deficits that arise due to aging (e.g., Reeves et al., 2009). While these compensatory mechanisms have been thoroughly investigated at the joint level, design of targeted rehabilitation techniques, interventions and devices are hindered by a limited understanding of the contributions of individual muscles. Understanding the contributions of individual muscles to unimpaired stair ascent builds a critical foundation for understanding the resulting compensatory mechanisms in impaired individuals and developing techniques to restore mobility. Therefore, the goal of this study was to understand how muscles work in synergy to perform stair ascent by developing a muscle-actuated forward dynamics simulation of unimpaired stair ascent and quantifying each muscle's contribution to vertical propulsion, anteroposterior propulsion, mediolateral control and leg swing.

The muscle excitations resulting from the simulation are generally in agreement with those measured experimentally (Appendix A: Figure A.4 - Bovi et al., 2011; Joseph and Watson, 1967; McFadyen and Winter, 1988; Moffet et al., 1993). However, while the net plantarflexor and dorsiflexor power trajectories of the current study are in agreement with the findings of Ghafari et al. (2009), the more proximal muscle groups exhibited

different net power trajectories. Their model was restricted to the sagittal plane and as a result muscles were not required to modulate power in order to regulate mediolateral motion. This likely resulted in over- or under-estimation of the net power, and the power curves identified in the present study are likely more indicative of the power generated, absorbed and transferred by the individual muscles.

In general, several different ipsilateral leg muscle groups contributed critically to stair ascent, generating forces which, through the redistribution of power between body segments (e.g., Zajac et al., 2002), propelled the body vertically and anteroposteriorly, controlled the mediolateral motion of the body COM and accomplished leg swing.

Vertical propulsion

Throughout stance, vertical propulsion was primarily generated by the knee extensors (VAS) and the plantarflexors (SOL, GAS) with additional contributions from the hip extensors (GMAX) and hip abductors (GMEDP, GMEDA). The combined contribution to vertical propulsion from the plantarflexors was largely equal to the contribution from VAS while both were approximately five times larger than the contributions from GMAX or the hip abductors (GMEDP, GMEDA). This indicates the importance of strengthening both the knee extensors and plantarflexors to improve vertical propulsion in individuals who have difficulty ascending stairs. The primary role of the leg extensors in generating vertical propulsion is consistent with a previously posed hypothesis based on EMG timings that the ipsilateral leg extensors likely provide vertical propulsion during pull-up when the majority of vertical progression occurs (Joseph and Watson, 1967; McFadyen and Winter, 1988). These results are also consistent with those of Wilken et al. (2011) who identified a correlation between peak

knee and ankle joint power and vertical acceleration during the first and second halves of stance, respectively. In addition, these findings are supported by Novak et al. (2011) who identified the plantarflexors and knee extensors as the primary contributors to the support moment with additional contributions from the hip. Finally, these results are consistent with the previous study by Lin et al. (2015) which identified the contributions of five muscle groups (gluteus maximus, gluteus medius, vasti, soleus and gastrocnemius) to vertical propulsion in stair ascent and found similar contributions.

Several of the primary contributors to vertical propulsion identified in this study are also contributors to body support in level walking. In level walking, the vasti, gluteus maximus and gluteus medius are the primary contributors to body support during the first half of stance while the plantarflexors are the primary contributors during the second half of stance (Liu et al., 2006; Neptune et al., 2001; Neptune et al., 2004) with additional contributions provided by gravity during both halves of the gait cycle (Anderson and Pandy, 2003; Neptune et al., 2004). In the first half of stance, the primary difference between body support in level walking and vertical propulsion in stair ascent is the importance of the uniarticular plantarflexors (SOL) in stair ascent. This difference may be due to several factors including the elevated position of the leading foot, altered joint kinematics and increased demands of propelling the COM vertically in stair ascent compared to supporting the body in level walking. The increased importance of SOL is consistent with previous studies that found increased positive ankle power (Nadeau et al., 2003) and work (Bovi et al., 2011) and an increased ankle plantarflexion moment in early stance (Lin et al., 2005; Nadeau et al., 2003) during stair ascent compared to level walking. In the second half of stance, HAM was found to oppose vertical propulsion in stair ascent while significantly contributing to forward propulsion. While this is not the case in level walking (Liu et al., 2006; Neptune et al., 2004), the hamstrings do have the

potential to reduce body support while accelerating the body forward during the second half of stance in level walking (Liu et al., 2006).

Anteroposterior propulsion

During stance, the hip abductors (GMEDP, TFL), hip extensors (GMAX, HAM), knee extensors (RF, VAS), plantarflexors (SOL, GAS) and dorsiflexors (TA) worked synergistically to control the distribution of AP power to the legs and trunk to achieve anteroposterior propulsion. Specifically, the hip extensors (GMAX, HAM) were the most critical to forward propulsion which highlights the importance of strengthening the hip extensors to improve forward propulsion during stair ascent in impaired individuals. Lin et al. (2015) noted that in the first half of stance, gluteus maximus and gluteus medius contributed to forward propulsion while soleus and gastrocnemius contributed to braking, consistent with the results of the current study. However, contrary to the results of Lin et al. (2015), the present study found that the vasti contributed to forward propulsion instead of braking during the first half of stance. During the second half of stance, the contributions from the five muscle groups investigated by Lin et al. (2015) were consistent with the results of the current study. It is possible that body-segment kinematic differences between studies in the first half of stance may have led to the observed differences in vasti function during early stance.

Similar to level walking, forward progression occurs throughout stair ascent (Zachazewski et al., 1993). However, the COM must traverse a shorter distance and the COM AP translation is often coupled with vertical movement leading to differences in muscle function between stair ascent and level walking. In the first half of stance during level walking, the hamstrings contribute to forward propulsion (Neptune et al., 2004),

which opposes the braking generated by the vasti (Liu et al., 2006; Neptune et al., 2004) and plantarflexors (Liu et al., 2006; Neptune et al., 2001; Neptune et al., 2004). While the plantarflexors remained important contributors to braking in stair ascent, RF and TFL replaced the vasti as primary contributors to braking and GMAX, TA, VAS, GMEDA and GMEDP contributed to forward propulsion instead of the hamstrings. In the second half of stance during level walking, the plantarflexors (Liu et al., 2006; Neptune et al., 2001) along with gluteus medius (Liu et al., 2006) contribute to forward propulsion and the knee extensors contribute to braking (Neptune et al., 2004). In stair ascent, HAM became the primary contributor to forward propulsion while the knee extensors (RF, VAS) remained the primary contributors to braking. These results are consistent with previous work suggesting that during the second half of stance in stair ascent, the plantarflexors are responsible for elevation of the body (vertical propulsion) but are not the main source of AP progression (McFadyen and Winter, 1988).

Mediolateral control

To achieve mediolateral control during the first half of stance when the COM moves first laterally over the ipsilateral leg and then medially (Zachazewski et al., 1993), the knee extensors (VAS) were the primary contributors to lateral control while the hip abductors (GMEDA and GMEDP) were the primary contributors to medial control. During the second half of stance, when the COM moves first laterally onto the contralateral limb and then medially again (Zachazewski et al., 1993), the hip extensors (HAM) and hip adductors (AL) were the primary contributors to lateral control while the hip abductors (GMEDP, GMEDA) and knee extensors (RF) were the primary contributors to medial control. This highlights the importance of strengthening these

muscle groups in individuals who exhibit impaired mediolateral control during stair ascent. These results are consistent with the previous study by Lin et al. (2015) which found that the vasti contributed to lateral control in the first half of stance and gluteus medius contributed to medial control throughout stance. In addition, our results are consistent with the previously observed function of the hip abductors to pull or balance the body over the limb (Joseph and Watson, 1967; McFadyen and Winter, 1988) and with the notion that abductor moments are important in maintaining the body's COM within the base of support while also countering the destabilizing forces associated with the trunk and mass of the swing leg (MacKinnon and Winter, 1993).

Mediolateral control in stair ascent was found to be very similar to level walking. In level walking, the vasti, hip adductors (Allen and Neptune, 2012; Pandy et al., 2010), and hamstrings (Allen and Neptune, 2012) contribute to lateral control, all of which also contributed to lateral control in stair ascent. Previously, gluteus medius (Allen and Neptune, 2012; Pandy et al., 2010) and gluteus maximus (Allen and Neptune, 2012) were identified as important contributors to medial control in level walking, and in the present study we found that the hip abductors (GMEDA and GMEDP) were the primary contributors to medial control during stair ascent. In both level walking and stair ascent, gravity contributed to lateral control in the first half of stance and medial control in the second half of stance (Pandy et al., 2010). The similarities in these contributions reflect the similarities in the task of mediolateral control between level walking and stair ascent, which are both straight-line activities where progression is achieved by cyclically alternating between limbs.

Leg swing

Throughout leg swing, antagonistic muscles spanning the hip, knee and ankle (e.g. TA and SOL; HAM and VAS) generated or absorbed power from the ipsilateral leg but also functioned synergistically to modulate the transfer of power between the trunk, ipsilateral leg and contralateral leg to achieve controlled and stable leg swing and appropriate foot placement during stair ascent. Antagonistic muscles were recruited to ensure that necessary power was delivered to the leg segments while also ensuring the leg avoided contact with the intermediate step through increased limb flexion (Andriacchi et al., 1980; Joseph and Watson, 1967; McFadyen and Winter, 1988; Nadeau et al., 2003) and hip abduction (Joseph and Watson, 1967; Nadeau et al., 2003) and was placed correctly on the subsequent step. In addition, compared to the other biomechanical subtasks, leg swing required increased contributions from contralateral leg muscles, likely due to the contralateral limb's role in moving the entire swing leg upward and forward through motion of the pelvis (McFadyen and Winter, 1988).

Leg swing is a similar task in both stair ascent and level walking, with the primary difference being the degree to which the swing leg is flexed (Nadeau et al., 2003). As a result, similar muscles contribute to leg swing in level walking and stair ascent. Similar to level walking (Neptune et al., 2004), GAS and IL played an important role in leg swing initiation during stair ascent. However, while the rectus femoris is primarily responsible for opposing leg swing initiation in level walking (Neptune et al., 2004), alternative knee extensors (VAS) were primarily responsible in stair ascent, although RF still opposed swing initiation. During early swing in level walking, iliacus and biceps femoris short head accelerate the leg forward (Neptune et al., 2004). In stair ascent, IL remained the primary contributor while HAM arose as an important contributor to leg acceleration in place of biceps femoris short head. In late swing, while HAM decelerated the leg in

preparation for ground contact, consistent with its function in level walking (Neptune et al., 2004), the plantarflexors also became important contributors to leg braking during stair ascent.

Study limitations

A principal strength of musculoskeletal modeling and simulation techniques is that they can provide valuable insight into quantities that cannot be measured experimentally. However, one resulting limitation is that simulation results cannot be directly validated, and therefore indirect measures of model validation must be used. In this study two indirect measures were used. First, the optimization algorithm minimized differences between simulated and experimental joint kinematics and GRFs in addition to minimizing muscle stress. By requiring the simulation to closely replicate experimental data while minimizing muscle co-contraction, a physiologically relevant and biomechanically consistent simulation was produced. Second, muscle excitation timings were compared to experimental timings available in the literature (Bovi et al., 2011; Joseph and Watson, 1967; McFadyen and Winter, 1988; Moffet et al., 1993) to assure that muscles were producing force at the appropriate points in the gait cycle. Although differences are evident (Appendix A: Figure A.4), these differences are largely similar to the variability seen between the experimental studies.

A second potential limitation of musculoskeletal modeling is that some assumptions for musculoskeletal parameters, including segment mass and inertial properties, musculoskeletal geometry and musculotendon properties, are required. However, the optimization algorithm can compensate for imprecise model parameters by adjusting the magnitude of the muscle excitations to produce the muscle forces necessary

to track the experimentally-measured biomechanics. Therefore, it is likely that the muscle forces, and resulting contributions to the subtasks of stair ascent, are minimally affected by these modeling assumptions.

CONCLUSIONS

The overall goal of this study was to use a musculoskeletal modeling and simulation framework to elucidate the contributions of individual muscles and the mechanisms by which they work in synergy to accomplish the subtasks of unimpaired stair ascent, including vertical propulsion, anteroposterior propulsion, mediolateral control and leg swing. The knee extensors (VAS) and plantarflexors were the primary contributors to vertical propulsion during the first and second halves of stance, respectively, while the hip extensors (GMAX – first half of stance, HAM – second half of stance) were the primary contributors to forward propulsion throughout stance. The hip abductors (GMEDA, GMEDP) were the primary contributors to medial control throughout stance while the knee extensors (VAS) were the primary contributors to lateral control during the first half of stance (when they are also contributing to vertical propulsion) and the hip extensors (HAM) were the primary contributors to lateral control during the second half of stance (when they are also contributing to forward propulsion). Throughout swing, antagonistic muscles spanning the hip, knee and ankle joints distributed power throughout the body to achieve controlled and stable leg swing. By understanding the function and coordination of these muscle groups, targeted interventions and rehabilitation programs can be designed to address patient-specific deficits in stair ascent.

Chapter 3: Muscle Function and Coordination of Amputee Stair Ascent

INTRODUCTION

Individuals with unilateral transtibial amputations utilize compensatory mechanisms to restore mobility. The functional loss of the uniarticular and biarticular plantarflexors, which are critical contributors to body support, forward propulsion, leg swing and mediolateral balance (Allen and Neptune, 2012; Liu et al., 2006; Neptune et al., 2001; Pandy et al., 2010), must be compensated for by either the prosthesis or the remaining muscles of the residual and intact legs. In level walking, this loss and subsequent compensations often result in increased energy cost (Genin et al., 2008; Houdijk et al., 2009), altered and asymmetric kinematics and kinetics (for review, see Prinsen et al., 2011), and diminished dynamic balance control (Silverman and Neptune, 2011), suggesting that the remaining muscles and current prosthetic devices are unable to fully compensate for the loss of the plantarflexors.

Stair ascent is a more challenging mobility task than level walking, which requires the center-of-mass (COM) to be simultaneously propelled horizontally and vertically. This increased need to elevate the COM is accomplished largely by extending the leg during stance after weight acceptance (Figure 3.1). In non-amputees, extension of the leg during stair ascent is accomplished by contributions from the knee extensors (DeVita et al., 2007; Nadeau et al., 2003; Novak and Brouwer, 2011; Wilken et al., 2011) and ankle plantarflexors (DeVita et al., 2007; Novak and Brouwer, 2011; Wilken et al., 2011). However, the loss of the plantarflexors coupled with the increased task demands of stair ascent requires amputees to develop additional compensatory mechanisms compared to level walking, which often result in increased lower-limb muscle activity

(Powers et al., 1997; Schmalz et al., 2007) and significant asymmetries between the residual and intact legs (Alimusaj et al., 2009; Powers et al., 1997; Schmalz et al., 2007; Yack et al., 1999). In the residual leg, amputees often utilize a hip strategy to ascend stairs. In addition, compensations are necessary in the intact leg, particularly at the ankle (Alimusaj et al., 2009; Sinitski et al., 2012; Yack et al., 1999) and also at the knee and hip (Alimusaj et al., 2009; Schmalz et al., 2007; Yack et al., 1999).

Several studies have focused on improving the design of prostheses in order to minimize these compensations and reduce limb asymmetries during stair ascent. These studies have assessed the effects of a variety of prosthesis designs, including solid ankle cushion heel (Agrawal et al., 2013b; Torburn et al., 1994), energy storage and return (Agrawal et al., 2013b; Aldridge et al., 2012; Torburn et al., 1994) and powered (Agrawal et al., 2013b; Aldridge et al., 2012; Alimusaj et al., 2009) prostheses on amputee stair ascent. However, while these studies have noted normalization of some kinematic and kinetic parameters, inter-limb asymmetries often still persist (Aldridge et al., 2012; Alimusaj et al., 2009). One challenge associated with improving prosthesis designs is our current limited understanding of how the prosthesis as well as the remaining musculature contribute to the subtasks of stair ascent. Understanding these contributions would help guide the development of improved prostheses and muscle-targeted rehabilitation programs for stair ascent.

One approach to determining the underlying contributions from individual muscles and the prosthesis is through muscle-actuated forward dynamics simulations. Such simulations have been used previously to elucidate the contributions of the prosthesis and individual muscles to the altered gait patterns observed in amputee level walking (Silverman and Neptune, 2012) and the contributions that would be required for amputees to emulate unimpaired walking (Zmitrewicz et al., 2007). These studies found

that the prosthesis was able to replicate the functions of the uniarticular soleus by providing a similar amount of body support (Silverman and Neptune, 2012; Zmitrewicz et al., 2007), but was unable to generate the full forward propulsion typically provided by the plantarflexors (Zmitrewicz et al., 2007) and the leg swing initiation typically provided by the biarticular gastrocnemius (Silverman and Neptune, 2012; Zmitrewicz et al., 2007). In addition, these studies found significant muscle compensations in the residual and intact legs compared to unimpaired level walking (Silverman and Neptune, 2012; Zmitrewicz et al., 2007). Muscle-actuated forward dynamics simulations have also been used to investigate unimpaired stair ascent and have found the plantarflexors, among other muscles, to be important contributors to the biomechanical subtasks of stair ascent (e.g., Chapter 2). Therefore, compared to unimpaired subjects, amputees likely require altered contributions from the remaining muscles in addition to contributions from the prosthesis in order to achieve stair ascent.

While these studies have identified the contributions from individual muscles to amputee level walking and unimpaired stair ascent in addition to the contributions from the prosthesis to amputee level walking, no study has investigated these contributions in amputee stair ascent. The purpose of this study was to develop a three-dimensional muscle-actuated forward dynamics simulation of unilateral transtibial amputee stair ascent to identify the contributions of individual muscles and the prosthesis to the biomechanical subtasks of stair ascent including vertical propulsion, anteroposterior propulsion, mediolateral control and leg swing. Identifying the functional roles of both the prosthesis and the individual muscles during amputee stair ascent will help elucidate the compensatory mechanisms used by unilateral transtibial amputees and could help guide the design and development of improved prostheses and targeted rehabilitation programs aimed at enhancing an amputee's ability to ascend stairs.

METHODS

A three-dimensional muscle-actuated forward dynamics simulation was developed for amputee stair ascent by modeling the musculoskeletal system, prosthesis, foot-ground contact and muscle force generation and using a dynamic optimization algorithm to identify muscle excitation patterns. The optimized muscle excitation patterns minimized the differences between the simulated and group-averaged experimental joint kinematics and ground reaction forces (GRFs) for 10 subjects with unilateral transtibial amputations. The contributions of individual muscles and the prosthesis to the subtasks of stair ascent were then identified using GRF decomposition and segment power analyses. These steps are described in greater detail below.

Musculoskeletal model

A previously developed three-dimensional unimpaired bipedal musculoskeletal model (Chapter 2) was modified to represent a unilateral transtibial amputee. The model was developed using SIMM/Dynamics Pipeline (MusculoGraphics, Inc., Santa Rosa, CA) with previously defined musculoskeletal geometry (Delp et al., 1990) and consisted of 14 rigid body segments representing the head-arms-trunk (HAT), pelvis and bilaterally the thigh, shank, patella, talus, calcaneus and toes. The segments were articulated with a total of 23 degrees-of-freedom (DOF), including a 6 DOF (3 translations, 3 rotations) joint between the pelvis and ground, 3 DOF spherical joints between the trunk and pelvis and at each hip, and 1 DOF revolute joints at each knee, ankle, subtalar and metatarsal joint. To model the altered mass and inertia of the prosthesis, the mass of the residual shank was reduced by 50% compared to the intact shank and the residual shank COM was shifted proximally to be 25% of the knee-to-ankle distance below the knee (Silverman and Neptune, 2012). In addition, to represent a unilateral transtibial amputee,

the muscles spanning the ankle joint (i.e., medial gastrocnemius, lateral gastrocnemius, soleus, tibialis anterior, tibialis posterior, extensor digitorum longus and flexor digitorum longus) were removed from the residual leg. The model was driven by the remaining 69 muscles (38 on the intact leg and 31 on the residual leg) and the prosthesis.

To model the prosthesis, the average experimental amputee ankle moment data across trials was fit with a second-order torsional spring with damping using the following regression model (Silverman and Neptune, 2012):

$$\tau = C_0 + C_1\theta + C_2\dot{\theta} + C_3\theta^2 + C_4\theta\dot{\theta} \qquad (3.1)$$

where τ is the torque applied by the prosthesis, C_i represents the coefficients (i equal to 0 through 4) determined by fitting the experimental data with the model, θ is the ankle angle and $\dot{\theta}$ is the ankle angular velocity. The prosthesis torque determined in Equation 3.1 was then applied as a passive torque to the ankle joint. In addition, passive torques representing the forces generated by passive tissues and joint structures were applied at each joint (Davy and Audu, 1987). To model foot-ground contact, 31 viscoelastic elements with Coulomb friction were attached to each foot and evenly distributed across the prosthetic foot as well as the intact calcaneus and toes (Neptune et al., 2000b). The system equations of motion were generated using SD/FAST (PTC, Needham, MA).

Muscle excitations at time *t* (*e(t),* Equation 3.2) for the 69 musculotendon actuators were represented using bimodal excitation patterns:

$$e(t) = \sum_{i=1}^{2} \begin{cases} \frac{A_i}{2}\left(1 - \cos\left(\frac{2\pi(t-onset_i)}{offset_i - onset_i}\right)\right) & onset_i \le t \le offset_i \\ 0 & t < onset_i \;||\; t > offset_i \end{cases} \qquad (3.2)$$

where the *onset*, *offset* and amplitude (A) of each mode (i) are the optimization parameters for each muscle. Muscle activation and deactivation dynamics were modeled by a non-linear first-order differential equation (Raasch et al., 1997) with previously derived activation and deactivation time constants (Winters and Stark, 1988). Muscle contraction dynamics were governed by Hill-type muscle properties (Zajac, 1989).

Dynamic optimization

A muscle-actuated forward dynamics simulation of unilateral transtibial amputee stair ascent was generated over 120% of the gait cycle (from intact foot-strike to the second residual toe-off) using a simulated annealing optimization algorithm (Goffe et al., 1994) to identify the optimal parameters for each muscle (timing and amplitude) that minimized the objective function. The previously defined objective function (Chapter 2) was comprised of two portions designed to: 1) achieve optimal tracking by minimizing the differences between simulated and experimental joint kinematics and GRFs and 2) eliminate unnecessary muscle co-activation by minimizing total muscle stress. To assess the overall quality of the simulation, the root-mean-square (RMS) errors of the simulated compared to experimental kinematics and GRFs were analyzed and the timings of simulated muscle excitations were compared with EMG timings available in the literature (Powers et al., 1997; Schmalz et al., 2007).

Simulation analyses

To identify the contributions of individual muscles and the prosthesis to the biomechanical subtasks of stair ascent, GRF decomposition and segment power analyses (Neptune et al., 2008; Neptune et al., 2004) were performed. The contribution of each

muscle and the prosthesis to vertical propulsion, anteroposterior propulsion and mediolateral control during the first (weight acceptance through pull-up, Figure 3.1) and second (forward continuance through push-up, Figure 3.1) halves of stance was quantified by its contribution to the vertical, anteroposterior (AP) and mediolateral (ML) GRF, respectively, during each region. The contribution of each muscle and the prosthesis to leg swing was quantified by the power delivered to the leg during swing initiation (push-up, Figure 3.1), early swing (early swing – foot clearance, Figure 3.1) and late swing (late swing – foot placement, Figure 3.1). In addition, throughout stance the mechanical power generated, absorbed and transferred by each muscle and the prosthesis to the trunk (HAT), residual leg and intact leg was examined in the vertical, AP and ML directions. Positive (negative) contributions to the AP and ML GRFs indicated contributions to forward propulsion (braking) and lateral (medial) control, respectively, while positive (negative) power indicated acceleration (deceleration) of the segment in the direction of motion. For analysis, muscles with similar biomechanical function and anatomical classification were combined into 15 muscle groups in the intact leg and 12 muscle groups in the residual leg (Table 3.1) by summing the contributions of the muscles within each group. In addition, the contribution of gravity to the biomechanical subtasks of stair ascent was also determined since it has been shown to be important in both unimpaired level walking (Anderson and Pandy, 2003; Lin et al., 2011) and stair ascent (Chapter 2).

Table 3.1: Muscles included in the musculoskeletal model and their corresponding analysis groups in both the intact and residual legs. The muscles labeled as "REMOVED" have been removed from the residual leg.

Muscles	Analysis Groups	
	Intact Leg	Residual Leg
Iliacus Psoas	IL	IL
Adductor Longus Adductor Brevis Pectineus Quadratus Femoris	AL	AL
Superior Adductor Magnus Middle Adductor Magnus Inferior Adductor Magnus	AM	AM
Sartorius	SAR	SAR
Rectus Femoris	RF	RF
Vastus Medialis Vastus Lateralis Vastus Intermedius	VAS	VAS
Anterior Gluteus Medius Middle Gluteus Medius Anterior Gluteus Minimus Middle Gluteus Minimus	GMEDA	GMEDA
Posterior Gluteus Medius Posterior Gluteus Minimus Piriformis Gemellus	GMEDP	GMEDP
Tensor Fasciae Latae	TFL	TFL
Superior Gluteus Maximus Middle Gluteus Maximus Inferior Gluteus Maximus	GMAX	GMAX
Semitendinosus Semimembranosus Gracilis Biceps Femoris Long Head	HAM	HAM
Biceps Femoris Short Head	BFSH	BFSH
Medial Gastrocnemius Lateral Gastrocnemius	GAS	REMOVED
Soleus Tibialis Posterior Flexor Digitorum Longus	SOL	
Tibialis Anterior Extensor Digitorum Longus	TA	

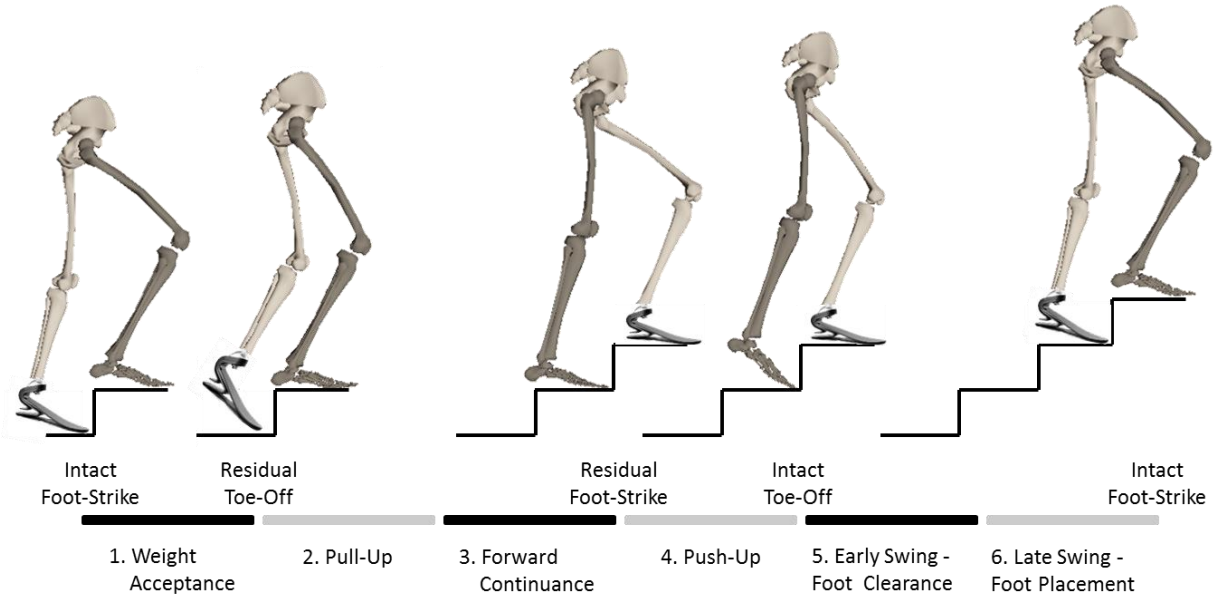

Figure 3.1: The six regions of the intact leg (dark shaded leg) gait cycle: 1) weight acceptance (intact foot-strike to residual toe-off), 2) pull-up and 3) forward continuance (residual toe-off to residual foot-strike divided into two equal regions), 4) push-up (residual foot-strike to intact toe-off), 5) early swing - foot clearance and 6) late swing - foot placement (intact toe-off to intact foot-strike divided into two equal regions).

Experimental data

Ten subjects with traumatic unilateral transtibial amputations (10 male; 29.4 ± 5.7 years; 87.4 ± 13.6 kg; 1.8 ± 0.1 m) and prescribed energy storage and return prostheses participated in this institutionally-approved study, which was conducted in the Military Performance Laboratory at the Center for the Intrepid in Fort Sam Houston, TX. All subjects were capable of walking independently for a minimum of 15 minutes, had been independent walkers for a minimum of 5 months and had no comorbidities on the intact leg. Written informed consent was obtained from each subject before they completed the experimental protocol that included ascending a 16-step instrumented staircase (2

forceplates, 1200 Hz: AMTI, Inc., Watertown, MA) step-over-step at a fixed cadence of 80 steps per minute. Three-dimensional whole-body kinematics (Wilken et al., 2012) were collected using a 26-camera optoelectronic motion capture system (120 Hz, Motion Analysis Corp., Santa Rosa, CA) and a body segment marker set consisting of 57 reflective markers. In addition, 20 anatomical bony landmarks were identified through a digitization process (C-motion, Inc., Germantown, MD).

Following data collection, all biomechanical data were processed in Visual3D (C-motion, Inc., Germantown, MD). For each subject, a 13-segment model was scaled to the subject's body mass and height (Dempster, 1955) using the anatomical bony landmarks to define the joint centers and joint coordinate systems (Grood and Suntay, 1983; Wu and Cavanagh, 1995; Wu et al., 2002). Marker and GRF data were low-pass filtered using a fourth-order Butterworth filter with cut-off frequencies of 6 Hz and 50 Hz, respectively. Joint kinematics were computed using Euler angles with previously defined pelvis, hip, knee and ankle Cardan rotation sequences (Baker, 2001; Grood and Suntay, 1983; Wu et al., 2002). For five complete gait cycles for each leg, GRFs were normalized by subject body weight and both GRFs and three-dimensional joint kinematics were time-normalized to 100% of the gait cycle and exported to MATLAB (MathWorks, Inc., Natick, MA) where they were averaged across gait cycles and subjects for each leg.

RESULTS

Simulation quality

The simulated kinematics and GRFs produced by the optimal set of muscle excitations successfully emulated the experimental data, with most quantities within 2 standard deviations (SDs) of the experimental data, and therefore statistically

indistinguishable from the experimental data (Appendix B: Figures B.1 – B.3). The average RMS error between the simulated and experimental pelvis translations, joint kinematics and GRFs across the gait cycle was 0.034 meters (2 SDs = 0.101 m), 10.74 degrees (2 SDs = 11.31 deg) and 0.129 percent body weight (2 SDs = 0.099 %BW), respectively. In addition, the timing profiles of the optimized muscle excitations were representative of the EMG data available in the literature (Appendix B: Figure B.4, Powers et al., 1997; Schmalz et al., 2007).

Vertical propulsion

The primary contributors to vertical propulsion during the first half of stance were similar in both the residual and intact legs with primary contributions from VAS and additional contributions from GMAX, GMEDA and GMEDP (Figure 3.2), all of which generated vertical power to the trunk and/or one of the legs (Appendix B: Figures B.5 and B.6). In the residual leg, the prosthesis also contributed critically to vertical propulsion (Figure 3.2) by providing power to the trunk and residual leg (Figure 3.3) while HAM and BFSH opposed vertical propulsion (Figure 3.2), absorbing vertical power from the body (Appendix B: Figure B.5). In the second half of stance, the primary contributors to vertical propulsion in the intact leg were the plantarflexors (Figure 3.2), which generated power to the trunk and intact leg (Figure 3.3) while the prosthesis was the primary contributor in the residual leg (Figure 3.2) by absorbing power from the trunk and residual leg while transferring some power to the intact leg (Figure 3.3). At the end of residual leg stance the pelvis was moving downward, so by absorbing power from the trunk the prosthesis decelerated the pelvis' downward motion, contributing to vertical

propulsion. Gravity also provided critical contributions to the vertical GRF throughout stance, particularly in the residual leg during the second half of stance.

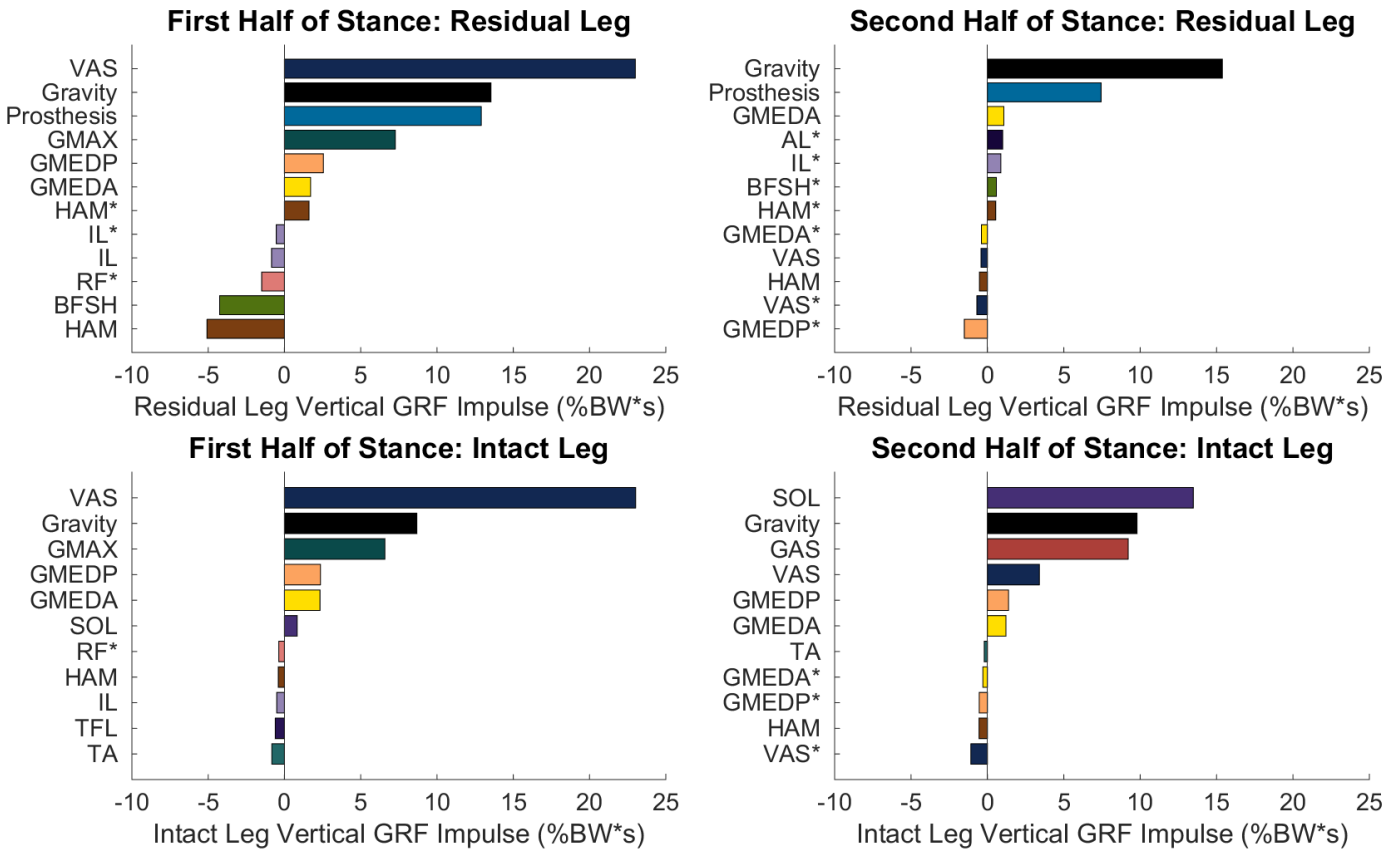

Figure 3.2: Primary positive and negative contributors to vertical propulsion of the body COM (i.e. the vertical ground reaction force (GRF) impulse) during the two halves of residual and intact leg stance: 1) weight acceptance through pull-up, and 2) forward continuance through push-up. Each muscle is depicted using a unique, muscle-specific color to enable comparison across figures. Muscle names without an asterisk (*) are from the leg specified in the plot title while muscle names with an asterisk (*) are from the opposite leg. For muscle group abbreviations, please see Table 3.1.

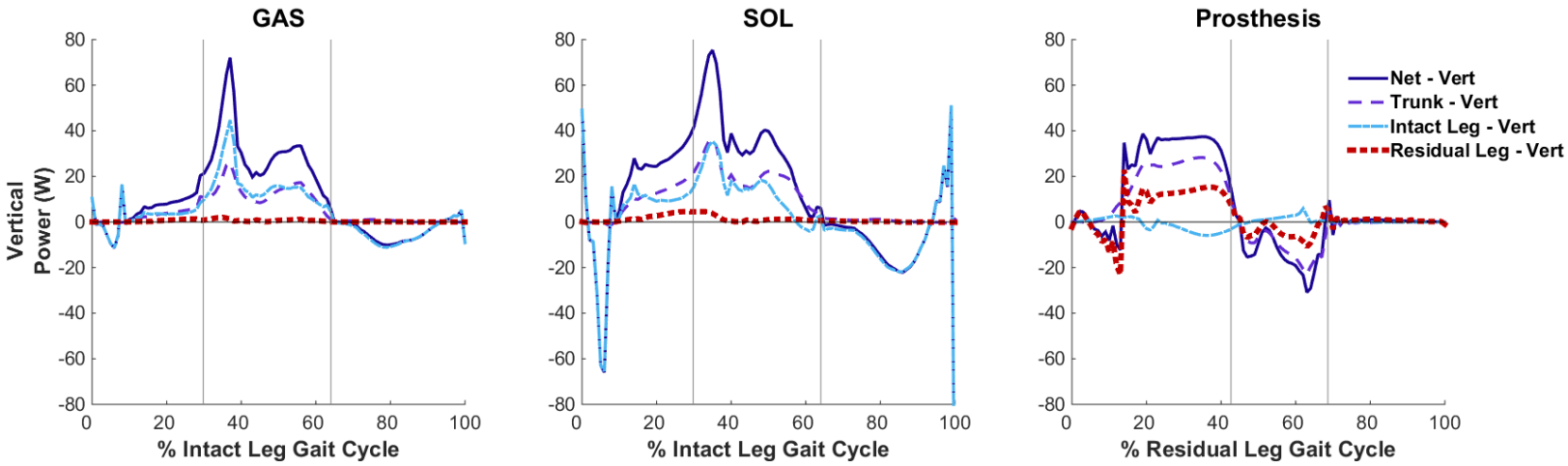

Figure 3.3: Musculotendon mechanical power output from the intact plantarflexors (gastrocnemius: GAS; soleus: SOL) and the prosthesis across the intact and residual leg gait cycles, respectively, and distributed to the trunk, intact leg and residual leg in the vertical direction. Positive (negative) net values indicate power generated (absorbed) by the musculotendon actuator. Positive (negative) values for the leg or trunk indicate that power is being generated to (absorbed from) the leg or trunk. The gray lines divide the gait cycle into three regions: 1) weight acceptance through pull-up, 2) forward continuance through push-up, and 3) swing (foot clearance through foot placement). For muscle group abbreviations, please see Table 3.1.

Anteroposterior propulsion

During the first half of stance, the primary contributors to forward propulsion (positive AP propulsion) were GMAX and HAM in the intact and residual legs, respectively (Figure 3.4) which generated AP power to the legs and transferred some power from the trunk to the legs (Appendix B: Figures B.7 and B.8). GMAX was also a primary contributor in the residual leg while VAS was a primary contributor in the intact leg (Figure 3.4). During this region, the plantarflexors, primarily SOL, contributed to braking (negative AP propulsion) in the intact leg (Figure 3.4), absorbing AP power from the trunk and intact leg (Figure 3.5), while the prosthesis was the primary contributor to braking in the residual leg (Figure 3.4), initially absorbing AP power from the trunk before absorbing power from the intact leg (Figure 3.5). Gravity contributed to forward propulsion in the intact leg and contributed minimally to braking in the residual leg.

During the second half of stance, the primary contributor to forward propulsion in both legs was VAS (Figure 3.4), which provided AP power to the trunk through generation and/or transfer of power from the ipsilateral leg (Appendix B: Figures B.7 and B.8). In addition, HAM was a primary contributor in both legs while GMAX, GMEDP and SOL contributed to forward propulsion in the intact leg (Figure 3.4). Gravity also contributed to forward propulsion in both legs but to a much greater extent in the residual leg. During this region, the prosthesis was the primary contributor to braking in the residual leg (Figure 3.4) by absorbing AP power from the residual leg despite a substantial amount of this power being transferred to the trunk (Figure 3.5). In the intact leg, RF and IL were the primary contributors to braking during the second half of stance (Figure 3.4). However, while RF absorbed power from the intact leg and transferred some of this power to the trunk, due to the low segmental velocities of the residual leg femur

and tibia, IL generated net AP power during this region, absorbing only minimal power from the residual leg (Appendix B: Figure B.8).

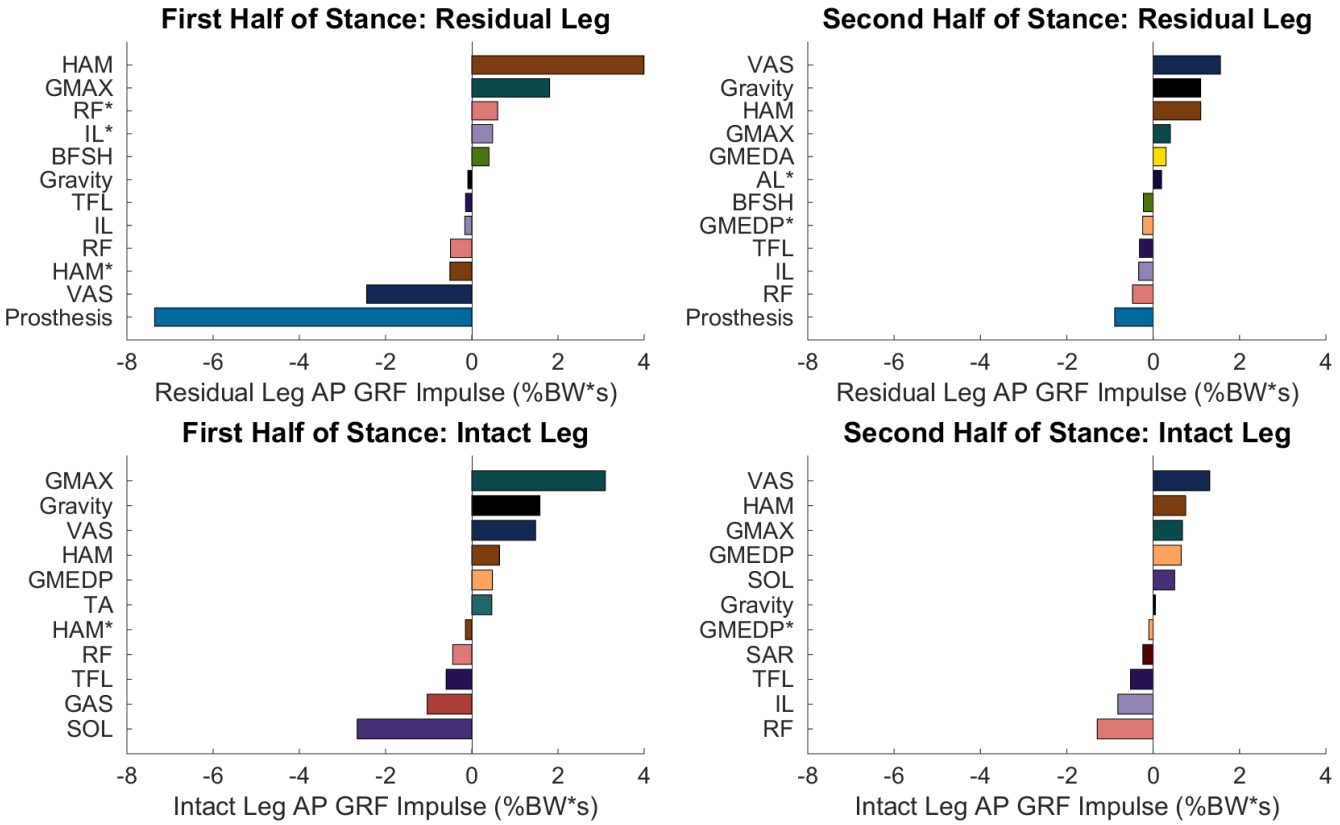

Figure 3.4: Primary positive and negative contributors to anteroposterior propulsion of the body COM (i.e. the anteroposterior (AP) ground reaction force (GRF) impulse) during the two halves of intact and residual leg stance: 1) weight acceptance through pull-up, and 2) forward continuance through push-up. Positive (negative) GRF impulses indicate contributions to forward propulsion (braking) of the COM. Each muscle is depicted using a unique, muscle-specific color to enable comparison across figures. Muscle names without an asterisk (*) are from the leg specified in the plot title while muscle names with an asterisk (*) are from the opposite leg. For muscle group abbreviations, please see Table 3.1.

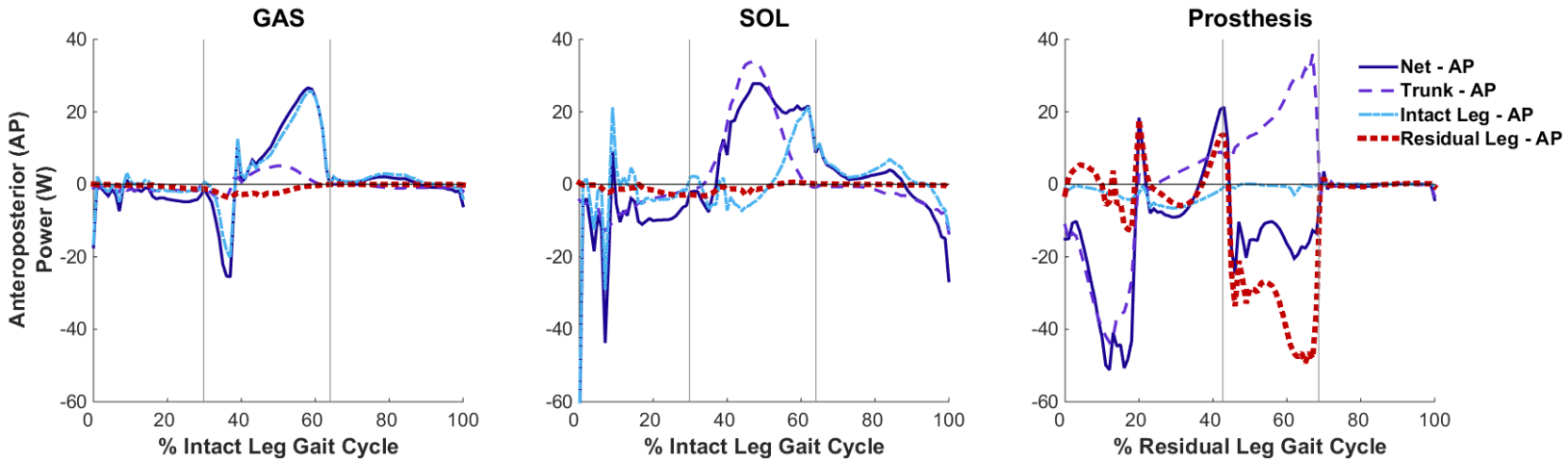

Figure 3.5: Musculotendon mechanical power output from the intact plantarflexors (gastrocnemius: GAS; soleus: SOL) and the prosthesis across the intact and residual leg gait cycles, respectively, and distributed to the trunk, intact leg and residual leg in the anteroposterior (AP) direction. Positive (negative) net values indicate power generated (absorbed) by the musculotendon actuator. Positive (negative) values for the leg or trunk indicate that power is being generated to (absorbed from) the leg or trunk. The gray lines divide the gait cycle into three regions: 1) weight acceptance through pull-up, 2) forward continuance through push-up, and 3) swing (foot clearance through foot placement). For muscle group abbreviations, please see Table 3.1.

Mediolateral control

Throughout stance, GMEDA and GMEDP were the primary contributors to medial control in both the residual and intact limbs, while the prosthesis and HAM were the primary contributors to lateral control in the residual leg and SOL, GAS, AL and AM were the primary contributors in the intact leg (Figure 3.6). RF was also a critical contributor to medial control in the residual leg during the second half of stance while gravity contributed to medial control in both legs throughout stance. Depending on the direction of motion of the trunk, intact leg and residual leg throughout the gait cycle, these muscles contributed to lateral or medial control through a combination of power generation (acceleration of the segment in its direction of motion), absorption (deceleration of the segment in its direction of motion) and/or transfer between the segments (Appendix B: Figures B.9 and B.10). Although the plantarflexors and prosthesis both contributed to lateral control, their power contributions during the first half of stance were generally small and during the second half of stance the plantarflexors absorbed ML power from the intact leg and transferred some of this power to the trunk while the prosthesis provided power directly to the trunk (Figure 3.7), propelling it laterally.

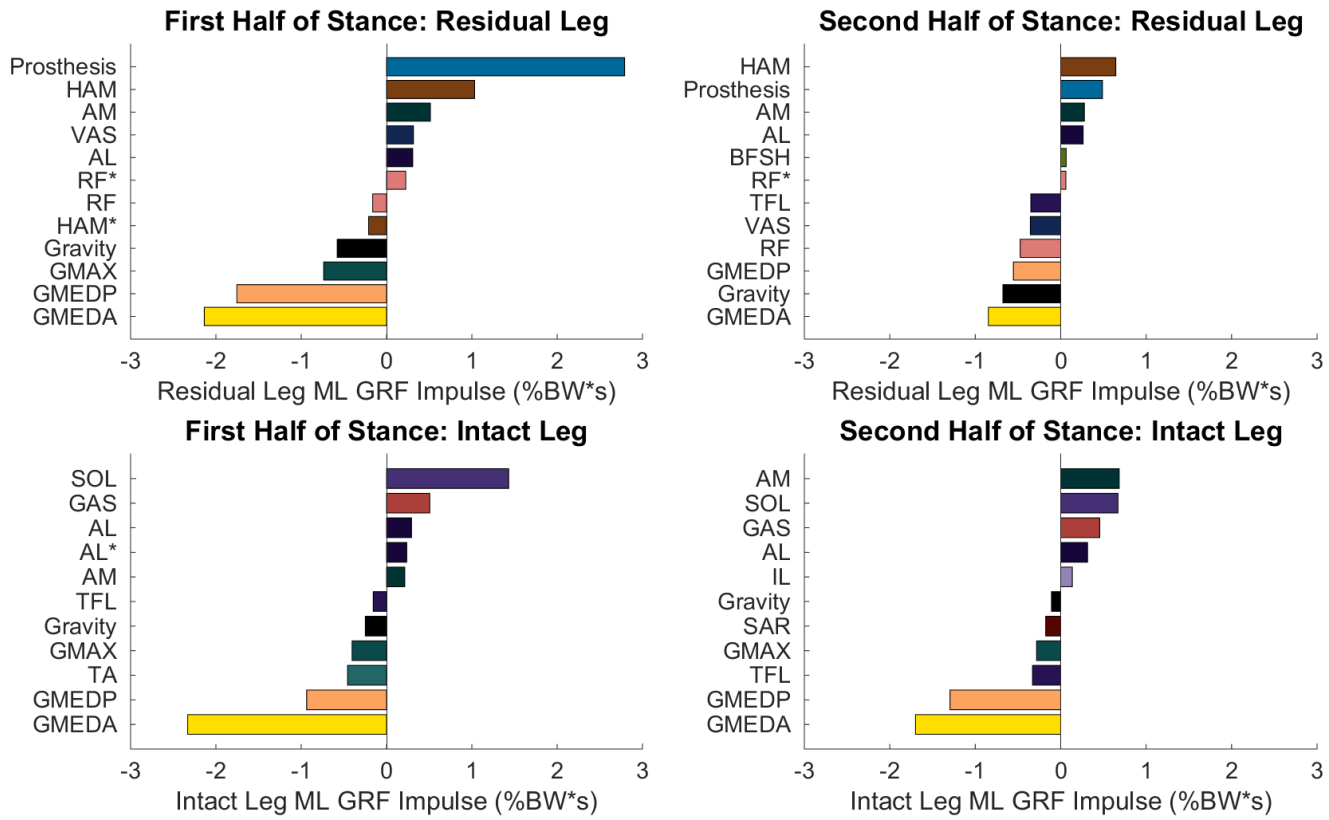

Figure 3.6: Primary positive and negative contributors to mediolateral control of the body COM (i.e. the mediolateral (ML) ground reaction force (GRF) impulse) during the two halves of intact and residual leg stance: 1) weight acceptance through pull-up, and 2) forward continuance through push-up. Positive (negative) GRF impulses indicate contributions to lateral (medial) control of the COM. Each muscle is depicted using a unique, muscle-specific color to enable comparison across figures. Muscle names without an asterisk (*) are from the leg specified in the plot title while muscle names with an asterisk (*) are from the opposite leg. For muscle group abbreviations, please see Table 3.1.

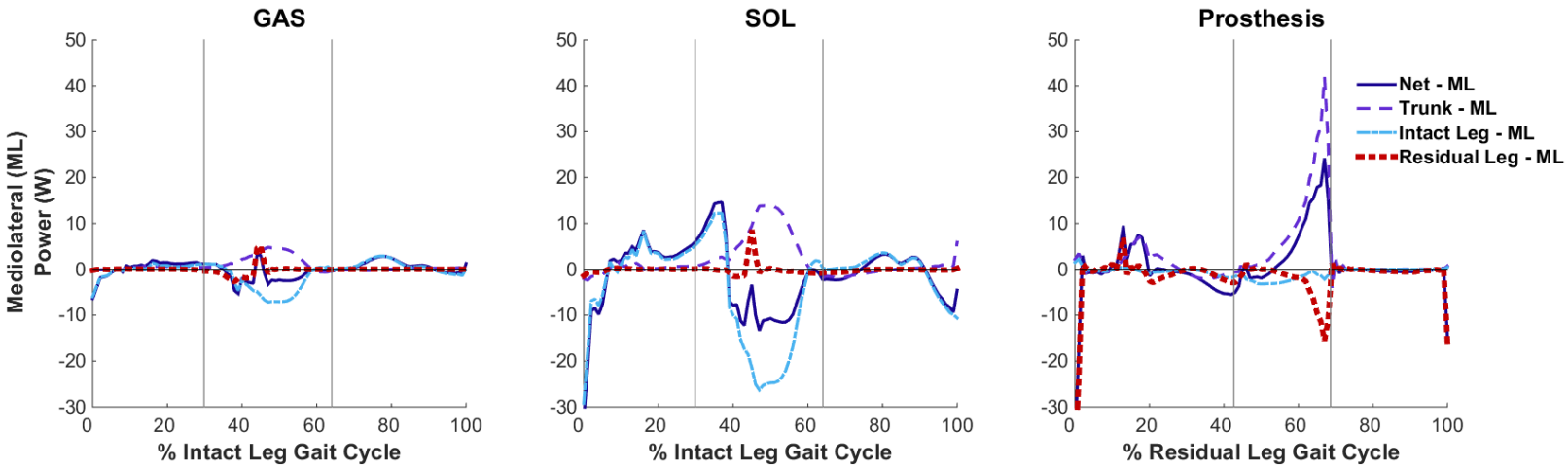

Figure 3.7: Musculotendon mechanical power output from the intact plantarflexors (gastrocnemius: GAS; soleus: SOL) and the prosthesis across the intact and residual leg gait cycles, respectively, and distributed to the trunk, intact leg and residual leg in the mediolateral direction. Positive (negative) net values indicate power generated (absorbed) by the musculotendon actuator. Positive (negative) values for the leg or trunk indicate that power is being generated to (absorbed from) the leg or trunk. The gray lines divide the gait cycle into three regions: 1) weight acceptance through pull-up, 2) forward continuance through push-up, and 3) swing (foot clearance through foot placement). For muscle group abbreviations, please see Table 3.1.

Leg swing

During swing initiation of the residual leg, intact HAM, AM and AL in addition to residual HAM were the primary generators of residual leg power while the prosthesis and VAS were the primary absorbers of power from the residual leg, therefore opposing swing initiation (Figure 3.8). The prosthesis absorbed power from the residual leg and transferred some of this power to the trunk, similar to the role of the intact SOL during this region but not the intact GAS (Figure 3.9). During residual leg swing (early and late), residual IL was the primary generator of power to the residual leg while gravity was a primary absorber of power from the residual leg with additional power absorption from VAS during late swing.

During swing initiation and early swing of the intact leg, intact IL was the primary generator of power to the intact leg with additional power generation from residual GMEDA during both regions, intact GAS, AL and AM during swing initiation and intact RF during early swing (Figure 3.8). During these regions, gravity was the primary absorber of power from the residual leg, decelerating its motion. During late swing, intact GMEDP and TA arose as the primary generators of power to the intact leg while intact AL absorbed power from the leg in preparation for contact with the ground.

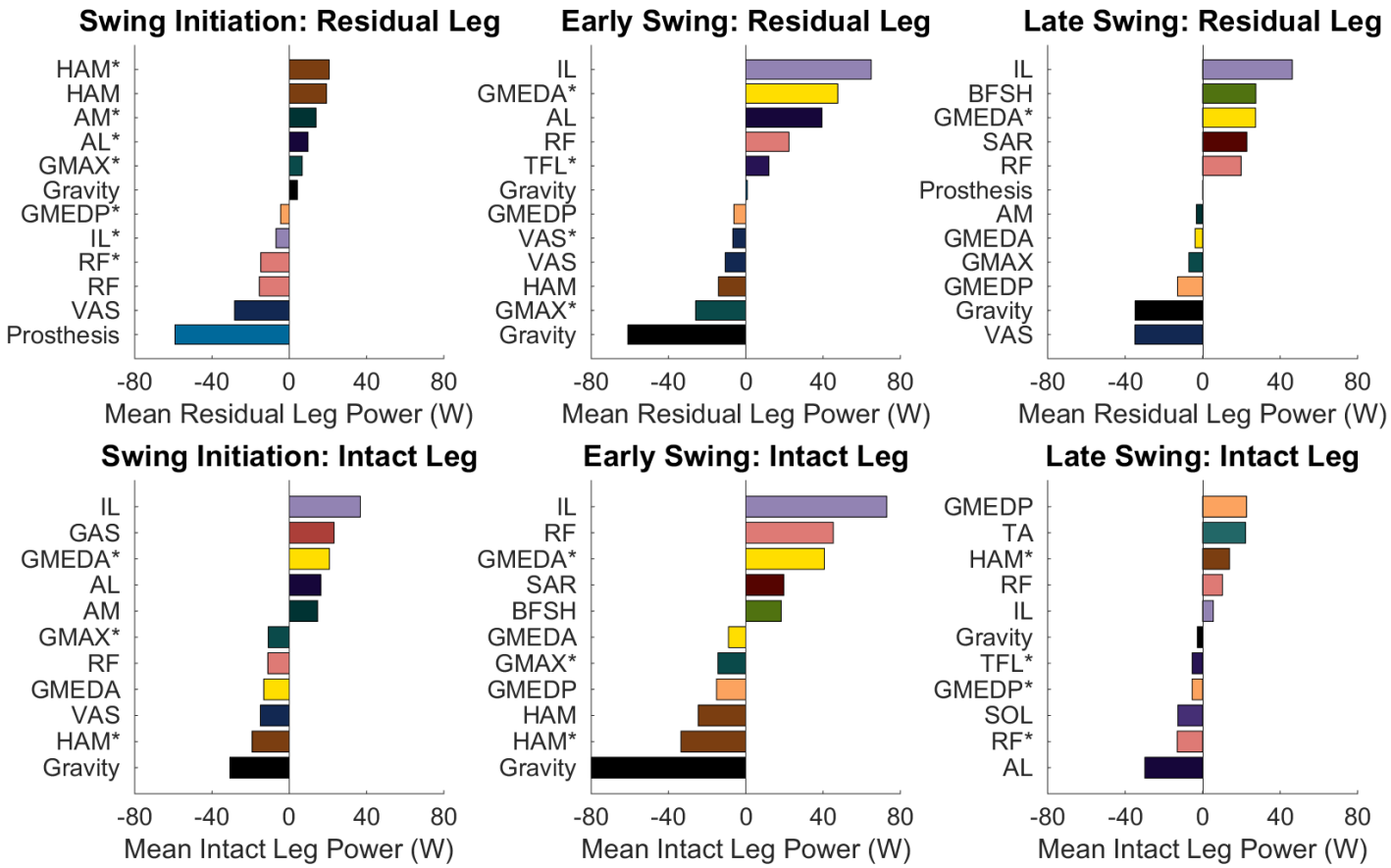

Figure 3.8: Primary contributors to the net mean mechanical power generation (positive) to and absorption (negative) from the intact and residual legs during: 1) swing initiation (push-up), 2) early swing (foot clearance), and 3) late swing (foot placement). Each muscle is depicted using a unique, muscle-specific color to enable comparison across figures. Muscle names without an asterisk (*) are from the leg specified in the plot title while muscle names with an asterisk (*) are from the opposite leg. For muscle group abbreviations, please see Table 3.1.

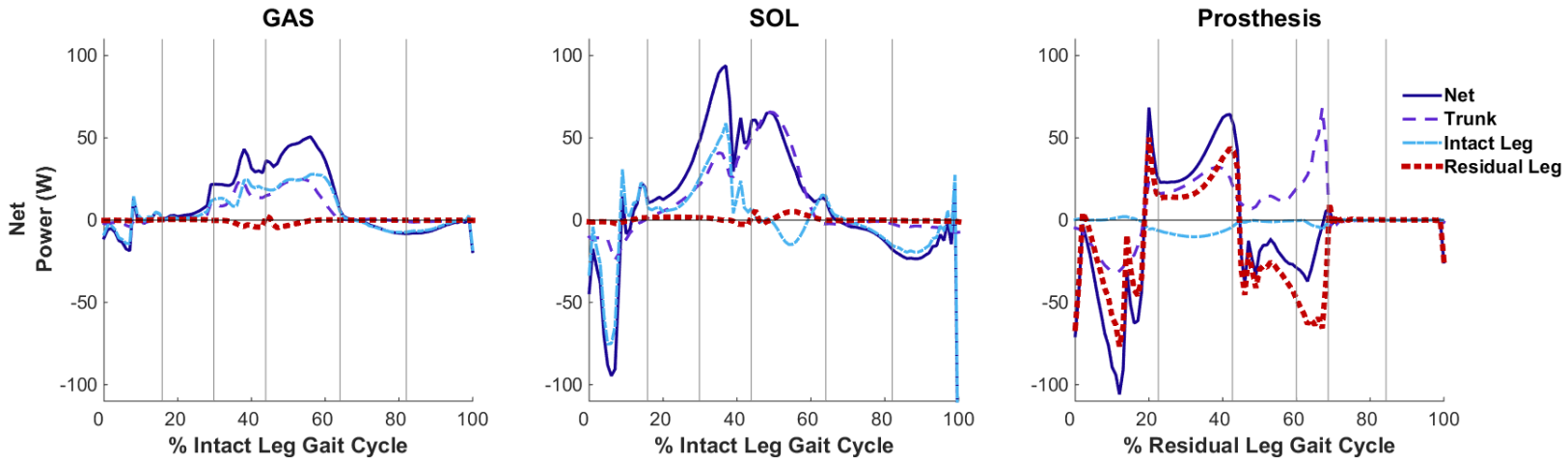

Figure 3.9: Musculotendon mechanical power output from the intact plantarflexors (gastrocnemius: GAS; soleus: SOL) and the prosthesis across the intact and residual leg gait cycles, respectively, and distributed to the trunk, intact leg and residual leg. Positive (negative) net values indicate power generated (absorbed) by the musculotendon actuator. Positive (negative) values for the leg or trunk indicate that power is being generated to (absorbed from) the leg or trunk. The gray lines divide the gait cycle into six regions: 1) weight acceptance, 2) pull-up, 3) forward continuance 4) swing initiation (push-up), 5) early swing (foot clearance) and 6) late swing (foot placement). For muscle group abbreviations, please see Table 3.1.

DISCUSSION

The purpose of this study was to determine how individual muscles and the prosthesis work in synergy during unilateral transtibial amputee stair ascent to accomplish the biomechanical subtasks of vertical propulsion, anteroposterior propulsion, mediolateral control and leg swing. The prosthesis was found to be a critical contributor to all of these subtasks in the residual leg while the plantarflexors, along with other muscles, were critical contributors to these subtasks in the intact leg. However, the prosthesis was unable to replicate all of the contributions of the unimpaired (i.e. non-amputee) plantarflexors (Chapter 2) during stair ascent and resulting muscle compensations were evident, consistent with the experimentally-observed compensations that arise due to limited prosthesis functionality (Powers et al., 1997; Ramstrand and Nilsson, 2009).

The primary contributors to vertical propulsion in both legs were largely consistent with the primary contributors in unimpaired stair ascent (Chapter 2) and amputee level walking (Silverman and Neptune, 2012), with VAS and GMAX, in addition to the prosthesis, contributing in the first half of stance and the plantarflexors or prosthesis contributing in the second half of stance. These results are also consistent with a previous study that identified a correlation between peak knee and ankle joint power and vertical acceleration during the first and second halves of stance in unimpaired stair ascent, respectively (Wilken et al., 2011). In the present study, the prosthesis provided greater vertical propulsion than the unimpaired plantarflexors (Chapter 2) during the first half of stance, which was compensated for by greater negative contributions from HAM and BFSH. Overall, with some minimal changes in muscle contributions, the prosthesis was able to provide vertical propulsion in the absence of the plantarflexors, similar to the role of the prosthesis in amputee level walking (Silverman and Neptune, 2012;

Zmitrewicz et al., 2007). However, it should be noted that while the intact and unimpaired plantarflexors (Chapter 2) both generated power to the trunk and ipsilateral leg throughout stance, the prosthesis provided a different power distribution during the second half of stance, primarily due to the trunk velocity decreasing and becoming negative at the end of residual leg stance.

The primary contributors to anteroposterior propulsion in the intact leg during the first half of stance were similar to the primary contributors in unimpaired stair ascent (Chapter 2), with GMAX providing the primary contribution to forward propulsion and the intact plantarflexors contributing to braking. Similarly, in the residual leg the prosthesis contributed to braking in this region, consistent with its role in amputee level walking (Silverman and Neptune, 2012). However, the prosthesis' contribution to braking was larger than the contribution from the intact or unimpaired (Chapter 2) plantarflexors and the prosthesis absorbed increased AP power from the trunk, similar to its role in amputee level walking (Zmitrewicz et al., 2007). To compensate for the prosthesis, HAM increased its contribution to forward propulsion but the residual leg still contributed to overall braking. As a result, the intact leg had to increase its overall contribution to forward propulsion by decreasing the contributions to braking from the plantarflexors and increasing the contributions to forward propulsion from GMAX compared to unimpaired stair ascent. This is consistent with the previous finding that decreased prosthesis mobility during weight acceptance limited an amputee's ability to advance over the foot which necessitated muscle compensations (Powers et al., 1997; Sinitski et al., 2012). However, compensations in the residual leg for the braking provided by the prosthesis were different in amputee level walking and stair ascent, with HAM increasing its contribution to forward propulsion in stair ascent while VAS and RF reduced their contributions to braking in level walking (Silverman and Neptune, 2012).

During the second half of stance in the intact leg, VAS and the plantarflexors, specifically SOL, arose as important contributors to forward propulsion, largely contrary to their role in unimpaired stair ascent (Chapter 2). However, the importance of the plantarflexors to forward propulsion is consistent with previous studies that found that ankle power generation during the second half of stance was greater in the intact leg compared to the unimpaired leg (Aldridge et al., 2012; Sinitski et al., 2012; Yack et al., 1999), and hypothesized that this additional energy generated by the plantarflexors could help propel the trunk onto the residual leg (Yack et al., 1999). This finding is also consistent with the role of the plantarflexors in amputee level walking (Silverman and Neptune, 2012). In the residual leg, the prosthesis contributed to braking, in contrast to its role in amputee level walking (Silverman and Neptune, 2012; Zmitrewicz et al., 2007) and to the role of the intact plantarflexors. The prosthesis was also unable to replicate the functional role of GAS in unimpaired stair ascent, which contributed to forward propulsion by generating power to the ipsilateral leg (Chapter 2). However, the functional role of the prosthesis was similar to the role of SOL during unimpaired stair ascent, which contributed to braking by transferring power from the ipsilateral leg to the trunk (Chapter 2). This indicates that the prosthesis was able to largely replicate the function of uniarticular SOL, providing AP power to the trunk, but did so at the expense of absorbing AP power from the residual leg and was therefore unable to replicate the function of biarticular GAS, consistent with the functional role of the prosthesis during amputee level walking (Silverman and Neptune, 2012; Zmitrewicz et al., 2007). While the role of the prosthesis was similar to SOL in unimpaired stair ascent, the prosthesis generated increased braking during the second half of stance and, to compensate, the residual VAS became the primary contributor to forward propulsion, contrary to its contribution to braking in unimpaired stair ascent (Chapter 2). In addition, while RF contributed to

braking in both the intact and residual legs, similar to unimpaired stair ascent (Chapter 2), RF decreased its contribution to braking in the residual leg compared to the intact and unimpaired legs to compensate for the increased braking provided by the prosthesis. It should also be noted that during the second half of stance, gravity played a critical role in residual leg forward propulsion. This is consistent with a previous study that found that amputees altered their body position to facilitate advancement of the body's center of gravity over the prosthetic ankle (Powers et al., 1997).

Lateral control throughout stance was generated primarily by the prosthesis and HAM in the residual leg and by the hip adductors (AM and AL) and the plantarflexors in the intact leg. The contributions from the hip adductors and HAM to lateral control are consistent with their contributions in amputee level walking (Silverman and Neptune, 2012) and unimpaired stair ascent (Chapter 2) and the role of the prosthesis is consistent with its role in amputee level walking (Silverman and Neptune, 2012). However, compared to unimpaired stair ascent (Chapter 2) and amputee level walking (Silverman and Neptune, 2012), in amputee stair ascent the contributions from VAS were decreased and the plantarflexors contributed to lateral control instead of medial control. While the intact plantarflexors and prosthesis both contributed to lateral control, during the second half of stance SOL and GAS absorbed ML power from the intact leg, transferring some of that power to the trunk, while the prosthesis generated ML power directly to the trunk. These disparate power distributions may be the reason that the residual leg relied on HAM for lateral control while the intact leg relied on the hip adductors.

Throughout stance, medial control was primarily generated by GMEDA and GMEDP, similar to unimpaired stair ascent (Chapter 2) and amputee level walking (Silverman and Neptune, 2012). However, their contributions increased to compensate for the increased lateral control provided by the intact plantarflexors and the prosthesis.

The increased overall contributions to medial and lateral control in amputee stair ascent compared to unimpaired stair ascent are consistent with the increased step width observed in amputees both previously (Ramstrand and Nilsson, 2009) and in the current study, in which increased hip abduction was observed in both legs compared to the unimpaired leg (Chapter 2). In addition, the altered muscle contributions to mediolateral control in amputee stair ascent compared to amputee level walking may be indicative of the increased instability of the task (Kendell et al., 2010).

The primary contributors to leg swing in both the intact and residual legs were largely different from unimpaired stair ascent (Chapter 2) and amputee level walking (Silverman and Neptune, 2012). However, in the intact leg, IL was the primary contributor to swing initiation and early swing and TA was a critical contributor to late swing, similar to unimpaired stair ascent. In addition, RF opposed swing initiation in both legs, similar to unimpaired stair ascent (Chapter 2) and level walking (Neptune et al., 2004) but contrary to the findings of Powers et al. (1997) who hypothesized that the RF activity during pre-swing acted to advance the leg. In addition, GAS was an important contributor to swing initiation of the intact leg, similar to its role in unimpaired stair ascent (Chapter 2) and amputee level walking (Silverman and Neptune, 2012) and SOL decelerated the leg in late swing in preparation for contact with the ground, similar to its role in unimpaired stair ascent (Chapter 2). During swing initiation, the prosthesis produced a similar power distribution to both the intact and unimpaired (Chapter 2) SOL, transferring power from the ipsilateral leg (residual for the prosthesis and intact for SOL) to the trunk, but was unable to emulate the power distribution produced by the intact or unimpaired GAS, which generated power to both the intact leg and trunk. This suggests that the prosthesis compromised leg swing in order to transfer power to the trunk, similar to the role of the prosthesis in amputee level walking (Silverman and Neptune, 2012;

Zmitrewicz et al., 2007). Consistently, in the residual leg the prosthesis opposed swing initiation, similar to the role of SOL in unimpaired stair ascent (Chapter 2), but to a much greater extent. In response to the prosthesis' increased opposition to swing initiation, the residual leg received increased positive contributions from the intact leg, specifically HAM, AL and AM. In addition, the residual IL and intact GMEDA increased their positive contributions throughout swing, consistent with a previous study that found increased residual leg hip flexion during swing (Aldridge et al., 2012).

While previous experimental studies found evidence to suggest that amputees use a hip-extensor strategy on the residual leg and a knee-extensor strategy on the intact leg during stair ascent (Agrawal et al., 2013b; Aldridge et al., 2012; Alimusaj et al., 2009; Powers et al., 1997; Schmalz et al., 2007; Yack et al., 1999), these strategies were not directly evident in the contributions of the hip and knee extensors to the biomechanical subtasks of stair ascent or in the distributions of power between segments in the vertical, AP and ML directions. Both the residual and intact leg knee and hip extensors provided critical contributions to vertical propulsion, anteroposterior propulsion, mediolateral control and leg swing (with the exception of the intact leg knee extensors in mediolateral control) by generating, absorbing and/or redistributing a significant amount of mechanical power. These results are in contrast with a previous experimental study which concluded the residual hip and intact leg were primarily responsible for energy generation during amputee stair ascent (Yack et al., 1999). However, consistent with a hip-extensor strategy on the residual leg and a knee-extensor strategy on the intact leg, GMAX generated greater net power in the residual leg compared to the intact leg and VAS generated greater net power in the intact leg compared to the residual leg (Appendix B: Figures B.11 and B.12) and unimpaired leg (Chapter 2). Therefore, while the use of a hip-strategy on the residual limb and a knee-strategy on the intact limb was not directly

observed in the contributions of the hip and knee extensors muscles to the subtasks of stair ascent, these strategies may have contributed to the overall differences in muscle contributions that were observed between amputee and unimpaired (Chapter 2) stair ascent. These results highlight the importance of using modeling and simulation techniques to investigate muscle function and identify contributions from muscles that may seem less important at the joint level but, due to dynamic coupling (Zajac and Gordon, 1989; Zajac et al., 2002), actually play a critical role in task execution.

Thus, musculoskeletal modeling and simulation techniques can provide valuable insight into quantities that cannot be measured experimentally. However, validation of these simulations can be challenging because these quantities cannot be directly validated by experimental data. Therefore, indirect measures of validation must be used instead. In this study a biomechanically consistent simulation was produced by requiring the simulation to closely replicate experimental data while also minimizing muscle co-contraction. In addition, simulated muscle excitation timings were compared to the experimental timings available in the literature for unilateral transtibial amputees (Powers et al., 1997; Schmalz et al., 2007) to assure that muscles were producing force at the appropriate times in the gait cycle. Because muscle function is state dependent (Zajac et al., 2002), by requiring the state and muscle excitation timings to closely emulate experimental data, we can confidently assess the functional role of the muscles during stair ascent using forward dynamics simulations.

Another potential limitation of musculoskeletal modeling is that some assumptions are required for musculoskeletal parameters. However, the optimization algorithm used in this study can compensate for model parameter inaccuracies by adjusting muscle excitation magnitudes to produce the muscle forces necessary to track the experimental biomechanics. Therefore, it is likely that these modeling assumptions

have a minimal effect on the muscle forces generated by the simulation and the resulting contributions to amputee stair ascent.

One additional limitation is that group-averaged experimental data was simulated. Amputees have been shown to demonstrate different individual compensations which may not be apparent in the averaged data (Powers et al., 1997; Silverman et al., 2008). Therefore, future work should focus on generating subject-specific simulations during stair ascent to enable the development of targeted rehabilitation programs tailored to an individual. However, this study is an important first step towards understanding individual muscle contributions to the subtasks of unilateral transtibial amputee stair ascent, including vertical propulsion, anteroposterior propulsion, mediolateral control and leg swing, and will have important clinical applications in the treatment of movement disorders.

CONCLUSIONS

The results of this study provide insight into the functional deficits of amputee stair ascent and the compensations necessary for transtibial amputees to ascend stairs. This work also has important implications for designing improved prostheses and restoring mobility in amputees. The passive prosthesis modeled in this study provided vertical propulsion throughout stance, similar to the role of the unimpaired plantarflexors in stair ascent. However, while the prosthesis contributed to braking throughout stance, similar to unimpaired SOL during stair ascent, it contributed to a greater extent. In addition, the prosthesis was unable to replicate the functions of unimpaired GAS, which contributes to forward propulsion during the second half of stance and leg swing initiation. To compensate HAM and VAS increased their contributions to forward

propulsion during the first and second halves of stance, respectively, but overall the residual leg still contributed to braking. The prosthesis also contributed to lateral control, contrary to the role of the plantarflexors in unimpaired stair ascent, which required increased contributions to medial control from the hip abductors (GMEDA and GMEDP). However, this was largely due to the increased step width observed in amputee stair ascent. Therefore, improved prostheses that provide additional forward propulsion (or reduced braking) and leg swing initiation could improve amputee stair ascent and minimize muscle compensations. In addition, targeted rehabilitation techniques could be designed to strengthen the muscles that demonstrated important compensatory mechanisms or to strengthen additional muscles that are able to functionally compensate for the loss of GAS by providing forward propulsion and leg swing initiation.

Chapter 4: Muscular Regulation of Dynamic Balance during Amputee and Non-amputee Stair Ascent

INTRODUCTION

Stair ascent is a common activity of daily living critical for maintaining independence in the home and community. However, previous studies have shown that dynamic balance is more difficult to maintain during stair ascent than level walking (Kendell et al., 2010), particularly in the frontal plane (Pickle et al., 2014; Silverman et al., 2014). As a result, populations with balance deficits often have difficulty ascending stairs and are at an increased risk for falls (e.g., Vanicek et al., 2010). Previous studies have attempted to mitigate fall risk through use of assistive devices such as handrails (Reeves et al., 2008; Reid et al., 2011) and canes (Hsue and Su, 2009, 2010), but few studies have investigated the underlying causes of altered dynamic balance.

Regulation of whole-body angular momentum has been identified as a critical aspect of maintaining dynamic balance during level walking (Herr and Popovic, 2008) and has been used as the foundation of control algorithms for bipedal robots (e.g., Goswami and Kallem, 2004; Hofmann et al., 2009; Kajita et al., 2003). Several studies have also suggested that controlling angular momentum is important in preventing falls during level walking (Simoneau and Krebs, 2000) and in recovering from a trip (Pijnappels et al., 2004, 2005a, 2005b) or unexpected step (van Dieen et al., 2007). In addition, regulation of angular momentum has been shown to be a promising indicator of balance in impaired populations (Bruijn et al., 2011; Nott et al., 2014; Silverman and Neptune, 2011).

Whole-body angular momentum, which is a measure of the body's rotation about its center-of-mass (COM), is often quantified by its time derivative (i.e., the time rate of

change of angular momentum), which is equal to the external moment about the body COM. The external moment is a function of the distance between the body COM and the center-of-pressure as well as the ground reaction forces (GRFs). As a result, angular momentum can be modulated through changes in the GRFs and external moment arms (e.g., foot placement). In human gait, muscles are the primary accelerators of the body segments and generators of the GRFs, and are therefore the primary regulators of whole-body angular momentum. Therefore, it is critical to understand how individual muscles contribute to the regulation of angular momentum in both unimpaired and impaired individuals in order to design effective rehabilitation programs and enhanced assistive devices aimed at improving dynamic balance.

Amputees are one group of individuals who are particularly susceptible to falls (Miller et al., 2001). A recent study analyzing whole-body angular momentum during level walking observed an increased range of frontal-plane angular momentum in amputees compared to non-amputees (Silverman and Neptune, 2011), which suggests a decrease in dynamic balance control. In addition, the range of sagittal-plane angular momentum was significantly different in amputees compared to non-amputees and was correlated with altered braking and propulsion, which highlighted how amputees modulate their braking and propulsion to help regulate sagittal-plane angular momentum during level walking. These changes in the regulation of sagittal-plane angular momentum are consistent with the loss of the ankle plantarflexors, which are important contributors to the regulation of non-amputee sagittal-plane angular momentum during level walking (Neptune and McGowan, 2011). In addition, others have shown that walking with a powered prosthesis, compared to a passive energy storage and return prosthesis, diminished sagittal-plane range of angular momentum (D'Andrea et al., 2014). This suggests that regulation of whole-body angular momentum, and thus dynamic

balance, has the potential to be improved with enhanced prosthesis designs that more fully replicate the role of the plantarflexors. However, despite these advances in understanding the regulation of angular momentum in amputee level walking, it remains unclear how amputees as well as non-amputees regulate whole-body angular momentum during the more challenging task of stair ascent.

Two recent studies found that regulation of angular momentum in both non-amputees (Silverman et al., 2014) and amputees (Pickle et al., 2014) was significantly altered in stair ascent compared to level walking. The primary difference in the regulation of angular momentum during amputee compared to non-amputee stair ascent was an increased range of sagittal-plane angular momentum, which was correlated with altered vertical GRF peaks in both the intact and residual limbs. This suggests that during stair ascent, compared to level walking, amputees likely modulate vertical propulsion instead of anteroposterior propulsion to regulate sagittal-plane angular momentum. While this result is consistent with the loss of the plantarflexors, which have been shown to be important contributors to vertical propulsion in non-amputee stair ascent (Chapter 2), the role of individual muscles in the regulation of angular momentum during amputee and non-amputee stair ascent as well as the contributions of the prosthesis and other necessary compensations remain unknown.

Muscle-actuated forward dynamics simulations have been used to identify the contributions of individual muscles to the time rate of change of angular momentum during non-amputee level walking (Neptune and McGowan, 2011). The purpose of this study was to use muscle-actuated forward dynamics simulations to identify the contributions of individual muscles, the prosthesis and gravity to whole-body angular momentum in the frontal, transverse and sagittal planes in order to gain insight into the differences in the biomechanical mechanisms used by amputees and non-amputees to

regulate angular momentum and maintain dynamic balance during stair ascent. Understanding which muscles are primarily responsible for regulating angular momentum and identifying the differences between amputees and non-amputees has important implications for the treatment of movement disorders and the design of targeted rehabilitation programs aimed at improving dynamic balance.

METHODS

Musculoskeletal model and dynamic optimization

Previously described three-dimensional muscle-actuated forward dynamics simulations of non-amputee (Chapter 2) and amputee (Chapter 3) stair ascent were developed using SIMM/Dynamics Pipeline (MusculoGraphics, Inc., Santa Rosa, CA) and consisted of rigid body segments representing the HAT (head, arms and trunk), pelvis and two legs, each consisting of a thigh, shank, patella, talus, calcaneus and toes. At each joint, passive torques representing the forces generated by passive tissues and ligaments were applied (Davy and Audu, 1987). Foot-ground contact was modeled using 31 viscoelastic elements with Coulomb friction distributed over the calcaneus and toes (Neptune et al., 2000b) or the prosthetic foot. The height of the ground was modified to represent the surface of the stairs (Rise/Run: 0.1778 m / 0.2794 m). The equations of motion were generated using SD/FAST (PTC, Needham, MA).

In the unilateral transtibial amputee simulation, the mass of the residual shank was reduced by 50% and the shank's center-of-mass (COM) was shifted proximally compared to the intact shank to represent the mass and inertia of the prosthesis and residual shank (Chapter 3). In addition, the muscles spanning the residual ankle joint (i.e., medial gastrocnemius, lateral gastrocnemius, soleus, tibialis posterior, tibialis anterior,

flexor digitorum longus and extensor digitorum longus) were removed. The prosthesis was modeled by fitting the average experimental amputee ankle moment data with a second-order torsional spring with damping. This prosthesis torque was then applied to the ankle joint as a passive torque.

The non-amputee model was driven by 38 Hill-type musculotendon actuators per leg, grouped into 15 muscle groups for analysis based on similar anatomical and functional classification (Table 4.1). The amputee model was driven by 69 muscles (38 on the intact leg and 31 on the residual leg), grouped into 15 muscle groups in the intact leg and 12 muscle groups in the residual leg (Table 4.1).

Forward dynamics simulations of non-amputee and amputee stair ascent were generated over 100% (right foot-strike to right foot-strike) and 120% (intact foot-strike to the second residual toe-off) of the gait cycle, respectively. A simulated annealing optimization algorithm (Goffe et al., 1994) was used to identify muscle excitation patterns that minimized the differences between experimental and simulated kinematics and GRFs in addition to minimizing muscle stress in order to reduce unnecessary muscle co-activation.

Table 4.1: Muscles included in the musculoskeletal model and their corresponding analysis groups in the non-amputee, intact and residual legs. The muscles labeled as "REMOVED" have been removed from the residual leg.

Muscles	Analysis Groups		
	Non-Amputee Leg	Intact Leg	Residual Leg
Iliacus Psoas	IL	IL	IL
Adductor Longus Adductor Brevis Pectineus Quadratus Femoris	AL	AL	AL
Superior Adductor Magnus Middle Adductor Magnus Inferior Adductor Magnus	AM	AM	AM
Sartorius	SAR	SAR	SAR
Rectus Femoris	RF	RF	RF
Vastus Medialis Vastus Lateralis Vastus Intermedius	VAS	VAS	VAS
Anterior Gluteus Medius Middle Gluteus Medius Anterior Gluteus Minimus Middle Gluteus Minimus	GMEDA	GMEDA	GMEDA
Posterior Gluteus Medius Posterior Gluteus Minimus Piriformis Gemellus	GMEDP	GMEDP	GMEDP
Tensor Fasciae Latae	TFL	TFL	TFL
Superior Gluteus Maximus Middle Gluteus Maximus Inferior Gluteus Maximus	GMAX	GMAX	GMAX
Semitendinosus Semimembranosus Gracilis Biceps Femoris Long Head	HAM	HAM	HAM
Biceps Femoris Short Head	BFSH	BFSH	BFSH
Medial Gastrocnemius Lateral Gastrocnemius	GAS	GAS	REMOVED
Soleus Tibialis Posterior Flexor Digitorum Longus	SOL	SOL	
Tibialis Anterior Extensor Digitorum Longus	TA	TA	

Simulation analysis

To identify the contributions of individual muscles and the prosthesis to dynamic balance, their contributions to the time rate of change of whole-body angular momentum ($\dot{\bar{H}}$) were determined (Neptune and McGowan, 2011; Neptune et al., 2011) using:

$$\dot{\bar{H}} = \bar{r} \times \bar{F}_{GRF} \qquad (4.1)$$

where $\bar{r}$ is the moment arm vector from the center-of-pressure on each foot to the body's COM, $\bar{F}_{GRF}$ is the vector of each muscle's and the prosthesis's contribution to the ground reaction force (GRF), and $\bar{r} \times \bar{F}_{GRF}$ is the vector of external moments (frontal, transverse and sagittal plane) generated about the body's COM by each muscle and the prosthesis (Figure 4.1). The contributions of each muscle and the prosthesis to the GRFs were determined using a previously described GRF decomposition technique (Neptune et al., 2004). The net contribution of each muscle group and the prosthesis to whole-body angular momentum in each plane was determined by integrating $\dot{\bar{H}}$ over the first and second halves of stance. The contribution of gravity was also computed since it has been shown to be an important contributor to the GRF in non-amputee (Chapter 2) and amputee stair ascent (Chapter 3).

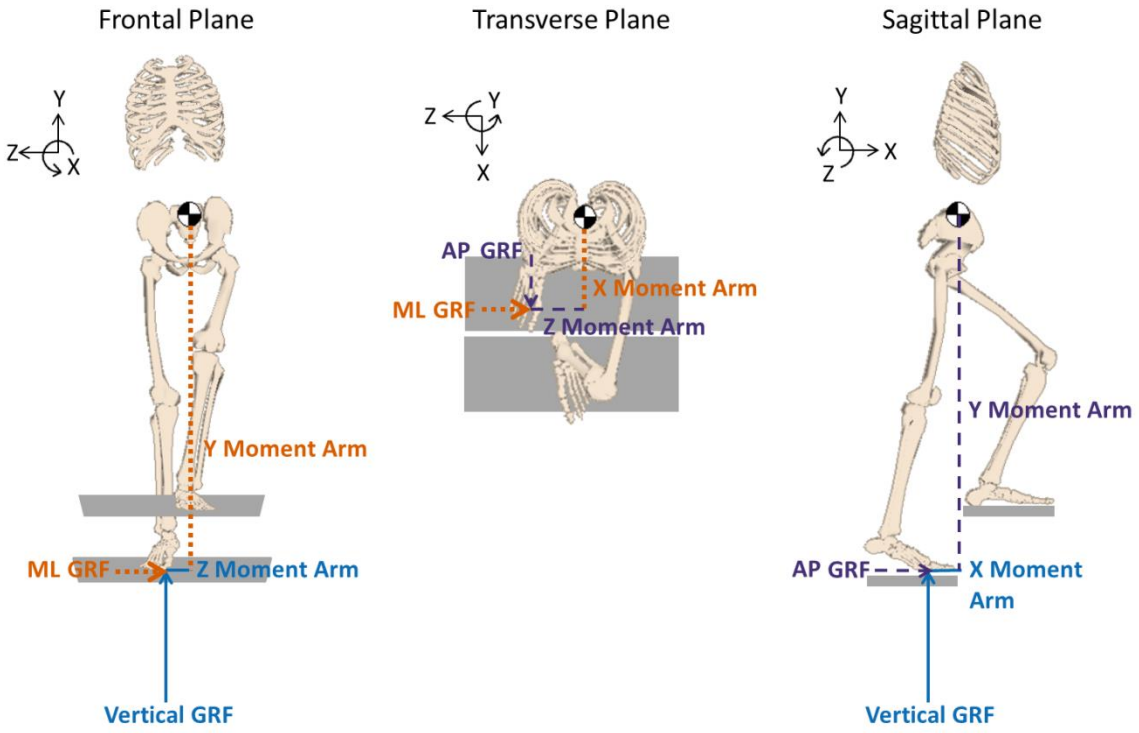

Figure 4.1. The time rate of change of whole-body angular momentum (external moment about the center-of-mass (COM)) in the frontal, transverse and sagittal planes, computed as the cross product of the external moment arms and ground reaction force (GRF) vectors (anteroposterior (AP), vertical, and mediolateral (ML)). The external moments in the frontal, transverse and sagittal planes were defined about the X, Y and Z axes, respectively. Note that for clarity, only the external moments generated by the right leg (non-amputee leg, intact leg) during stair ascent are depicted.

Experimental tracking data

Previously collected three-dimensional kinematics and GRFs from 27 non-amputee subjects and 10 traumatic unilateral transtibial amputees prescribed with a passive energy storage and return prosthesis were used to generate these simulations. Each subject ascended a 16-step instrumented staircase (2 forceplates, 1200 Hz: AMTI, Inc., Watertown, MA) step-over-step at a fixed cadence of 80 steps per minute while a

26-camera optoelectronic motion capture system (120 Hz, Motion Analysis Corp., Santa Rosa, CA) collected three-dimensional whole-body kinematics. For five complete gait cycles for each leg, GRFs (normalized by subject body weight) and joint kinematics were time-normalized to 100% of the gait cycle and averaged across gait cycles and subjects for each leg. For additional details on the experimental protocol for the non-amputees and amputees, see Chapter 2 and Chapter 3, respectively.

RESULTS

Frontal-plane angular momentum

Each muscle in addition to the prosthesis and gravity contributed to frontal-plane angular momentum through its contribution to the frontal-plane external moment, composed of its contribution to the vertical and/or ML GRF coupled with the moment arms from the COP to the body COM (Appendix C: Figures. C.1 – C.3). Throughout non-amputee (right leg of non-amputee simulation), intact (right leg of amputee simulation) and residual (left leg of amputee simulation) stance, the hip abductors (GMEDA, GMEDP) were the primary contributors to angular momentum that acted to rotate the body towards the ipsilateral leg (Figure 4.2). During the first half of non-amputee stance, VAS was the primary contributor to angular momentum that acted to rotate the body towards the contralateral leg. VAS was also a primary contributor during the first half of residual and intact stance but the prosthesis and uniarticular plantarflexors (SOL) contributed to a greater extent (Figure 4.2). In addition, HAM and GAS also made important contributions to angular momentum that acted to rotate the body towards the contralateral leg during residual and intact stance, respectively. During the second half of non-amputee stance, HAM was the primary contributor to angular momentum that acted

to rotate the body towards the contralateral leg, with additional contributions from AL and the plantarflexors (SOL, GAS) (Figure 4.2). During the second half of residual and intact stance, the prosthesis and plantarflexors (SOL, GAS) were the primary contributors to angular momentum that acted to rotate the body towards the contralateral leg with additional contributions from gravity and HAM in the residual leg and AM in the intact leg (Figure 4.2).

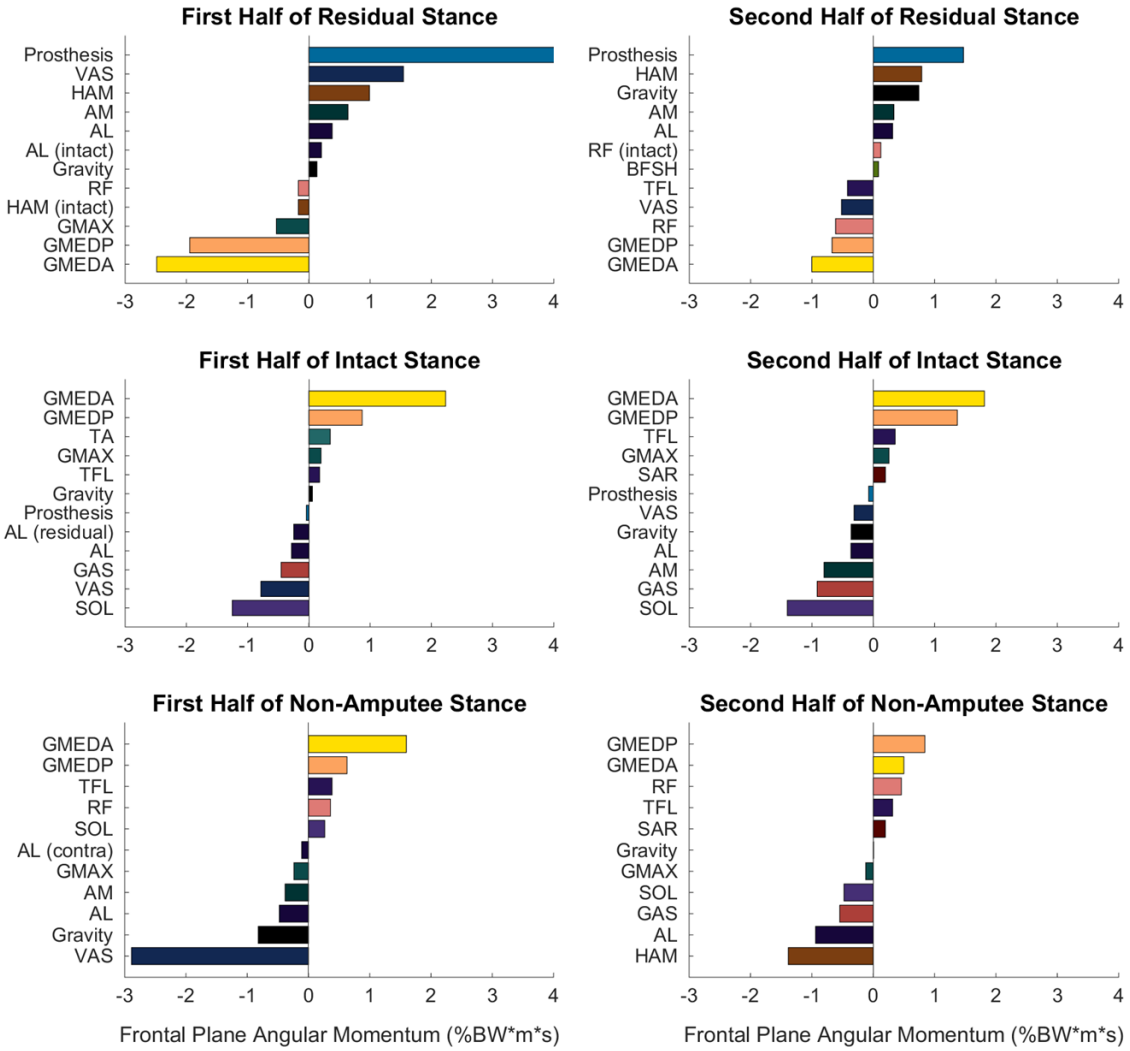

Figure 4.2: Primary positive and negative muscle contributions in addition to the contributions from the prosthesis and gravity to whole-body angular momentum in the frontal plane during the first and second halves of residual, intact and non-amputee stance. In residual stance (left leg of the amputee simulation), positive (negative) contributions indicate angular momentum that acts to rotate the body towards the contralateral (ipsilateral) leg. In intact and non-amputee stance (right leg of the amputee and non-amputee simulation, respectively), positive (negative) contributions indicate angular momentum that acts to rotate the body towards the ipsilateral (contralateral) leg. Each muscle is depicted using a muscle-specific color to enable comparisons across figures. Unless otherwise indicated, muscles are from the leg specified in the plot title (see Table 4.1 for muscle group abbreviations). In the non-amputee plots, "contra" indicates the contralateral non-amputee leg.

Transverse-plane angular momentum

Each muscle in addition to the prosthesis and gravity contributed to transverse-plane angular momentum through its contribution to the transverse-plane external moment, composed of its contribution to the AP and/or ML GRF coupled with the moment arms from the COP to the body COM (Appendix C: Figures C.4 – C.6). In the transverse plane, contributions were an order of magnitude smaller than the contributions in the frontal and sagittal planes. During the first half of non-amputee stance (right leg of the non-amputee simulation), GMAX, TA and gravity were the primary contributors to angular momentum that acted to rotate the body vertically towards the contralateral leg while SOL and RF were the primary contributors to angular momentum that acted to rotate the body vertically towards the ipsilateral leg (Figure 4.3). During the first half of residual stance (left leg of the amputee simulation), the hip abductors (GMEDA, GMEDP) and hip extensors (GMAX, HAM) were the primary contributors to angular momentum that acted to rotate the body towards the contralateral leg while the prosthesis, with additional contributions from VAS, was the primary contributor to angular momentum that acted to rotate the body towards the ipsilateral leg (Figure 4.3). During the first half of intact stance (right leg of the amputee simulation), the contributions to transverse-plane angular momentum were much smaller compared to residual stance. Gravity, GMAX, VAS and the hip abductors (GMEDP, GMEDA) made small contributions to angular momentum that acted to rotate the body towards the contralateral leg while minimal contributions were made to angular momentum that acted to rotate the body towards the ipsilateral leg (Figure 4.3).

During the second half of non-amputee stance, HAM was the primary contributor to angular momentum that acted to rotate the body vertically towards the contralateral leg while RF was the primary contributor to angular momentum that acted to rotate the body

vertically towards the ipsilateral leg (Figure 4.3). Similarly, during the second half of residual stance, HAM and VAS, with additional contributions from gravity, were the primary contributors to angular momentum that acted to rotate the body towards the contralateral leg while RF, TFL and the prosthesis were the primary contributors to angular momentum that acted to rotate the body towards the ipsilateral leg (Figure 4.3). In contrast to the primary contributors during non-amputee and residual stance, during the second half of intact stance, VAS, AM and SOL were the primary contributors to angular momentum that acted to rotate the body towards the contralateral leg while the hip abductors (GMEDA, GMEDP) were the primary contributors to angular momentum that acted to rotate the body towards the ipsilateral leg (Figure 4.3).

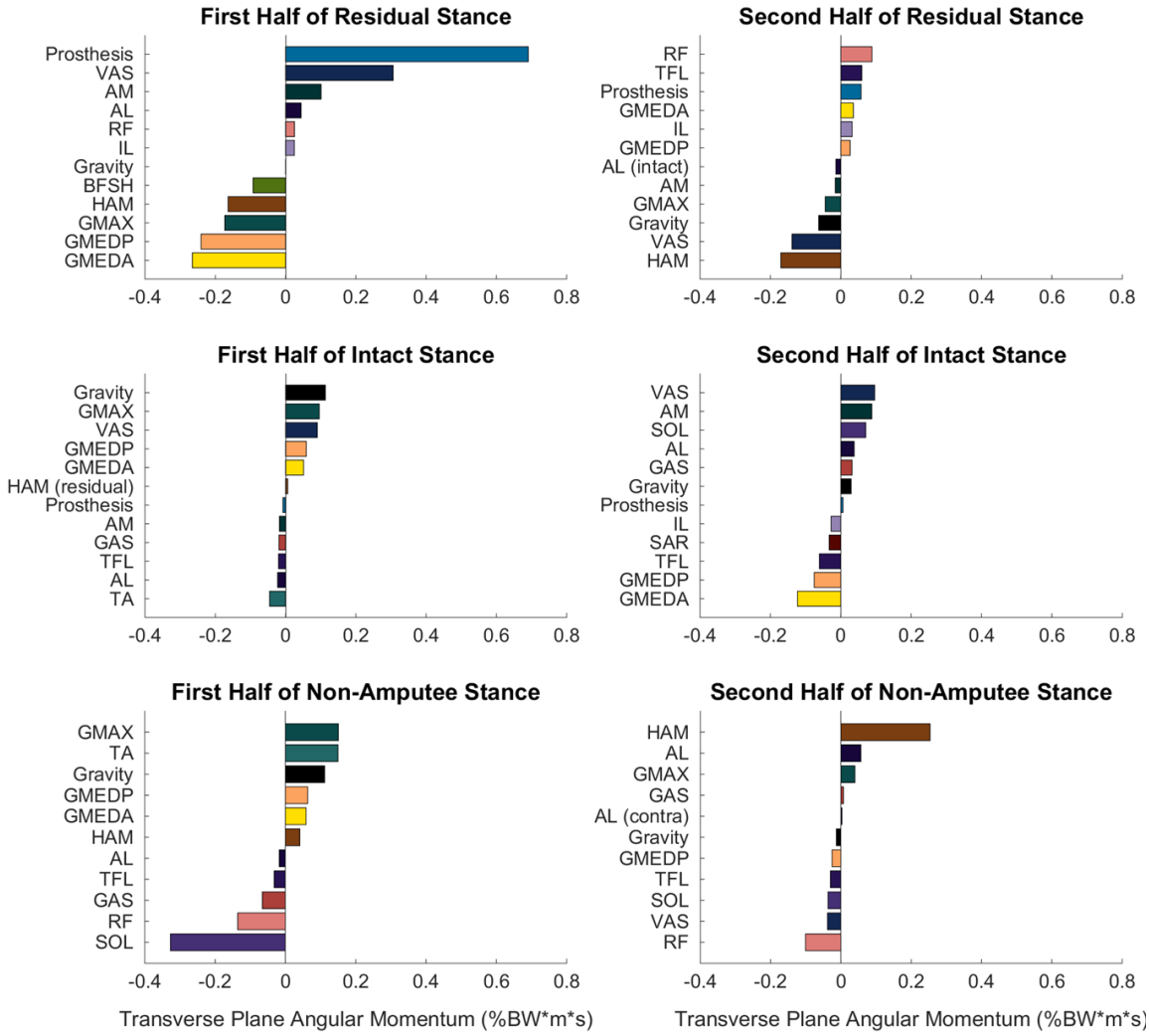

Figure 4.3: Primary positive and negative muscle contributions in addition to the contributions from the prosthesis and gravity to whole-body angular momentum in the transverse plane during the first and second halves of residual, intact and non-amputee stance. In residual stance (left leg of the amputee simulation), positive (negative) contributions indicate angular momentum that acts to rotate the body vertically towards the ipsilateral (contralateral) leg. In intact and non-amputee stance (right leg of the amputee and non-amputee simulations, respectively), positive (negative) contributions indicate angular momentum that acts to rotate the body vertically towards the contralateral (ipsilateral) leg. Each muscle is depicted using a muscle-specific color to enable comparisons across figures. Unless otherwise indicated, muscles are from the leg specified in the plot title (see Table 4.1 for muscle group abbreviations). In the non-amputee plots, "contra" indicates the contralateral non-amputee leg.

Sagittal-plane angular momentum

Each muscle in addition to the prosthesis and gravity contributed to sagittal-plane angular momentum through its contribution to the sagittal-plane external moment, composed of its contribution to the AP and/or vertical GRF coupled with the moment arms from the COP to the body COM (Appendix C: Figures C.7 – C.9). During the first half of non-amputee stance, the plantarflexors (particularly SOL) and RF contributed to forward (negative) angular momentum while GMAX contributed to backward (positive) angular momentum (Figure 4.4). The primary contributors during the first half of residual and intact stance were largely similar with the prosthesis or plantarflexors contributing to forward angular momentum and GMAX contributing to backward angular momentum, with additional contributions from HAM during residual stance (Figure 4.4). In addition, in the first half of stance gravity contributed to backward angular momentum in all three legs (Figure 4.4). During the second half of non-amputee stance, SOL, RF and VAS contributed to forward angular momentum while HAM contributed to backward angular momentum (Figure 4.4). Similar to the first half of stance, the primary contributors during the second half of residual and intact stance were similar to those of non-amputee stance. The prosthesis contributed to forward angular momentum in the residual leg and RF contributed to forward angular momentum in both legs while VAS and HAM were the primary contributors to backward angular momentum in both legs (Figure 4.4). During the second half of stance, gravity contributed to backward angular momentum in the residual leg but forward angular momentum in the intact and non-amputee legs (Figure 4.4).

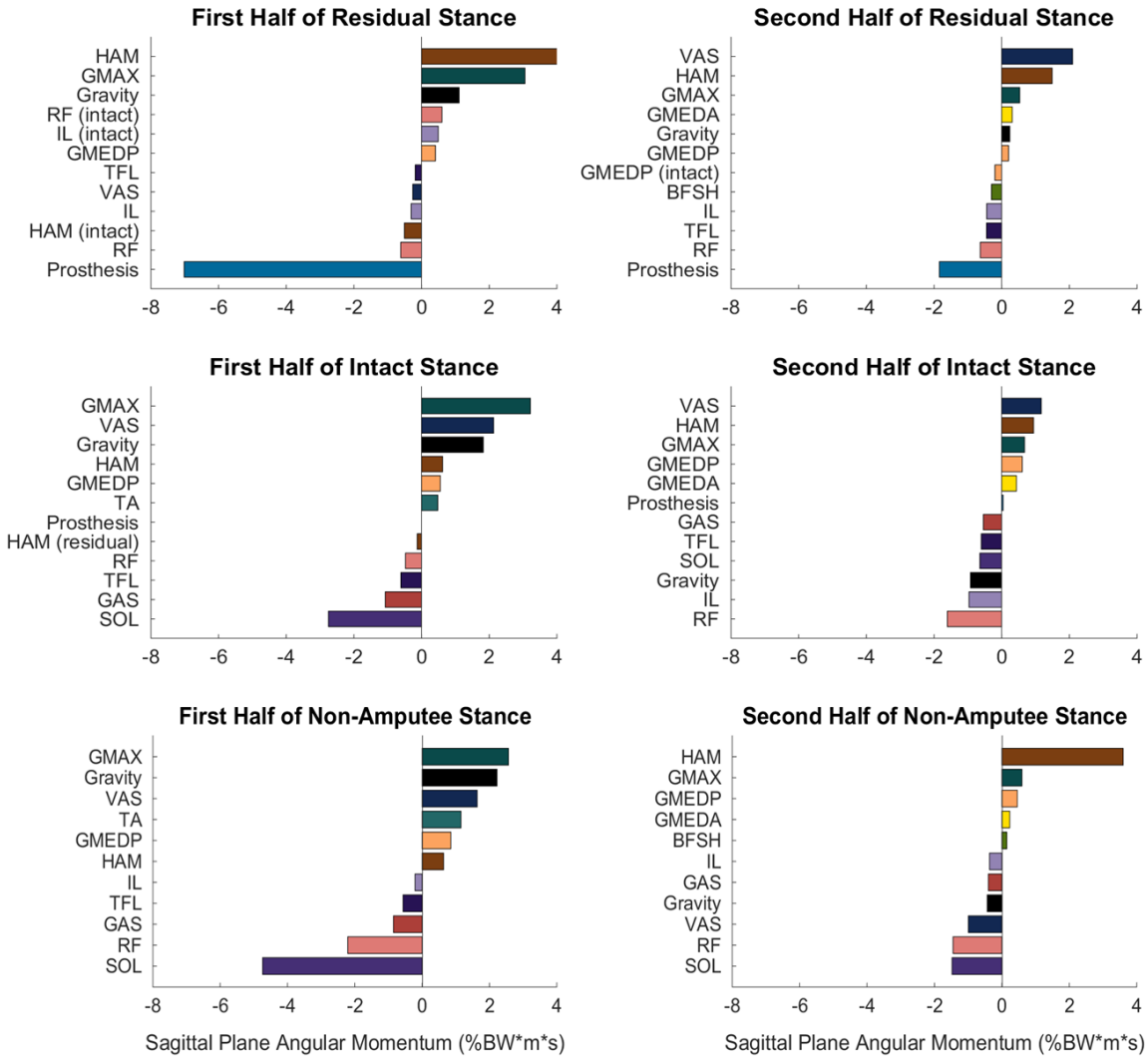

Figure 4.4: Primary positive and negative muscle contributions in addition to the contributions from the prosthesis and gravity to whole-body angular momentum in the sagittal plane during the first and second halves of residual, intact and non-amputee stance. Positive (negative) contributions indicate angular momentum that acts to rotate the body backward (forward). Each muscle is depicted using a muscle-specific color to enable comparisons across figures. Unless otherwise indicated, muscles are from the leg specified in the plot title (see Table 4.1 for muscle group abbreviations).

DISCUSSION

Dynamic balance is more difficult to maintain during stair ascent compared to level walking (Kendell et al., 2010; Lee and Chou, 2007) and as a result, individuals with balance deficits such as lower-limb amputees often have difficulty ascending stairs and are more susceptible to falls (Miller et al., 2001). During human locomotion, dynamic balance is highly regulated by minimizing changes in angular momentum (e.g., Herr and Popovic, 2008). The purpose of this study was to elucidate the differences in the biomechanical mechanisms used by amputees and non-amputees to regulate angular momentum and maintain dynamic balance during stair ascent by identifying the contributions of individual muscles, the prosthesis and gravity to whole-body angular momentum.

In the sagittal plane, the prosthesis was able to largely replicate the function of the non-amputee plantarflexors in the regulation of angular momentum during stair ascent by contributing to forward angular momentum throughout residual limb stance. As a result, the primary contributors in the residual, intact and non-amputee legs were largely similar with GMAX, HAM, VAS and gravity contributing to backward angular momentum. The importance of the plantarflexors (SOL, GAS) or prosthesis, knee extensors (VAS) and hip extensors (GMAX) to sagittal-plane angular momentum is consistent with their critical role in anteroposterior and vertical propulsion during non-amputee (Chapter 2; Lin et al., 2015) and amputee (Chapter 3) stair ascent while the importance of HAM is consistent with its role in anteroposterior propulsion during non-amputee (Chapter 2) and amputee (Chapter 3) stair ascent.

Despite the decreased range of sagittal-plane angular momentum in non-amputee stair ascent compared to level walking (Silverman et al., 2014), in both tasks the muscles that extend the ankle, knee and hip were the most critical to the regulation of sagittal-

plane angular momentum (Neptune and McGowan, 2011). This is consistent with a previous study that showed leg extension strength to be the best predictor of an older adult's ability to recover from a trip in the sagittal plane (Pijnappels et al., 2008). Similar to both amputee and non-amputee stair ascent, in level walking GMAX, VAS, HAM and gravity generated backward angular momentum and SOL generated forward angular momentum during the first half of stance (Neptune and McGowan, 2011). However, unlike level walking where GAS generated forward angular momentum during the first half of stance and backward angular momentum during the second half of stance (Neptune and McGowan, 2011), in stair ascent GAS generated forward angular momentum throughout stance. As a result, during the second half of non-amputee stair ascent HAM became the primary contributor to backward angular momentum in place of GAS while both HAM and VAS contributed to backward angular momentum during the second half of residual and intact stance. These results contradict a previous hypothesis that the increased range of sagittal-plane angular momentum during residual stance compared to non-amputee stance could be mitigated if the prosthesis was able to replicate the function of gastrocnemius (Pickle et al., 2014). This emphasizes the need for rehabilitation programs that focus on strengthening GMAX, HAM and VAS which may improve an amputee's ability to control dynamic balance by generating the appropriate backward angular momentum.

The importance of the plantarflexors, hamstrings, gluteus maximus and vastii in the regulation of sagittal-plane angular momentum during amputee and non-amputee stair ascent is also consistent with previous studies examining recovery from a trip in the sagittal plane. These studies found that the increased forward angular momentum generated by tripping over an obstacle during level walking could be restrained by the plantarflexors, hamstrings and gluteus maximus in the support limb (Pijnappels et al.,

2005) in addition to hip and knee extensor moments in the recovery limb (Grabiner et al., 1993). While this emphasizes the importance of GMAX, HAM and VAS in generating backward angular momentum, in stair ascent the plantarflexors contribute solely to forward angular momentum and would not be a useful mechanism for restraining the increased forward angular momentum after a trip (c.f., during level walking Neptune and McGowan, 2011; Pijnappels et al., 2005). While the prosthesis was able to largely replicate the function of the non-amputee plantarflexors in the sagittal-plane, the range of sagittal-plane angular momentum is increased during residual stance compared to non-amputee stance which suggests decreased dynamic balance control (Pickle et al., 2014). In addition, the ability to respond to balance perturbations during standing has been previously shown to be limited in the prosthetic leg (Vrieling et al., 2008b). As a result, if an amputee were to trip during stair ascent it may be more difficult to restrain the sudden increase in forward angular momentum due to the inability of the prosthesis to limit the momentum. This further emphasizes the need for rehabilitation programs to strengthen the muscles that are capable of providing backward angular momentum (e.g., hip and knee extensors).

While the prosthesis replicated the role of the non-amputee plantarflexors in the sagittal plane, it was unable to do so in the frontal plane. In the frontal plane, the non-amputee plantarflexors contributed minimally while the prosthesis was found to be the primary contributor to angular momentum that acted to rotate the body towards the contralateral leg. To compensate, VAS and HAM decreased their contributions to angular momentum that acted to rotate the body towards the contralateral leg during the first and second halves, respectively, of residual and intact stance compared to non-amputee stance. However, increased angular momentum that acted to rotate the body towards the contralateral leg was still generated in the residual leg. In the intact leg, the plantarflexors

increased their contributions to angular momentum that acted to rotate the body towards the contralateral leg to compensate for the increased contributions provided by the prosthesis in the residual leg and the decreased contributions from VAS and HAM in the intact leg. In addition, the contributions from the hip abductors (GMEDA, GMEDP) to angular momentum that acted to rotate the body towards the ipsilateral leg increased in both the residual and intact legs to compensate for the increased contributions provided by the prosthesis and intact plantarflexors to angular momentum that acted to rotate the body towards the contralateral leg. However, despite these increased contributions in the residual and intact legs, the range of frontal-plane angular momentum is similar in non-amputee and amputee stair ascent (e.g., Pickle et al., 2014).

In stair ascent, the importance of the intact plantarflexors and prosthesis in the regulation of frontal-plane angular momentum is consistent with their roles in vertical propulsion and mediolateral control in non-amputee (Chapter 2) and amputee (Chapter 3) stair ascent while the importance of the hip abductors (GMEDA, GMEDP) and HAM is consistent with their role in mediolateral control in non-amputee (Chapter 2; Lin et al., 2015) and amputee (Chapter 3) stair ascent. VAS is also important to mediolateral control in non-amputee stair ascent (Chapter 2; Lin et al., 2015) and to vertical propulsion in non-amputee (Chapter 2; Lin et al., 2015) and amputee stair ascent (Chapter 3). Similar to stair ascent, in non-amputee level walking VAS was a primary contributor to angular momentum that acted to rotate the body towards the contralateral leg while gluteus medius was the primary contributor to angular momentum that acted to rotate the body towards the ipsilateral leg (Neptune et al., 2012). In addition, in non-amputee level walking the plantarflexors contributed to angular momentum that acted to rotate the body towards the contralateral leg (Neptune et al., 2012), similar to the role of the prosthesis and the intact plantarflexors but less similar to the role of the non-amputee plantarflexors

during stair ascent. The importance of the hip abductors in generating frontal-plane angular momentum during stair ascent is also consistent with the role of the hip abductors in maintaining mediolateral balance during level walking (Jansen et al., 2014; Pandy et al., 2010; Silverman and Neptune, 2012) in addition to the role of the hip abductor moment in resisting ML perturbations to standing balance (Curtze et al., 2012) and in maintaining lateral stability in the frontal plane during stair ascent (Novak and Brouwer, 2011).

In the transverse plane, the prosthesis was able to largely replicate the role of the unimpaired plantarflexors, particularly the role of the uniarticular plantarflexors. However, the prosthesis contributed to nearly twice as much angular momentum that acted to rotate the body vertically towards the ipsilateral leg as the non-amputee plantarflexors. As a result, compensations were evident in the residual leg muscles, specifically the knee extensors (VAS, RF), hip extensors (GMAX, HAM) and hip abductors (GMEDA, GMEDP). In addition, the overall contributions to transverse-plane angular momentum in the intact leg during the first half of stance decreased which indicates that amputees rely more on the muscles of the residual leg to regulate transverse-plane angular momentum during the first half of stance. During the second half of stance, additional compensations arose in both the residual and intact legs as the prosthesis replicated the function of the non-amputee SOL but not GAS. However, the contributions to transverse-plane angular momentum were small during the second half of stance which reflects an overall decreased need for regulating transverse-plane angular momentum during late stance. Consistently, compared to level walking the range of transverse-plane angular momentum was decreased in stair ascent in both amputees (Pickle et al., 2014) and non-amputees (Silverman et al., 2014). In amputees, the ML moment arms were increased due to increased amputee step width (Chapter 3; Ramstrand

and Nilsson, 2009), but it was not enough to significantly alter the range of transverse-plane angular momentum (Pickle et al., 2014).

In general, contributions to angular momentum in each plane were larger during the first half of stance compared to the second half. This indicates that during stair ascent, there is an increased demand on the musculature to control angular momentum during the first half of stance in both amputees and non-amputees. Strengthening the muscles that contribute to frontal-, transverse- and sagittal-plane angular momentum during the first half of stance, with emphasis on the muscles that contribute to sagittal-plane angular momentum where a trip is most likely to occur, may help improve dynamic balance and decrease the risk of falls during stair ascent in both impaired and unimpaired populations.

One potential limitation of this study is that while musculoskeletal modeling and simulation techniques can provide insight into quantities that cannot be measured experimentally, such as the contributions of individual muscles to the time rate of change of angular momentum, validation of these simulations can be challenging. However, in this study, biomechanically consistent simulations were produced by requiring the simulations to closely emulate experimental data while minimizing muscle co-contraction. In addition, simulated muscle excitation timings were previously compared to those available in the literature to assure that muscles were producing force at the appropriate points in the gait cycle (Chapters 2 and 3). Because muscle function is state dependent (Zajac et al., 2002), by requiring the state and muscle excitation timings to closely emulate experimental data, we can confidently assess the functional role of the muscles during stair ascent using forward dynamics simulations.

Another potential limitation is that the arms were not included in the musculoskeletal model. However, previous studies demonstrated that the arms contribute negligibly to sagittal- and frontal-plane angular momentum (Herr and Popovic, 2008) and

COM accelerations (Jansen et al., 2014). In addition, by requiring the simulation to closely replicate experimental data collected from subjects allowed to swing their arms, it is likely that the simulated lower limb muscle forces and their subsequent contributions to the GRF are minimally affected by this assumption.

Lastly, one additional limitation is that group-averaged experimental data was simulated for both amputee and non-amputee stair ascent. However, amputees have been shown to demonstrate different individual compensations which may not be apparent in the averaged data (Powers et al., 1997; Silverman et al., 2008). As a result, future work should focus on generating subject-specific simulations of stair ascent to assess individual deficits in angular momentum regulation and enable the development of targeted rehabilitation programs tailored to an individual. However, this study is an important first step towards understanding individual muscle contributions to the regulation of frontal-, transverse- and sagittal-plane angular momentum in non-amputee and unilateral transtibial amputee stair ascent and will have important clinical applications in the treatment of movement disorders which exhibit decreased dynamic balance control.

CONCLUSIONS

The results of this study provide insight into the mechanisms by which amputees and non-amputees regulate dynamic balance during stair ascent with emphasis on the necessary compensations in unilateral transtibial amputees. This work has important implications for designing targeted rehabilitation and strength training programs and refined prostheses in order to improve dynamic balance during stair ascent. The passive prosthesis was found to replicate the role of non-amputee plantarflexors in the sagittal

plane by providing forward angular momentum throughout stance. The prosthesis also replicated the role of the non-amputee plantarflexors in the transverse plane but caused a larger change in angular momentum. The biggest difference between amputee and non-amputee regulation of angular momentum was in the frontal plane, where the non-amputee plantarflexors contributed minimally but the prosthesis arose as a critical contributor to angular momentum that acted to rotate the body towards the contralateral leg. To compensate, VAS and HAM decreased their contributions to angular momentum that acted to rotate the body towards the contralateral leg during the first and second halves of stance respectively, while the hip abductors (GMEDA, GMEDP) increased their contributions to angular momentum that acted to rotate the body towards the ipsilateral leg. Therefore, improved prostheses with reduced contributions to transverse- and frontal-plane angular momentum could improve dynamic balance control during amputee stair ascent and minimize muscle compensations. It is likely that this could be accomplished by minimizing the prosthesis' contribution to the mediolateral GRF, possibly by increasing the stiffness of the prosthetic foot in the coronal plane to decrease the energy stored and returned in the mediolateral direction. In addition, targeted rehabilitation techniques could be implemented to strengthen the muscles that contribute to frontal-, transverse- and sagittal-plane angular momentum, specifically those that contribute during the first half of stance when the demand on the musculature to regulate angular momentum is higher. Strengthening these muscles could help improve dynamic balance control and reduce the risk of a fall during stair ascent in both non-amputees and amputees.

Chapter 5: Conclusions

The overall goal of this research was to use a musculoskeletal modeling and simulation framework to identify how individual muscles, gravity and the prosthesis contribute to the subtasks of stair ascent in non-amputees and unilateral transtibial amputees to provide a foundation for the design of targeted rehabilitation programs and more effective prostheses. This overall goal was addressed through a series of studies.

In the study in Chapter 2, a muscle-driven forward dynamics simulation of non-amputee stair ascent was developed and analyzed to determine the contributions of individual lower-extremity muscles to the subtasks of vertical propulsion, anteroposterior propulsion, mediolateral control and leg swing in non-amputee stair ascent and the mechanisms by which individual muscles work synergistically to perform these subtasks. Vertical propulsion was generated primarily by the knee extensors (VAS) and plantarflexors during the first and second halves of stance respectively, while forward propulsion was generated primarily by the hip extensors (GMAX – first half of stance, HAM – second half of stance) throughout stance. Medial control was generated by the hip abductors (GMEDA, GMEDP) throughout stance while lateral control was generated by the knee extensors (VAS) during the first half of stance (when they are also contributing to vertical propulsion) and the hip extensors (HAM) during the second half of stance (when they are also contributing to forward propulsion). Controlled and stable leg swing was achieved by antagonistic muscles spanning the hip, knee and ankle joints that distributed power throughout the body. By understanding the function and coordination of these muscle groups, targeted interventions and rehabilitation programs can be designed to address patient-specific deficits in stair ascent.

In the study in Chapter 3, the compensatory mechanisms used by unilateral transtibial amputees were identified by developing and analyzing a muscle-driven forward dynamics simulation of amputee stair ascent to identify the contributions of individual muscles and the prosthesis to the same biomechanical subtasks investigated in Chapter 2 during amputee stair ascent. The passive prosthesis modeled in this study was able to replicate some of the functions of the non-amputee plantarflexors (SOL, GAS), specifically those of the uniarticular plantarflexors (SOL), by providing vertical propulsion and braking throughout stance. However, the prosthesis provided more braking than the non-amputee SOL and the prosthesis was unable to replicate all of the functions of non-amputee GAS, which contributes to vertical and forward propulsion during the second half of stance in addition to leg swing initiation. To compensate, HAM and VAS increased their contributions to forward propulsion during the first and second halves of stance respectively, but overall the residual leg still contributed to braking. In addition, contrary to the role of the plantarflexors in non-amputee stair ascent, the prosthesis contributed to lateral control, which required increased contributions to medial control from the hip abductors (GMEDA and GMEDP). However, this was largely due to the increased step width observed in amputee stair ascent. The results of this study provide insight into the functional deficits of amputees and the compensations necessary for transtibial amputees to ascend stairs. Refined prostheses that provide additional forward propulsion (or reduced braking) and increased leg swing initiation could improve amputee stair ascent and minimize required muscle compensations. In addition, targeted rehabilitation techniques could be designed to strengthen the muscles that demonstrated important compensatory mechanisms or to strengthen additional muscles that are able to functionally compensate for the loss of GAS by providing forward propulsion and leg swing initiation (e.g., HAM).

In the study in Chapter 4, the biomechanical mechanisms by which amputees and non-amputees regulate dynamic balance during stair ascent were determined by quantifying the contributions of individual muscles and the prosthesis to whole-body angular momentum in the frontal, transverse and sagittal planes. The passive prosthesis was found to replicate the role of the non-amputee plantarflexors in the sagittal plane by providing forward angular momentum throughout stance. In addition, the prosthesis replicated the role of the non-amputee plantarflexors in the transverse plane but contributed to a greater extent. In the frontal plane the non-amputee plantarflexors contributed minimally but the prosthesis was found to be an important contributor to angular momentum that acted to rotate the body towards the contralateral leg. To compensate, HAM and VAS decreased their contributions to angular momentum that acted to rotate the body towards the contralateral leg while the hip abductors (GMEDA, GMEDP) increased their contributions to angular momentum that acted to rotate the body towards the ipsilateral leg. The results of this study provide insight into the biomechanical mechanisms by which amputees and non-amputees regulate dynamic balance. Refined prostheses with reduced contributions to transverse- and frontal-plane angular momentum, which can likely be accomplished by minimizing the prosthesis' contribution to the mediolateral GRF (e.g., through coronal-plane stiffness modulation), could improve dynamic balance control during amputee stair ascent and minimize muscle compensations. In addition, targeted rehabilitation therapies could strengthen the primary muscle contributors to frontal-, transverse- and sagittal-plane angular momentum, specifically the critical contributors during the first half of stance when the demand on the musculature to regulate angular momentum is higher. Targeted strengthening of these muscles could help improve dynamic balance control and reduce the risk of falls during stair ascent in both amputees and non-amputees.

Each study contributed to the overall goal of understanding individual muscle function and coordination in amputee and non-amputee stair ascent. Collectively, these studies have identified the compensatory mechanisms used by unilateral transtibial amputees and provided a foundation for designing refined prosthetic devices and targeted rehabilitation programs aimed at improving an individual's ability to ascend stairs while maintaining dynamic balance.

Chapter 6: Future Work

This body of work has provided an understanding of the contributions of individual muscles to the biomechanical subtasks of non-amputee and amputee stair ascent, with emphasis on the compensations necessary for unilateral transtibial amputees to ascend stairs. However, there are several avenues for expanding and building upon this work. For example, this research focused on stair ascent instead of stair descent since stair ascent was previously shown to be a more strenuous activity requiring increased muscle activity (Bae et al., 2009; Lyons et al., 1983; McFadyen and Winter, 1988), net joint work (DeVita et al., 2007) and metabolic energy (Teh and Aziz, 2002). However, while stair ascent is achieved primarily through force generation, stair descent is achieved predominantly by controlling the force due to gravity (McFadyen and Winter, 1988) and may be a more dynamic process (Zachazewski et al., 1993). In addition, falls are potentially more dangerous during stair descent (e.g., Startzell et al., 2000) and angular momentum is more tightly regulated (Pickle et al., 2014; Silverman et al., 2014). Therefore, to gain further insight into stair locomotion, future work should focus on identifying the contributions of individual muscles to the biomechanical subtasks of non-amputee and amputee stair descent.

While this research identified the contributions of individual muscles and the prosthesis to the subtasks of non-amputee and amputee stair ascent, an additional area of future work involves analyzing the joint contact forces generated during both non-amputee and amputee stair ascent. Knee contact forces measured in patients with instrumented knee replacements (e.g., Mundermann et al., 2008), determined by experimentally simulating stair ascent in cadaver knees (Gilbert et al., 2013) or estimated from subject-specific knee models (Costigan et al., 2002) are larger during stair ascent

compared to level walking. In addition, amputees often place additional stress on their intact limb to reduce stress on their residual limb, which can lead to the development of osteoarthritis (Gailey et al., 2008). Future work could use the simulations of stair ascent developed in this research to examine the joint loads experienced during stair ascent by both non-amputees and amputees and to determine the muscle contributions to these joint loads in order to identify the largest contributors. In addition, developing predictive simulations of stair ascent that minimize joint contact forces instead of tracking experimental data (e.g., Erdemir et al., 2007) could lead to an improved understanding of mechanisms for reducing joint loading during stair ascent. Overall, this work could provide insight into injury mechanisms and help guide the development of gait retraining programs to minimize joint loading in individuals who are particularly susceptible to the development of osteoarthritis or other degenerative joint diseases.

This research demonstrated the valuable insights that can be gained from analyses of simulations that emulate group-averaged data. However, amputees have been shown to demonstrate different individual compensations which may not be apparent in the averaged data (Powers et al., 1997; Silverman et al., 2008). Developing subject-specific simulations would enable clinicians to create customized therapies and devices. However, the use of simulations in the clinical environment is contingent upon the development of improved optimization frameworks that can more quickly produce biomechanically relevant simulations. Therefore, future work should focus on the development of more computationally efficient optimization techniques that facilitate the generation of subject-specific simulations.

Lastly, this work provided insights into the role of individual muscles and the prosthesis in non-amputee and amputee stair ascent, and future work should focus on developing and implementing targeted rehabilitation programs based on the results of

Chapters 2-4. In addition, future work should focus on developing improved prostheses that overcome the limitations of the current prostheses highlighted in Chapters 3 and 4. Therefore, while the studies presented in this dissertation provide valuable and novel insights into the contributions of individual muscles and the prosthesis to the subtasks of non-amputee and amputee stair ascent, there is significant potential for future work that expands upon this work.

Appendix A: Supplemental Material for Chapter 2

Table A.1: Muscles and analysis groups included in the musculoskeletal model and their parameters including maximum isometric force (F_o^M), optimal fiber length (l_o^M), tendon slack length (l_s^T), pennation angle (α) and activation (τ_{act}) and deactivation (τ_{deact}) time constants.

Muscles	Analysis Groups	F_O^M (N)	l_O^M (cm)	l_S^T (cm)	α (°)	τ_{act} (ms)	τ_{deact} (ms)
Iliacus	IL	429	10	9	7	12	48
Psoas		371	10.4	13	8	12	48
Adductor Longus	AL	418	13.8	11	6	12	48
Adductor Brevis		286	11.3	2	0	12	48
Pectineus		177	13.3	0.1	0	12	48
Quadratus Femoris		254	5.4	2.4	0	12	48
Superior Adductor Magnus	AM	346	8.7	6	5	12	48
Middle Adductor Magnus		312	12.1	13	3	12	48
Inferior Adductor Magnus		444	13.1	26	5	12	48
Sartorius	SAR	104	57.9	4	0	9	43
Rectus Femoris	RF	779	8.4	34.6	5	9	39
Vastus Medialis	VAS	1294	8.9	12.6	5	17	61
Vastus Lateralis		1871	8.4	15.7	5	16	58
Vastus Intermedius		1365	8.7	13.6	3	13	50
Anterior Gluteus Medius	GMEDA	546	5.35	7.8	8	12	48
Middle Gluteus Medius		382	8.45	5.3	0	12	48
Anterior Gluteus Minimus		180	6.8	1.6	10	12	48
Middle Gluteus Minimus		190	5.6	2.6	0	12	48
Posterior Gluteus Medius	GMEDP	435	6.46	5.3	19	12	48
Posterior Gluteus Minimus		215	3.8	5.1	21	12	48
Piriformis		296	2.6	11.5	10	12	48
Gemellus		109	2.4	3.9	0	12	48
Tensor Fasciae Latae	TFL	155	9.5	42.5	3	12	48
Superior Gluteus Maximus	GMAX	382	14.2	12.5	5	12	48
Middle Gluteus Maximus		546	14.7	12.7	0	12	48
Inferior Gluteus Maximus		368	14.4	14.5	5	12	48
Semitendinosus	HAM	328	20.1	26.2	5	12	48
Semimembranosus		1030	8	35.9	15	17	59
Gracilis		108	35.2	14	3	12	48
Biceps Femoris Long Head		717	10.9	34.1	0	17	60
Biceps Femoris Short Head	BFSH	402	17.3	10	23	11	45
Medial Gastrocnemius	GAS	1113	4.5	40.8	17	11	45
Lateral Gastrocnemius		488	6.4	38.5	8	9	38
Soleus	SOL	2839	3	26.8	25	31	111
Tibialis Posterior		1270	3.1	31	12	10	43
Flexor Digitorum Longus		310	3.4	40	7	9	39
Tibialis Anterior	TA	603	9.8	22.3	5	15	55
Extensor Digitorum Longus		341	10.2	34.5	8	7	37

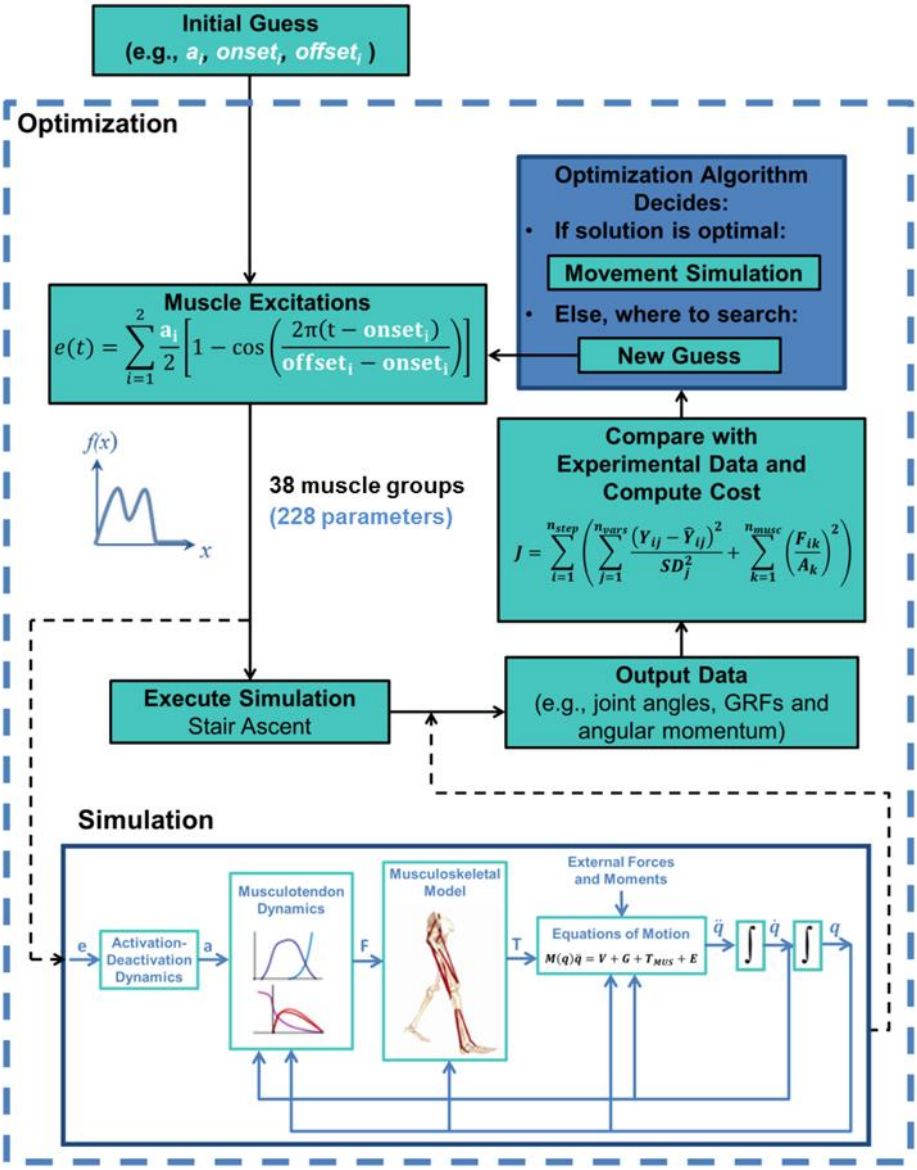

Figure A.1: Dynamic optimization framework for generating the stair ascent simulation.

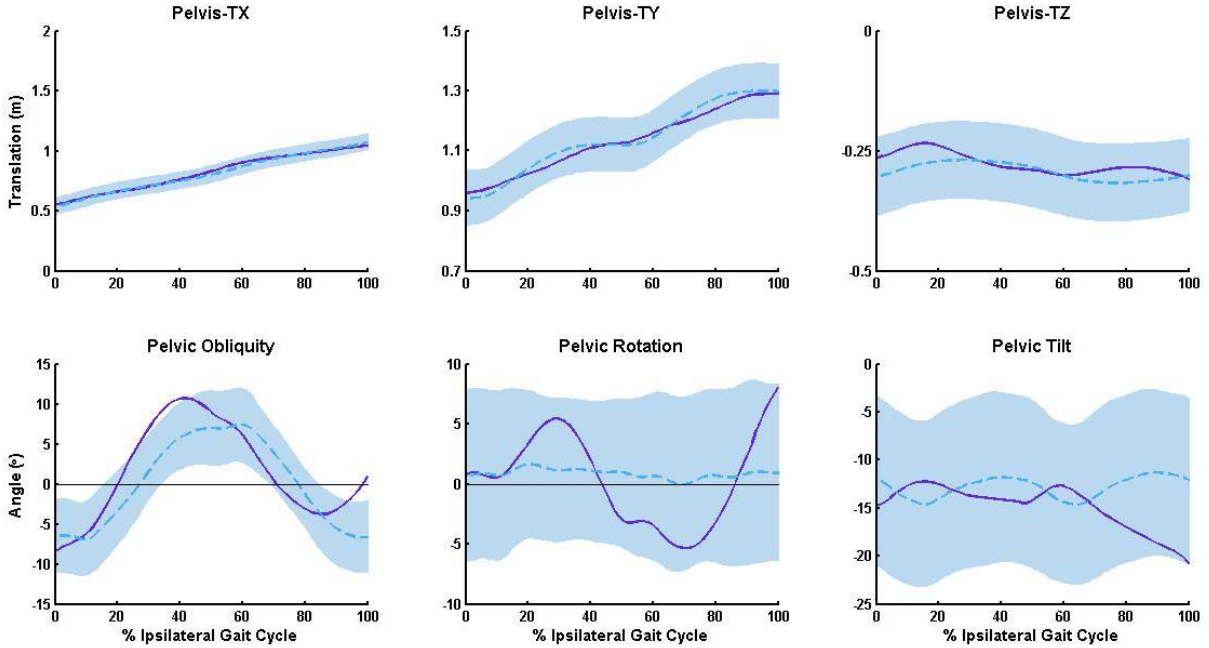

Figure A.2: Three-dimensional simulated (solid purple) and experimental (average - dashed blue; ± two experimental standard deviations - shaded blue) pelvis kinematics across the ipsilateral gait cycle during unimpaired stair ascent.

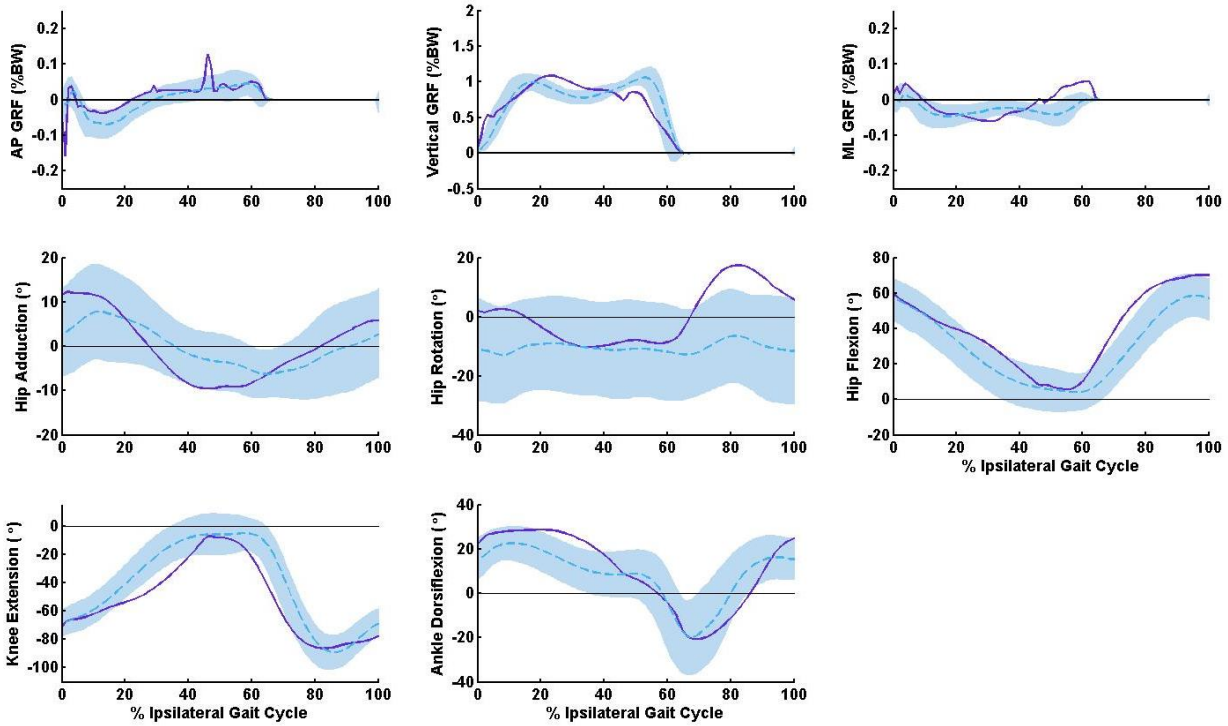

Figure A.3: Three-dimensional simulated (solid purple) and experimental (average - dashed blue; ± two experimental standard deviations - shaded blue) ground reaction forces (GRFs) and hip, knee and ankle kinematics for the ipsilateral leg across the ipsilateral gait cycle during unimpaired stair ascent. Positive values represent anterior, vertical and lateral GRFs, hip adduction, hip internal rotation, hip flexion, knee extension and ankle dorsiflexion.

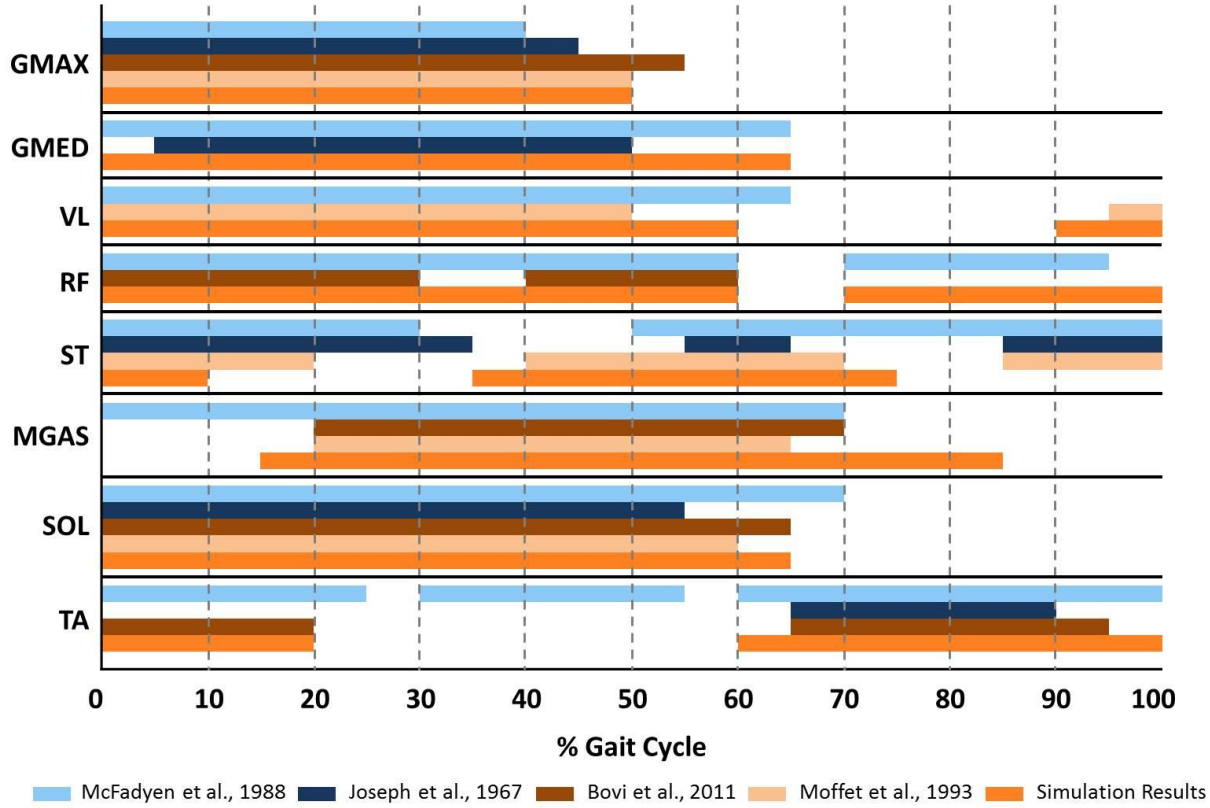

Figure A.4: Comparison of simulated (orange) and experimental (light blue, dark blue, burnt orange and beige) EMG timings for eight muscles available in the literature (Bovi et al., 2011; Joseph and Watson, 1967; McFadyen and Winter, 1988; Moffet et al., 1993) including gluteus maximus (superior, middle and inferior compartments summed: GMAX), gluteus medius (anterior, middle and posterior compartments summed: GMED), vastus lateralis (VL), rectus femoris (RF), semitendinosus (ST), medial gastrocnemius (MGAS), soleus (SOL) and tibialis anterior (TA).

Appendix B: Supplemental Material for Chapter 3

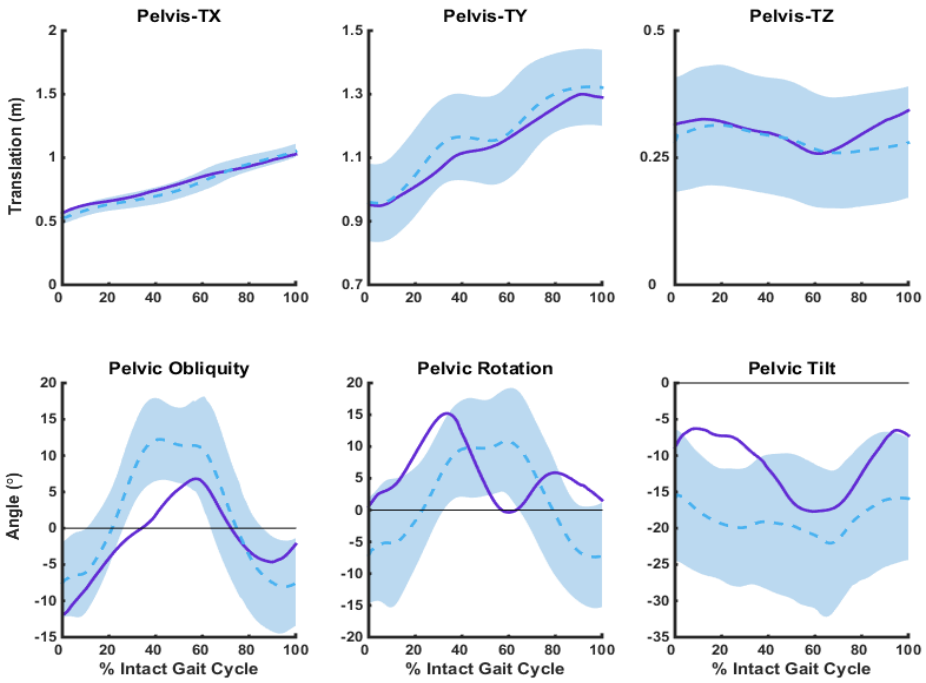

Figure B.1: Three-dimensional simulated (solid line) and experimental (average - dashed line; ± two experimental standard deviations - shaded area) pelvis kinematics across the intact leg gait cycle during amputee stair ascent.

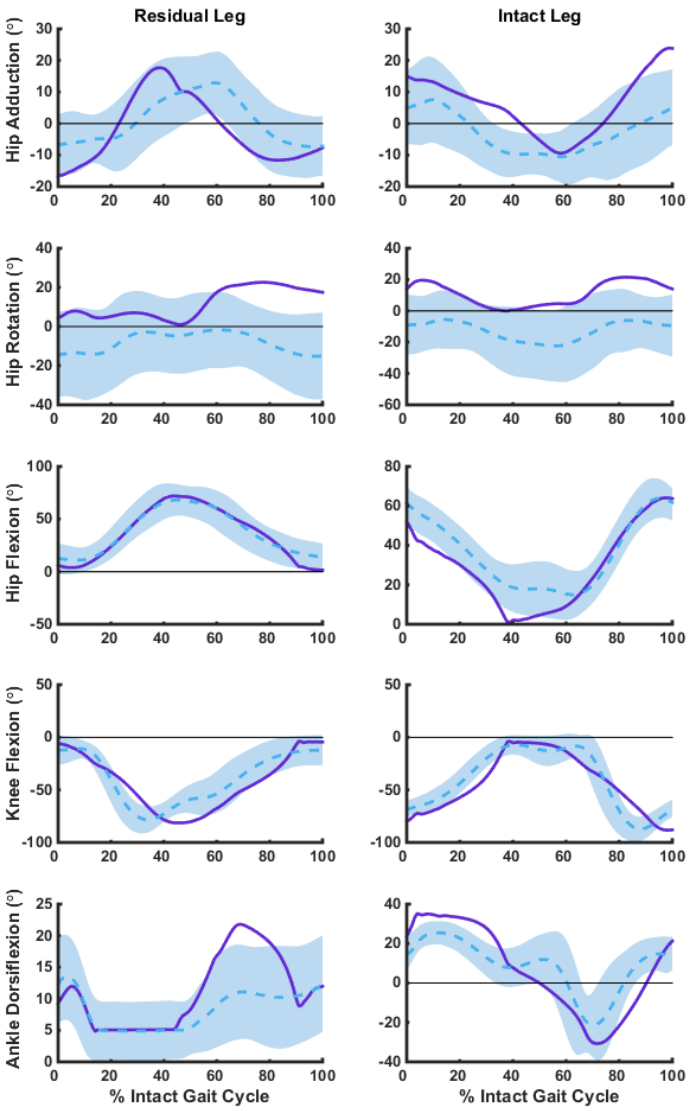

Figure B.2: Three-dimensional simulated (solid line) and experimental (average - dashed line; ± two experimental standard deviations - shaded area) hip, knee and ankle kinematics for the residual and intact legs across the intact leg gait cycle during amputee stair ascent. Positive values represent hip adduction, hip internal rotation, hip flexion, knee extension and ankle dorsiflexion.

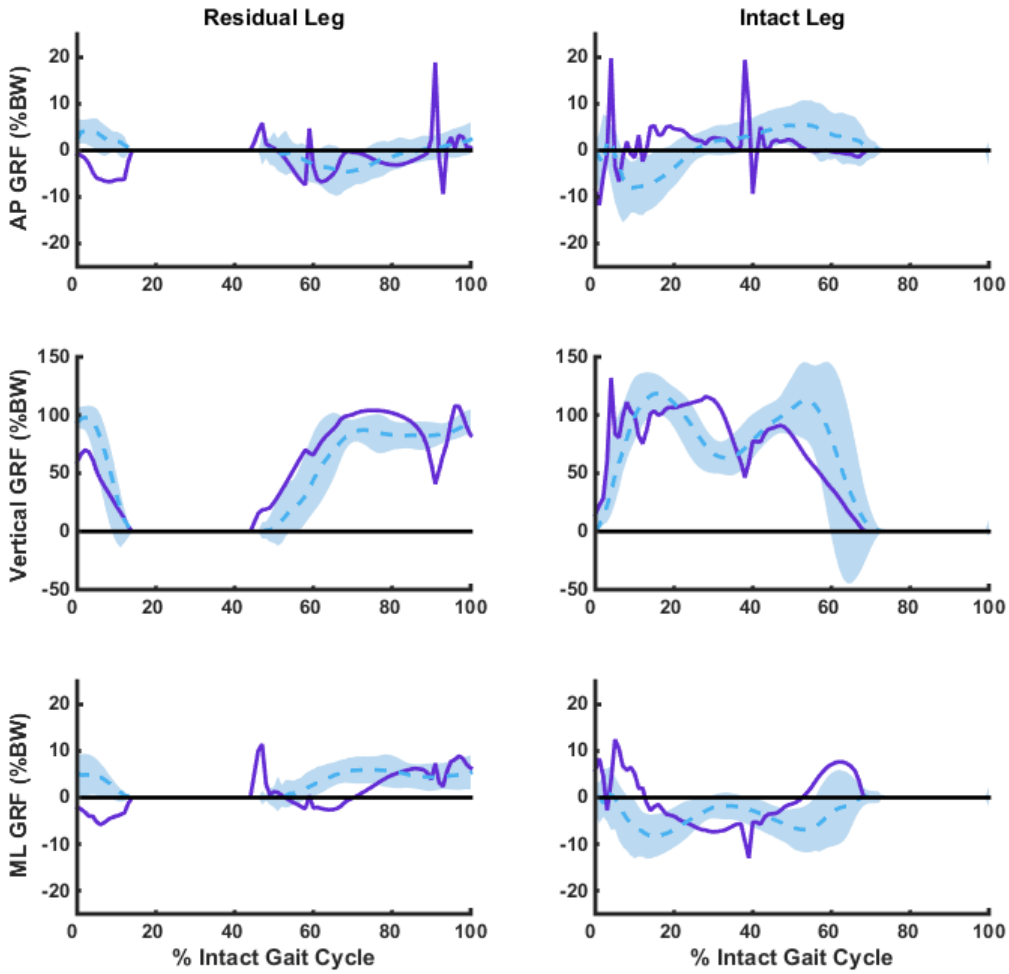

Figure B.3: Three-dimensional simulated (solid line) and experimental (average - dashed line; ± two experimental standard deviations - shaded area) anteroposterior (AP), vertical and mediolateral (ML) ground reaction forces (GRFs) for the residual and intact legs across the intact leg gait cycle during amputee stair ascent. In the residual (left) leg, positive values represent anterior, vertical and medial GRFs. In the intact (right) leg, positive values represent anterior, vertical and lateral GRFs.

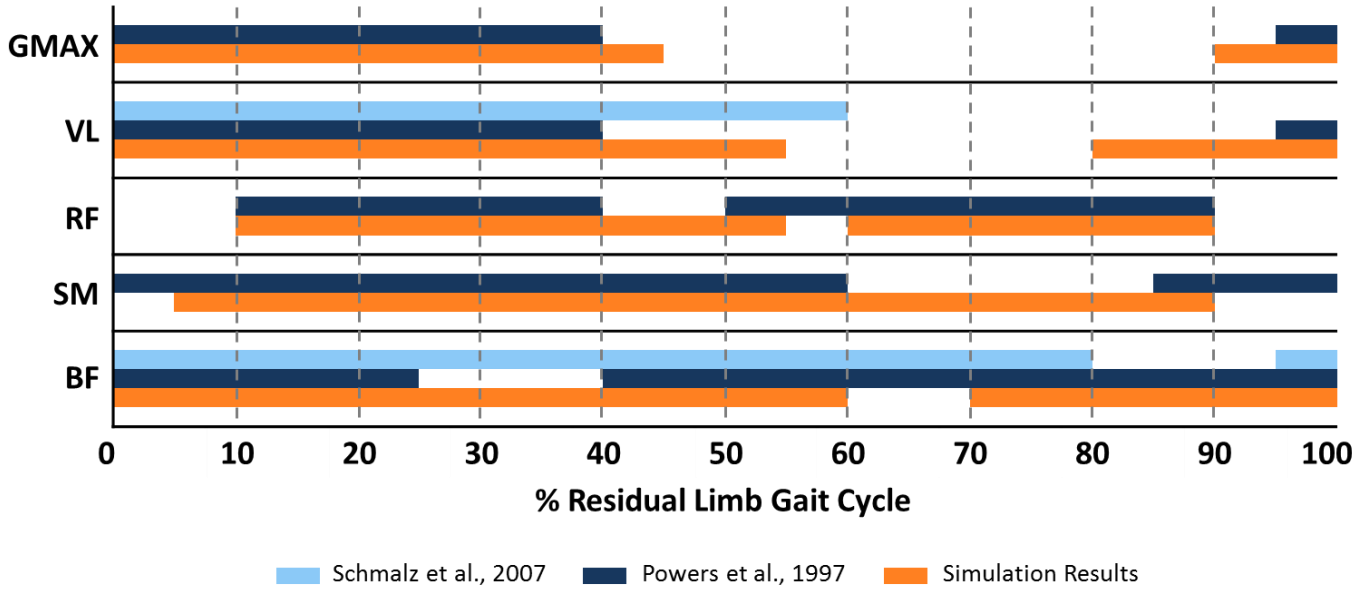

Figure B.4: Comparison of simulated (orange) and experimental (light blue and dark blue) EMG timings for five muscles available in the literature (Powers et al., 1997; Schmalz et al., 2007) including gluteus maximus (superior, middle and inferior compartments summed: GMAX), vastus lateralis (VL), rectus femoris (RF), semimembranosus (SM), and biceps femoris (long and short heads summed: BF).

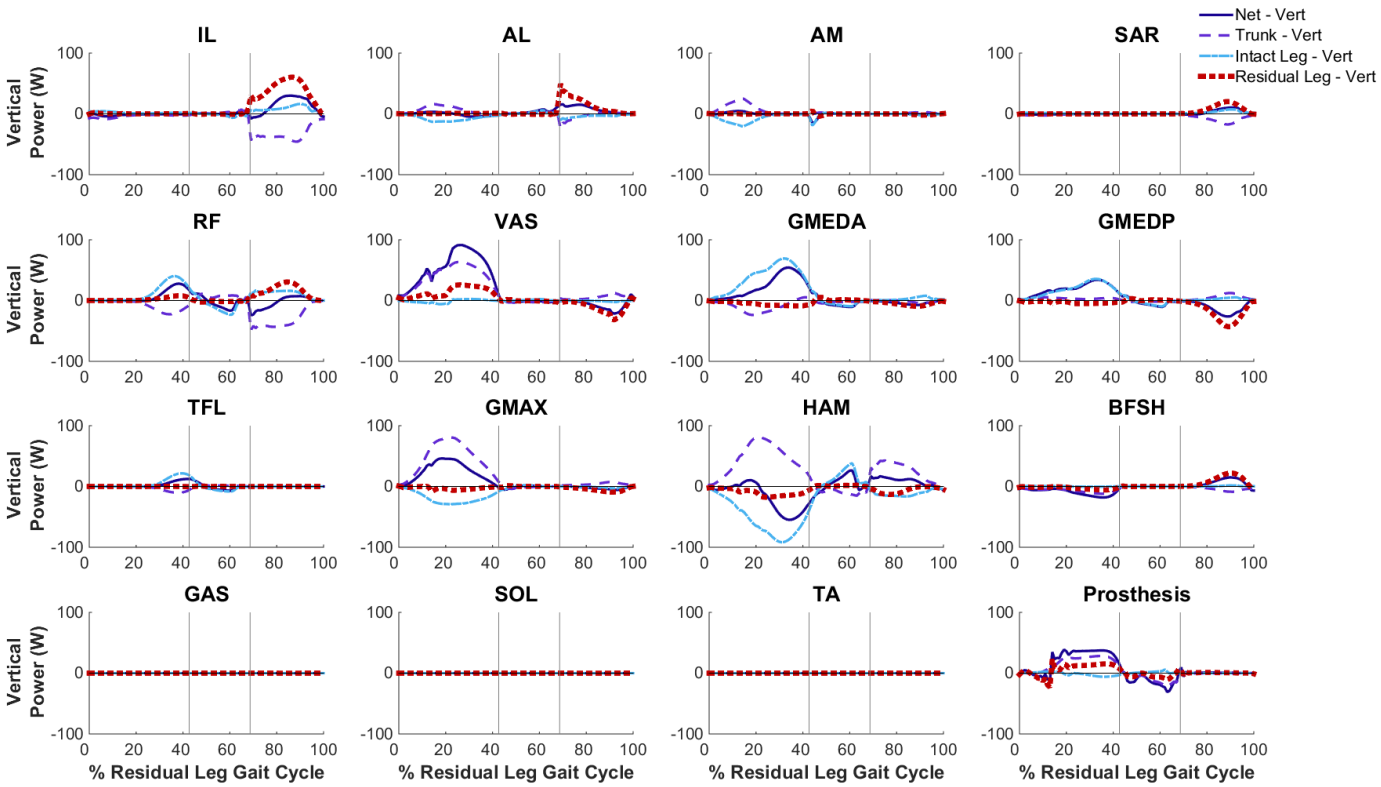

Figure B.5: Musculotendon mechanical power output from the residual leg muscles across the residual leg gait cycle and distributed to the trunk, intact leg and residual leg in the vertical direction. Positive (negative) net values indicate power generated (absorbed) by the musculotendon actuator. Positive (negative) values for the leg or trunk indicate that power is being generated to (absorbed from) the leg or trunk. The gray lines divide the gait cycle into three regions: 1) weight acceptance through pull-up, 2) forward continuance through push-up, and 3) swing (foot clearance through foot placement). For muscle group abbreviations, please see Table 3.1.

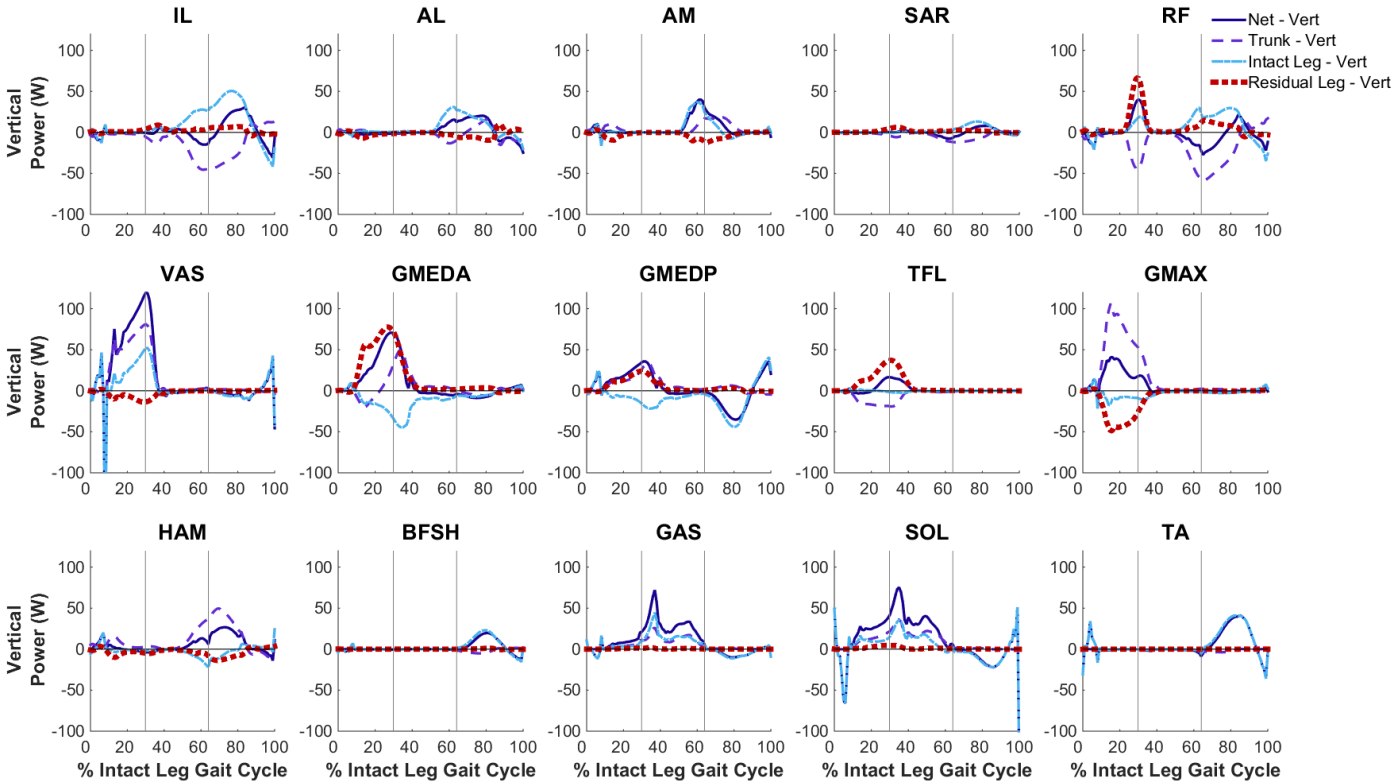

Figure B.6: Musculotendon mechanical power output from the intact leg muscles across the intact leg gait cycle and distributed to the trunk, intact leg and residual leg in the vertical direction. Positive (negative) net values indicate power generated (absorbed) by the musculotendon actuator. Positive (negative) values for the leg or trunk indicate that power is being generated to (absorbed from) the leg or trunk. The gray lines divide the gait cycle into three regions: 1) weight acceptance through pull-up, 2) forward continuance through push-up, and 3) swing (foot clearance through foot placement). For muscle group abbreviations, please see Table 3.1.

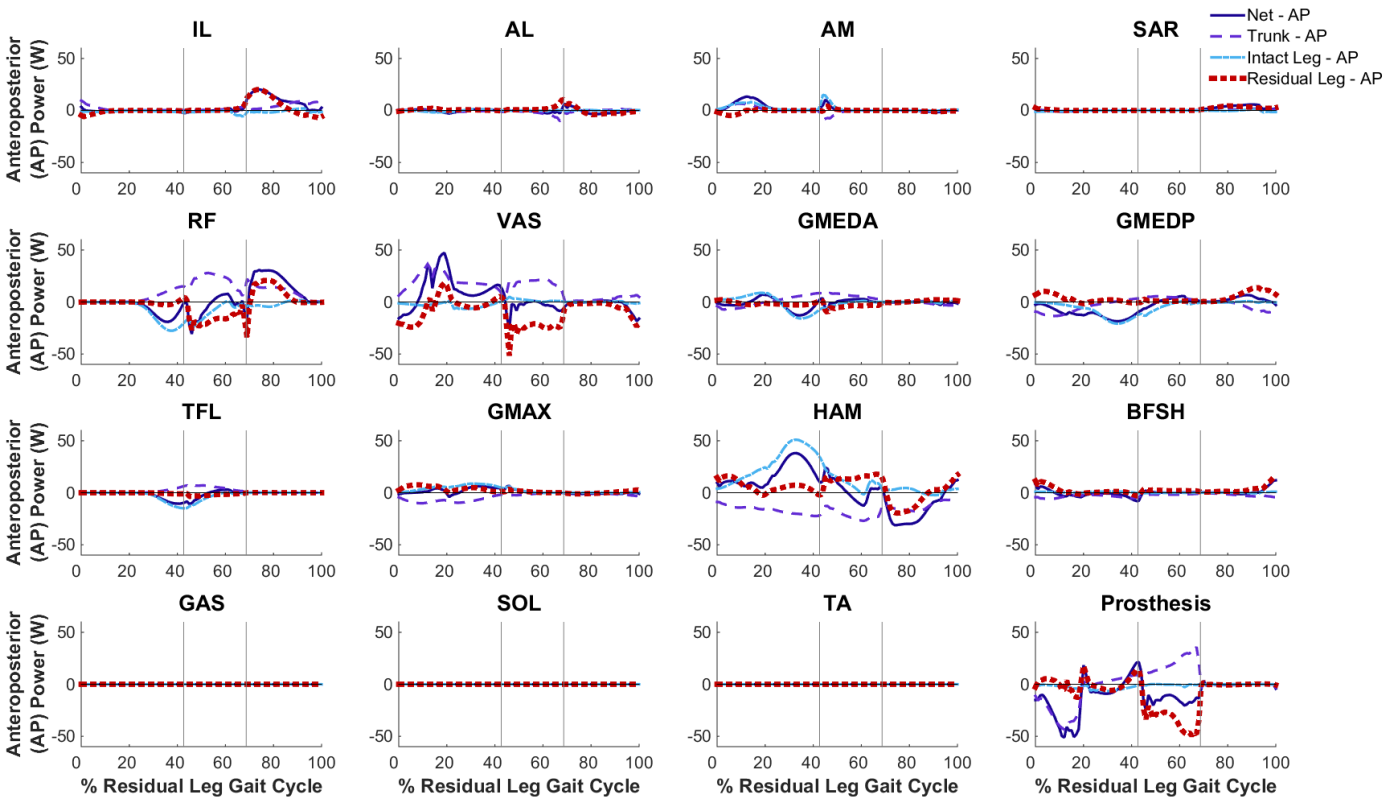

Figure B.7: Musculotendon mechanical power output from the residual leg muscles across the residual leg gait cycle and distributed to the trunk, intact leg and residual leg in the anteroposterior (AP) direction. Positive (negative) net values indicate power generated (absorbed) by the musculotendon actuator. Positive (negative) values for the leg or trunk indicate that power is being generated to (absorbed from) the leg or trunk. The gray lines divide the gait cycle into three regions: 1) weight acceptance through pull-up, 2) forward continuance through push-up, and 3) swing (foot clearance through foot placement). For muscle group abbreviations, please see Table 3.1.

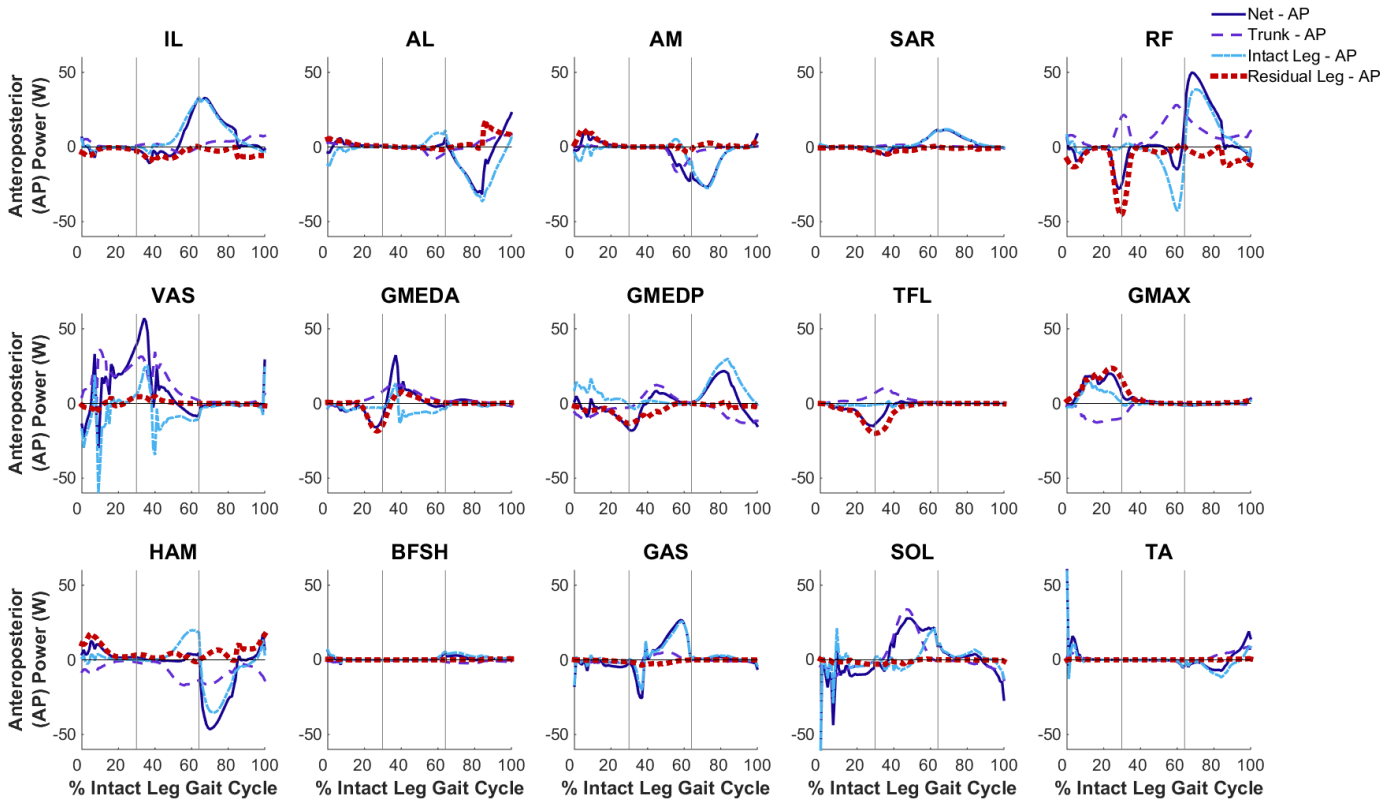

Figure B.8: Musculotendon mechanical power output from the intact leg muscles across the intact leg gait cycle and distributed to the trunk, intact leg and residual leg in the anteroposterior (AP) direction. Positive (negative) net values indicate power generated (absorbed) by the musculotendon actuator. Positive (negative) values for the leg or trunk indicate that power is being generated to (absorbed from) the leg or trunk. The gray lines divide the gait cycle into three regions: 1) weight acceptance through pull-up, 2) forward continuance through push-up, and 3) swing (foot clearance through foot placement). For muscle group abbreviations, please see Table 3.1.

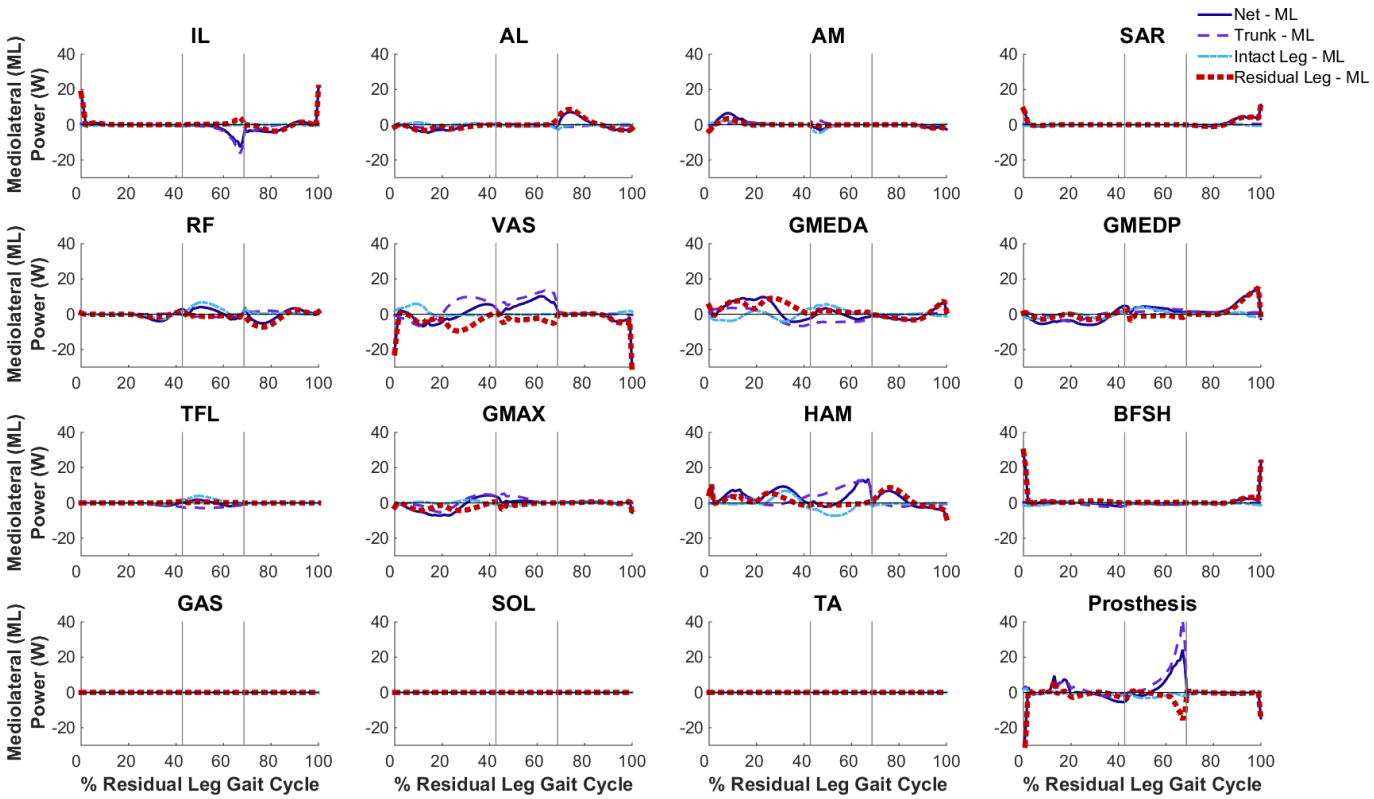

Figure B.9: Musculotendon mechanical power output from the residual leg muscles across the residual leg gait cycle and distributed to the trunk, intact leg and residual leg in the mediolateral (ML) direction. Positive (negative) net values indicate power generated (absorbed) by the musculotendon actuator. Positive (negative) values for the leg or trunk indicate that power is being generated to (absorbed from) the leg or trunk. The gray lines divide the gait cycle into three regions: 1) weight acceptance through pull-up, 2) forward continuance through push-up, and 3) swing (foot clearance through foot placement). For muscle group abbreviations, please see Table 3.1.

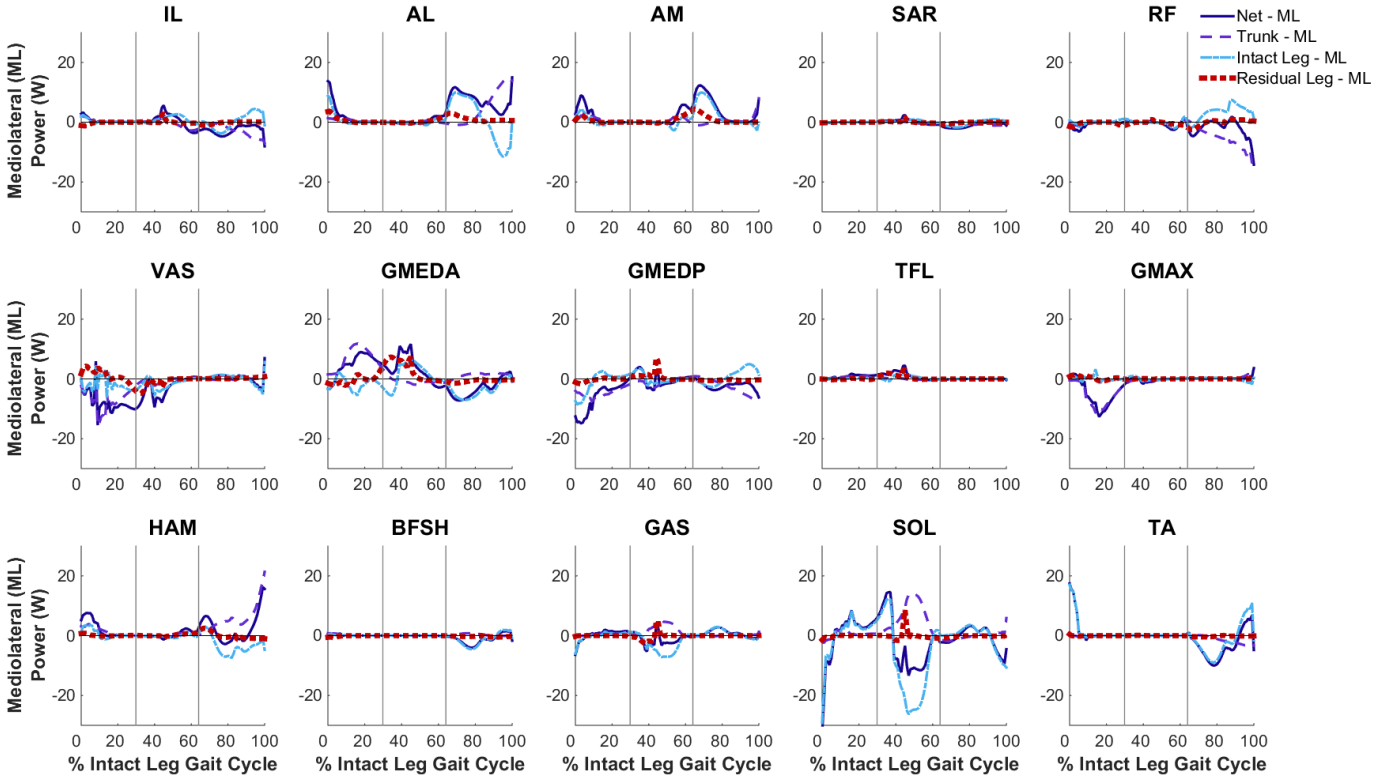

Figure B.10: Musculotendon mechanical power output from the intact leg muscles across the intact leg gait cycle and distributed to the trunk, intact leg and residual leg in the mediolateral (ML) direction. Positive (negative) net values indicate power generated (absorbed) by the musculotendon actuator. Positive (negative) values for the leg or trunk indicate that power is being generated to (absorbed from) the leg or trunk. The gray lines divide the gait cycle into three regions: 1) weight acceptance through pull-up, 2) forward continuance through push-up, and 3) swing (foot clearance through foot placement). For muscle group abbreviations, please see Table 3.1.

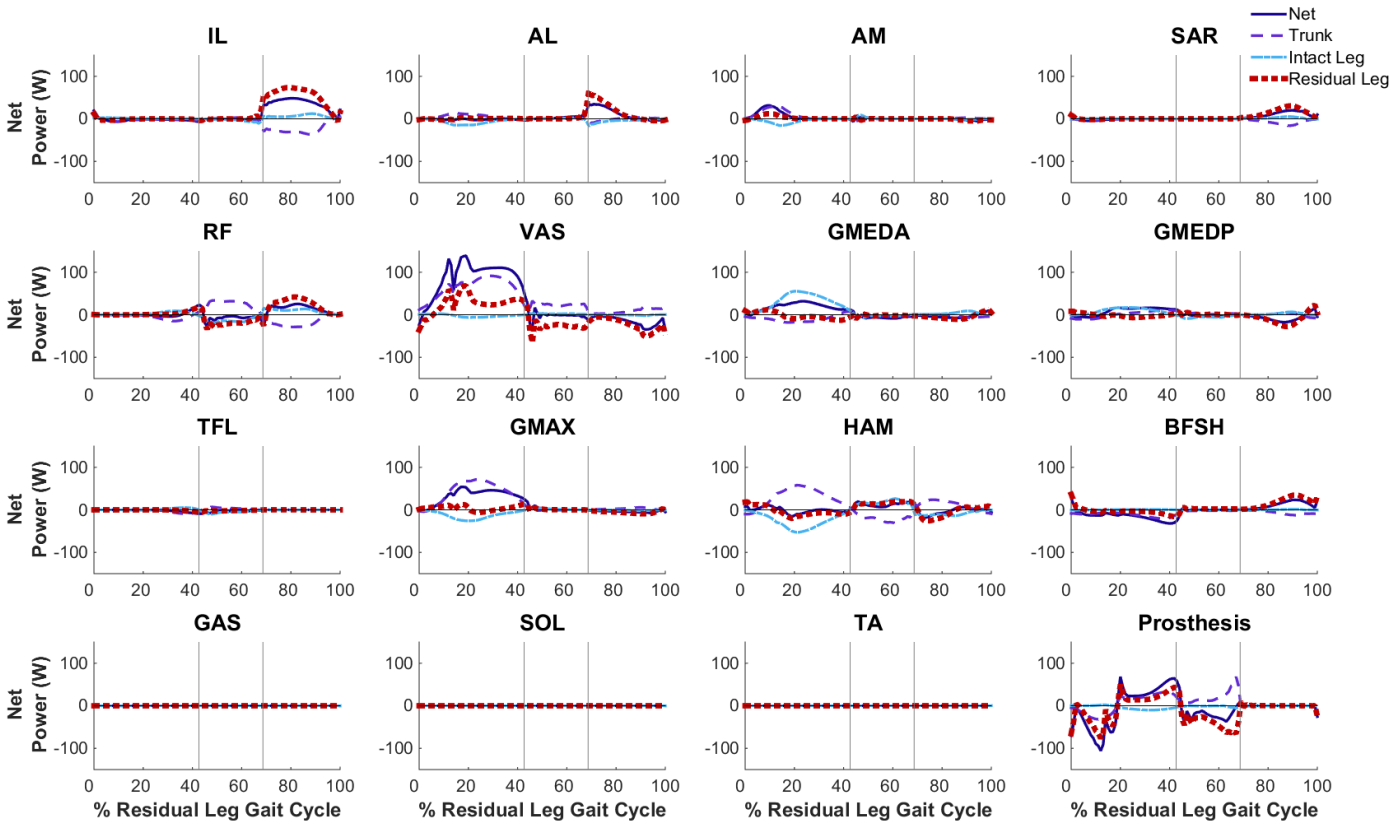

Figure B.11: Musculotendon mechanical power output from the residual leg muscles across the residual leg gait cycle and distributed to the trunk, intact leg and residual leg. Positive (negative) net values indicate power generated (absorbed) by the musculotendon actuator. Positive (negative) values for the leg or trunk indicate that power is being generated to (absorbed from) the leg or trunk. The gray lines divide the gait cycle into three regions: 1) weight acceptance through pull-up, 2) forward continuance through push-up, and 3) swing (foot clearance through foot placement). For muscle group abbreviations, please see Table 3.1.

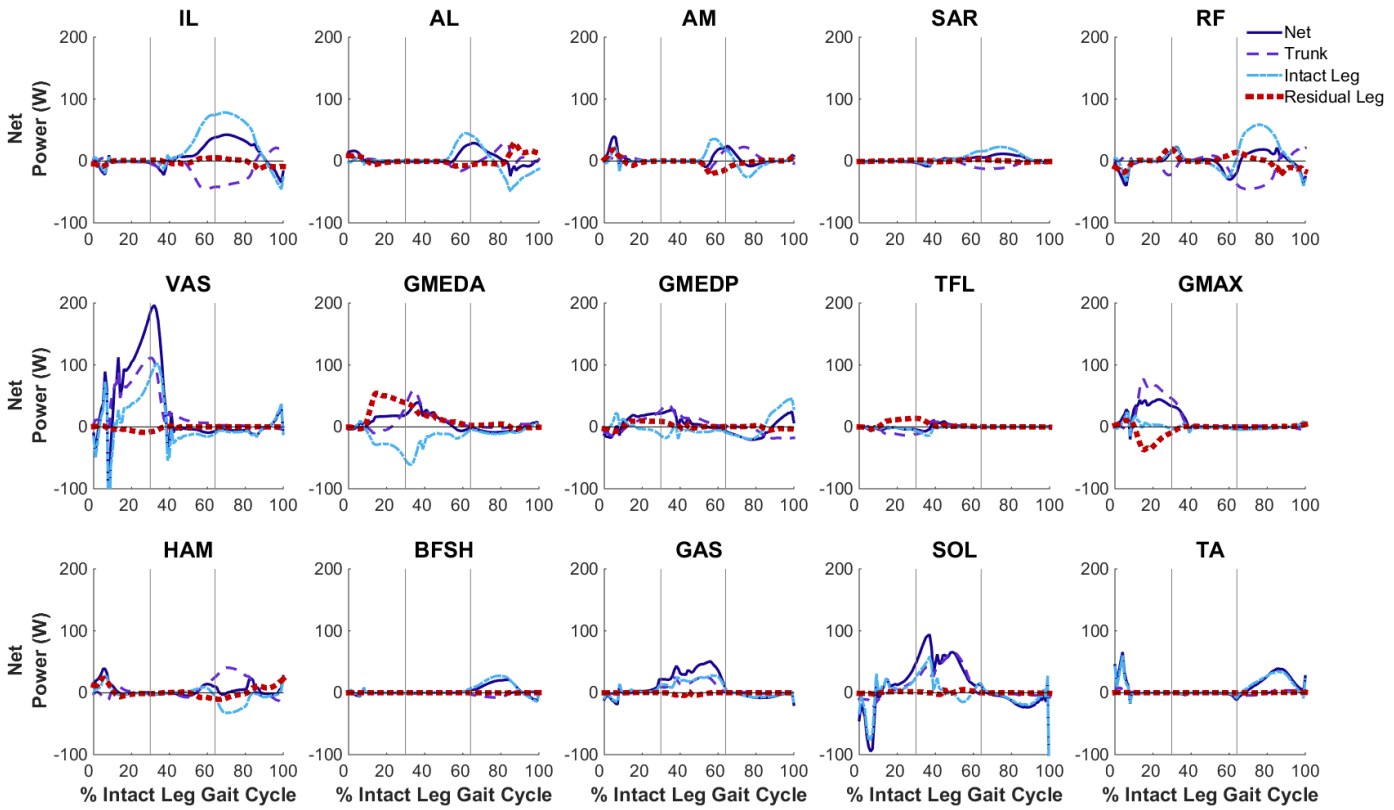

Figure B.12: Musculotendon mechanical power output from the intact leg muscles across the intact leg gait cycle and distributed to the trunk, intact leg and residual leg. Positive (negative) net values indicate power generated (absorbed) by the musculotendon actuator. Positive (negative) values for the leg or trunk indicate that power is being generated to (absorbed from) the leg or trunk. The gray lines divide the gait cycle into three regions: 1) weight acceptance through pull-up, 2) forward continuance through push-up, and 3) swing (foot clearance through foot placement). For muscle group abbreviations, please see Table 3.1.

Appendix C: Supplemental Material for Chapter 4

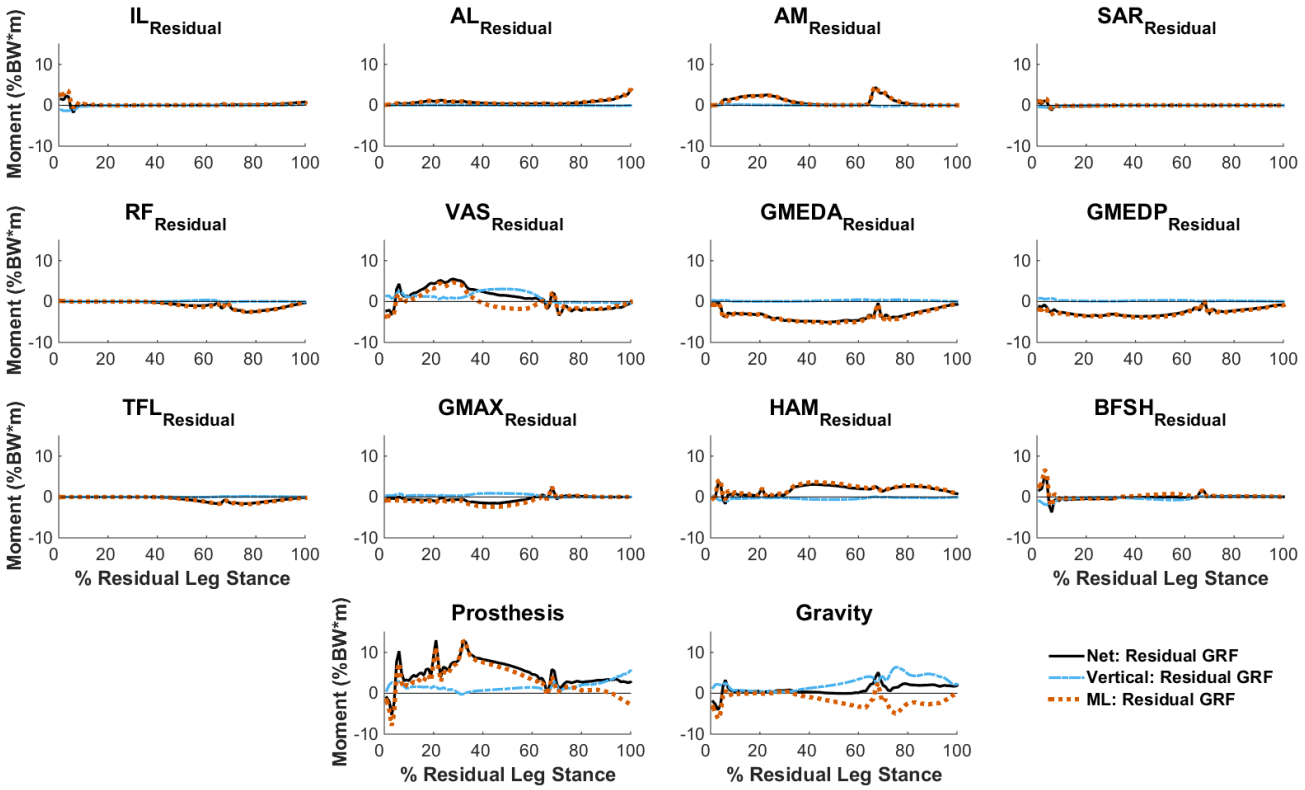

Figure C.1: External frontal-plane moments about the center-of-mass (time rate of change of angular momentum) during residual stance (left leg of the amputee simulation) generated by the contributions of muscles from the residual leg, the prosthesis and gravity to the residual vertical and mediolateral (ML) ground reaction forces (GRF). Positive (negative) values indicate angular momentum that acted to rotate the body towards the contralateral (ipsilateral) leg. Contributions to the residual vertical and ML GRFs from the intact leg were small. See Table 4.1 for muscle group abbreviations.

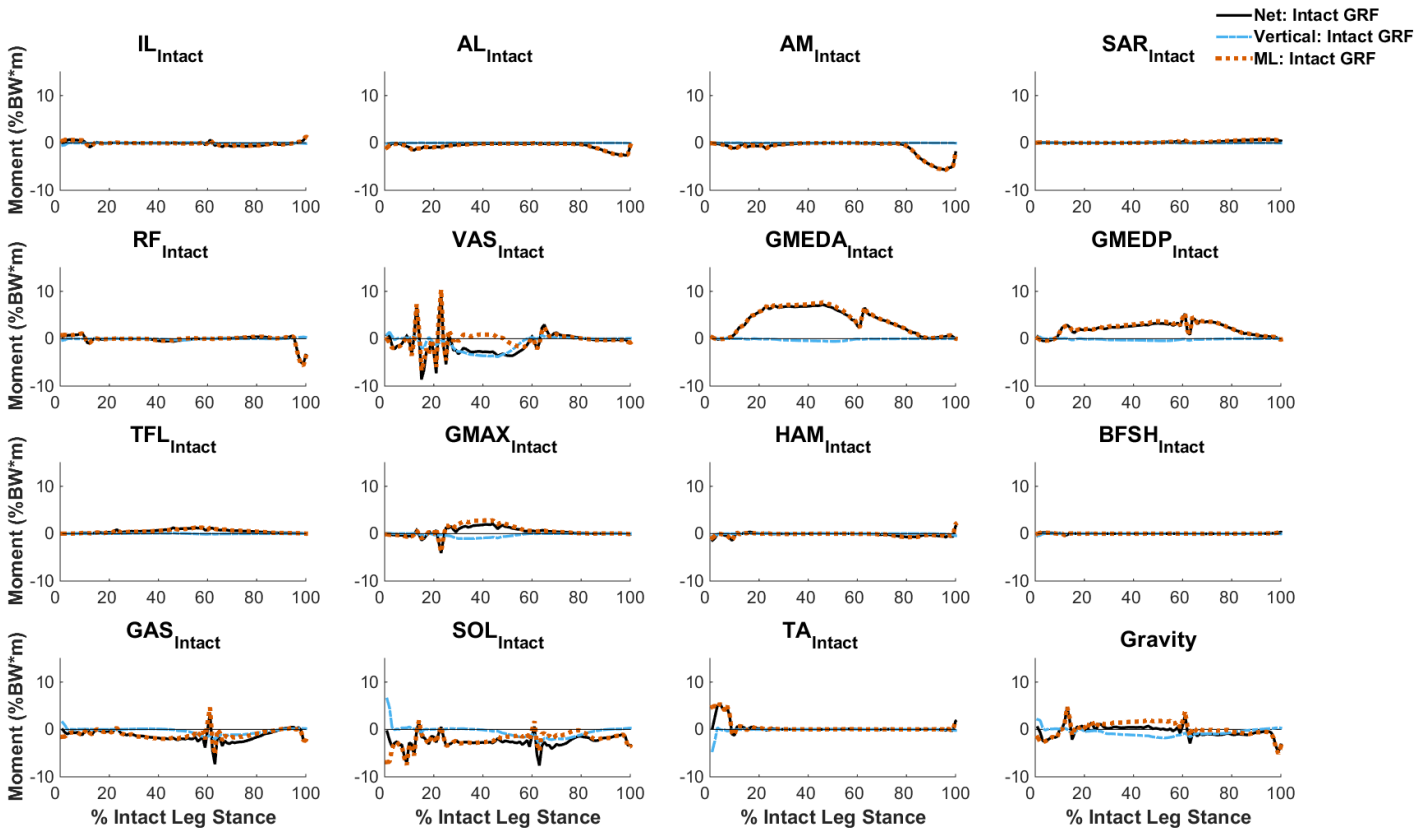

Figure C.2: External frontal-plane moments about the center-of-mass (time rate of change of angular momentum) during intact stance (right leg of the amputee simulation) generated by the contributions of muscles from the intact leg and gravity to the intact vertical and mediolateral (ML) ground reaction forces (GRF). Positive (negative) values indicate angular momentum that acted to rotate the body towards the ipsilateral (contralateral) leg. Contributions to the intact vertical and ML GRFs from the residual leg were small. See Table 4.1 for muscle group abbreviations.

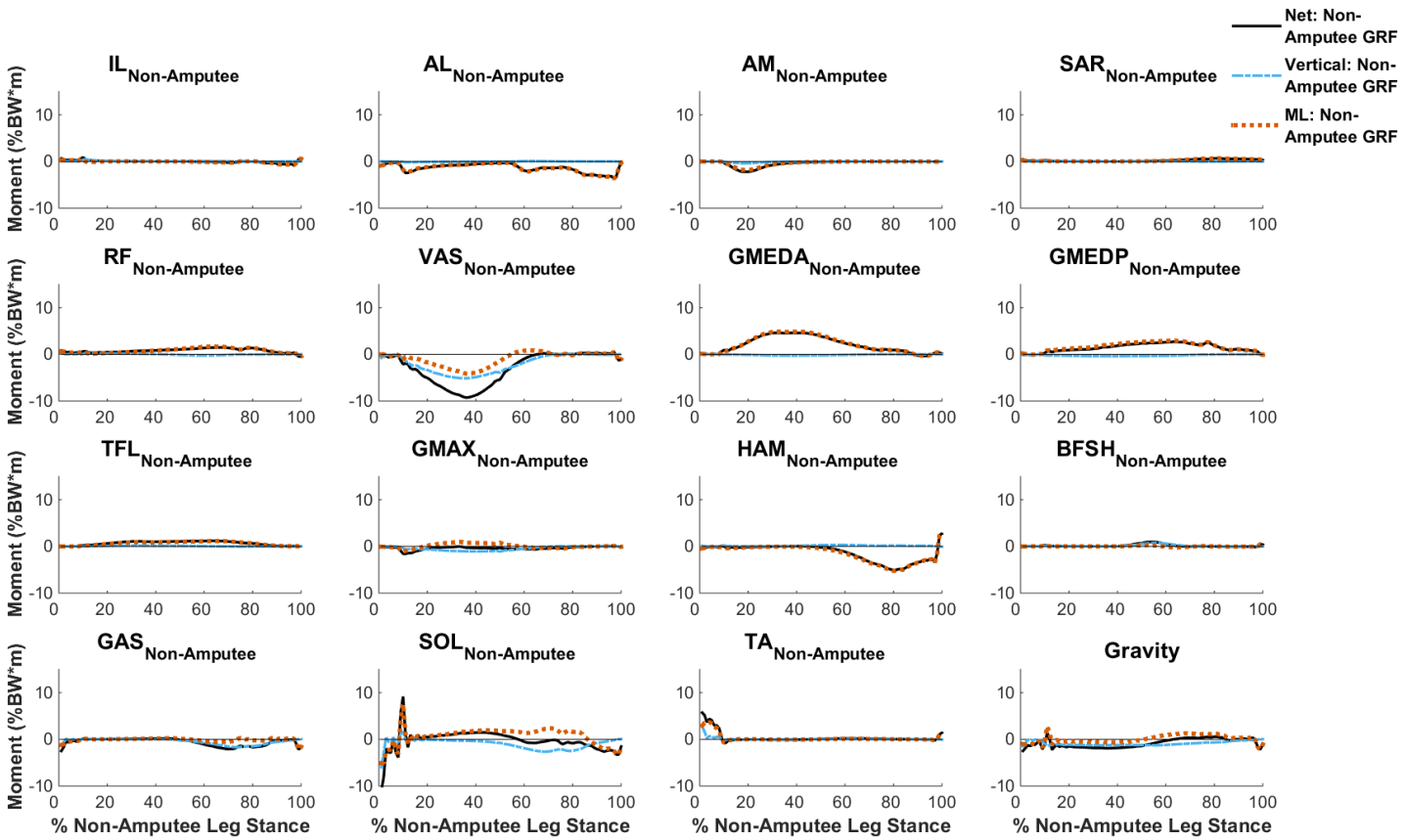

Figure C.3: External frontal-plane moments about the center-of-mass (time rate of change of angular momentum) during non-amputee stance (right leg of the non-amputee simulation) generated by the contributions of muscles from the non-amputee leg and gravity to the non-amputee vertical and mediolateral (ML) ground reaction forces (GRF). Positive (negative) values indicate angular momentum that acted to rotate the body towards the ipsilateral (contralateral) leg. Due to model symmetry, the contributions from both non-amputee legs were identical and only one leg is presented. See Table 4.1 for muscle group abbreviations.

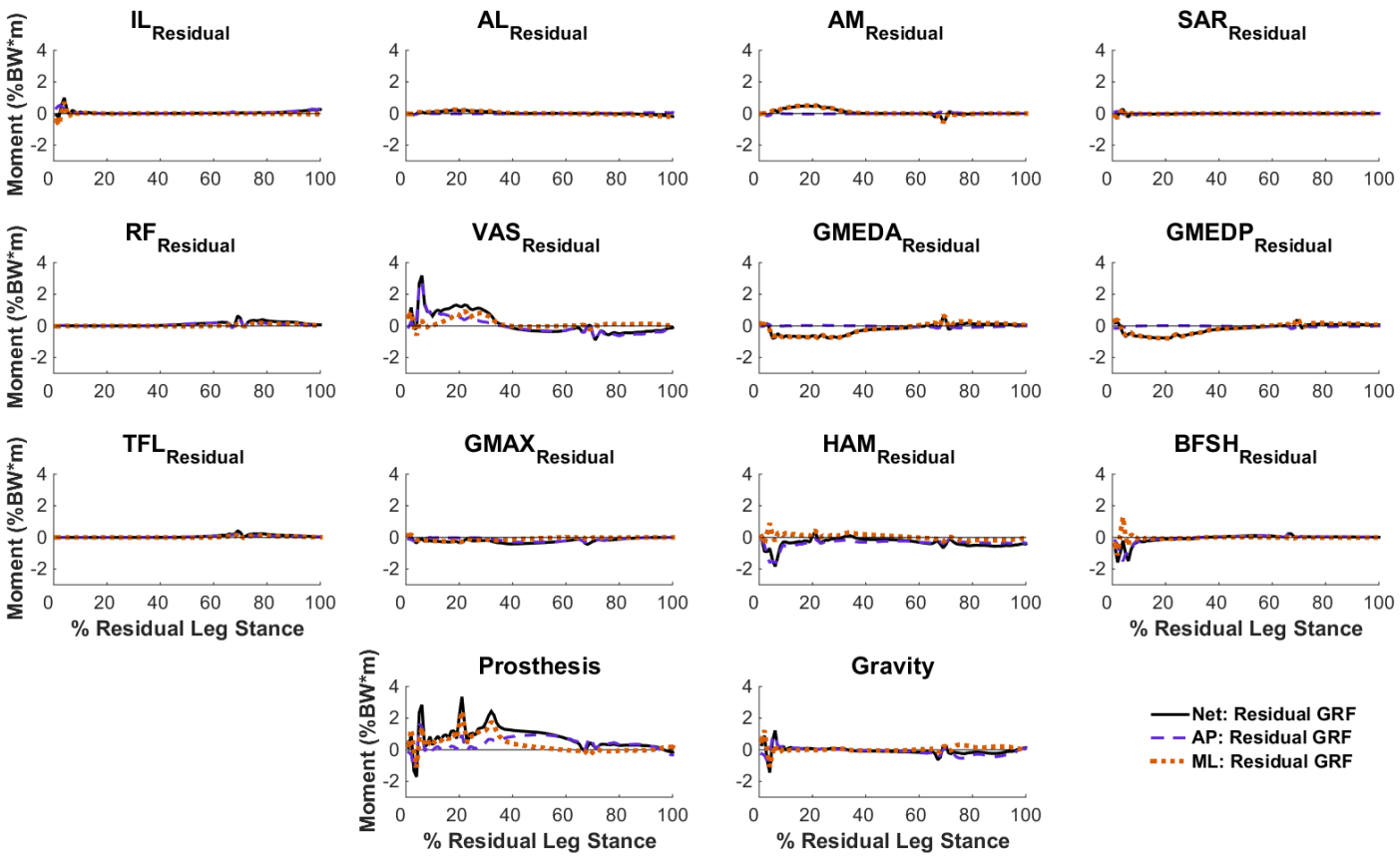

Figure C.4: External transverse-plane moments about the center-of-mass (time rate of change of angular momentum) during residual stance (left leg of the amputee simulation) generated by the contributions of muscles from the residual leg, the prosthesis and gravity to the residual anteroposterior (AP) and mediolateral (ML) ground reaction forces (GRF). Positive (negative) values indicate angular momentum that acted to rotate the body vertically towards the ipsilateral (contralateral) leg. Contributions to the residual AP and ML GRFs from the intact leg were small. See Table 4.1 for muscle group abbreviations.

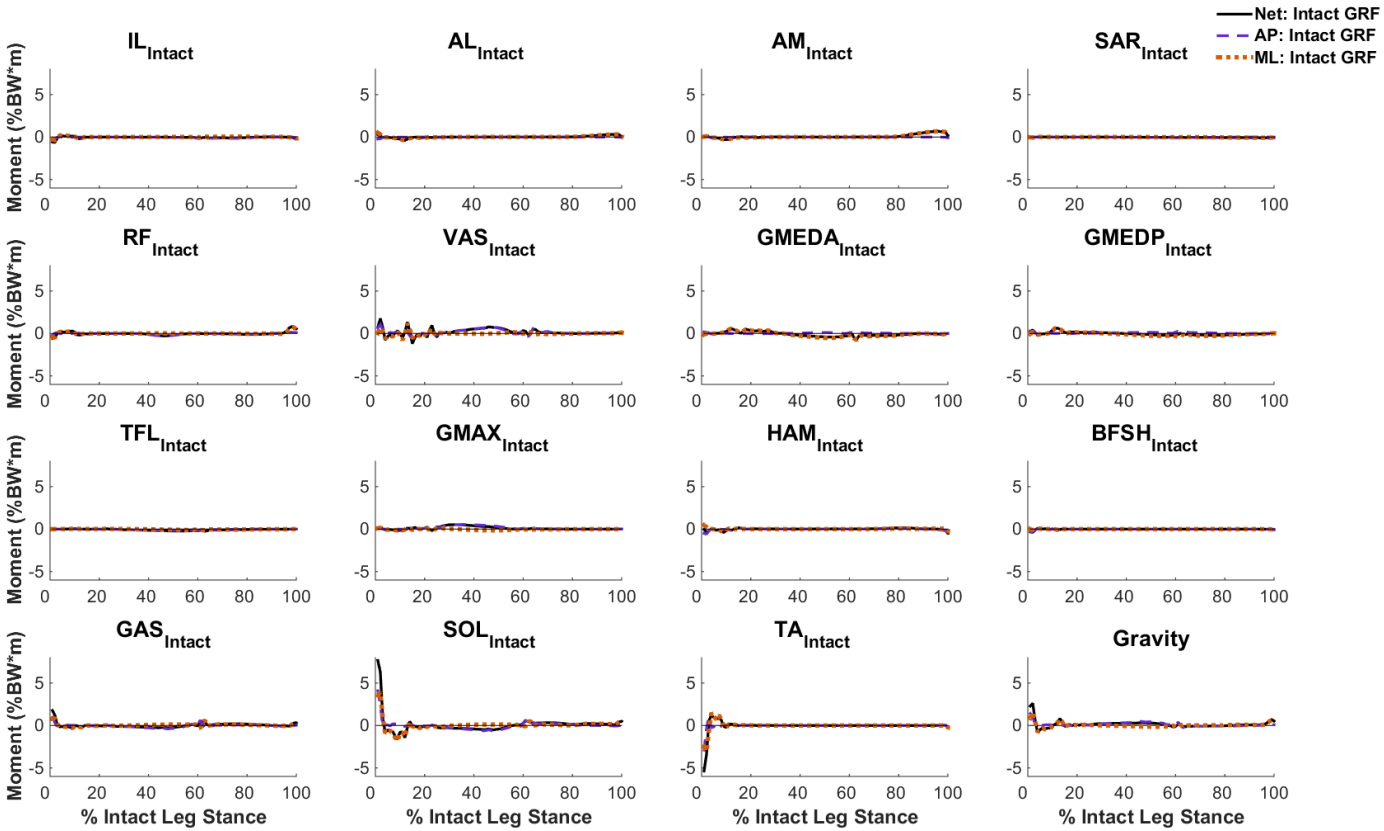

Figure C.5: External transverse-plane moments about the center-of-mass (time rate of change of angular momentum) during intact stance (right leg of the amputee simulation) generated by the contributions of muscles from the intact leg and gravity to the intact anteroposterior (AP) and mediolateral (ML) ground reaction forces (GRF). Positive (negative) values indicate angular momentum that acted to rotate the body vertically towards the contralateral (ipsilateral) leg. Contributions to the intact AP and ML GRFs from the residual leg were small. See Table 4.1 for muscle group abbreviations.

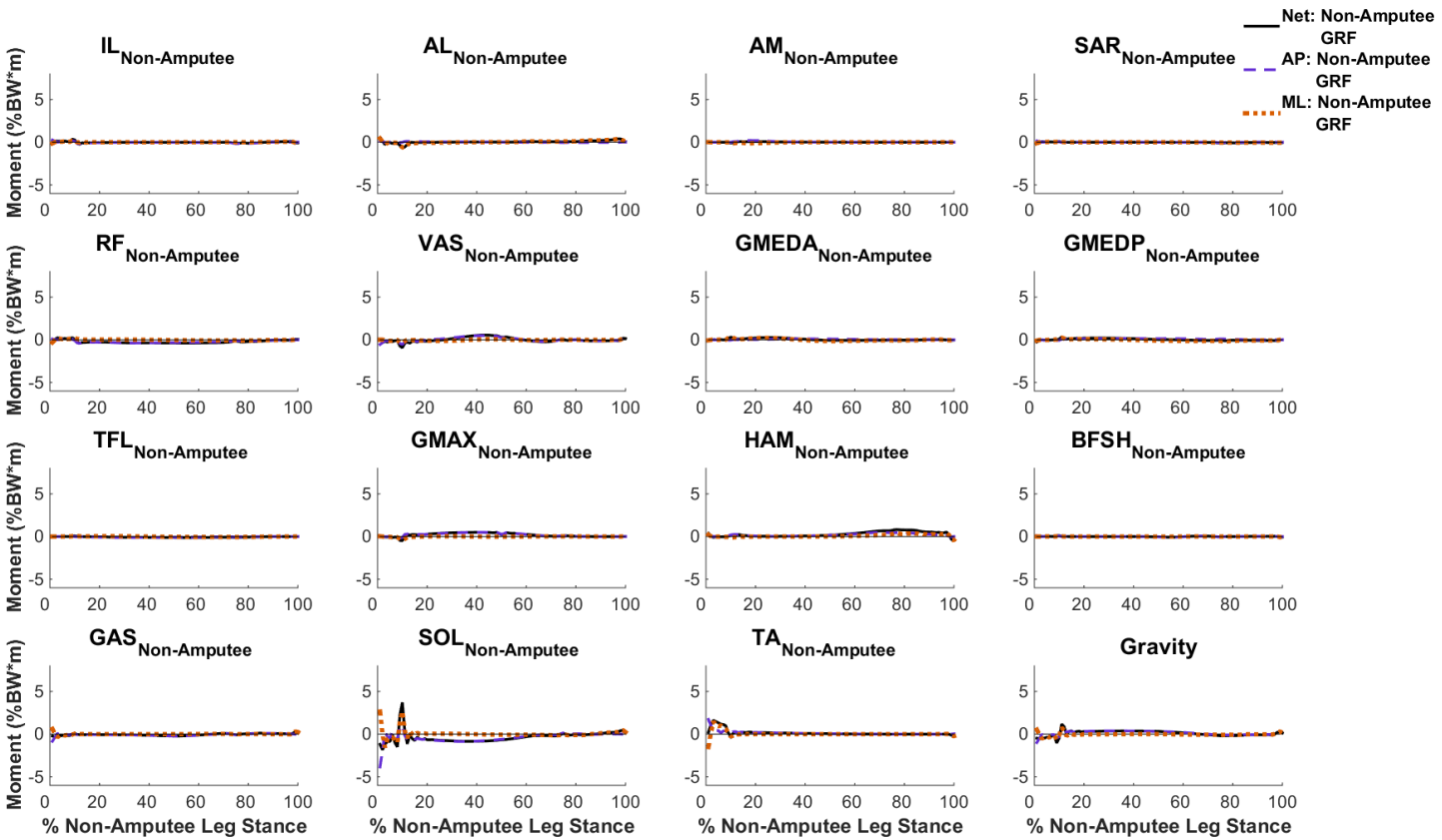

Figure C.6: External transverse-plane moments about the center-of-mass (time rate of change of angular momentum) during non-amputee stance (right leg of the non-amputee simulation) generated by the contributions of muscles from the non-amputee leg and gravity to the non-amputee anteroposterior (AP) and mediolateral (ML) ground reaction forces (GRF). Positive (negative) values indicate angular momentum that acted to rotate the body vertically towards the contralateral (ipsilateral) leg. Due to model symmetry, the contributions from both non-amputee legs were identical and only one leg is presented. See Table 4.1 for muscle group abbreviations.

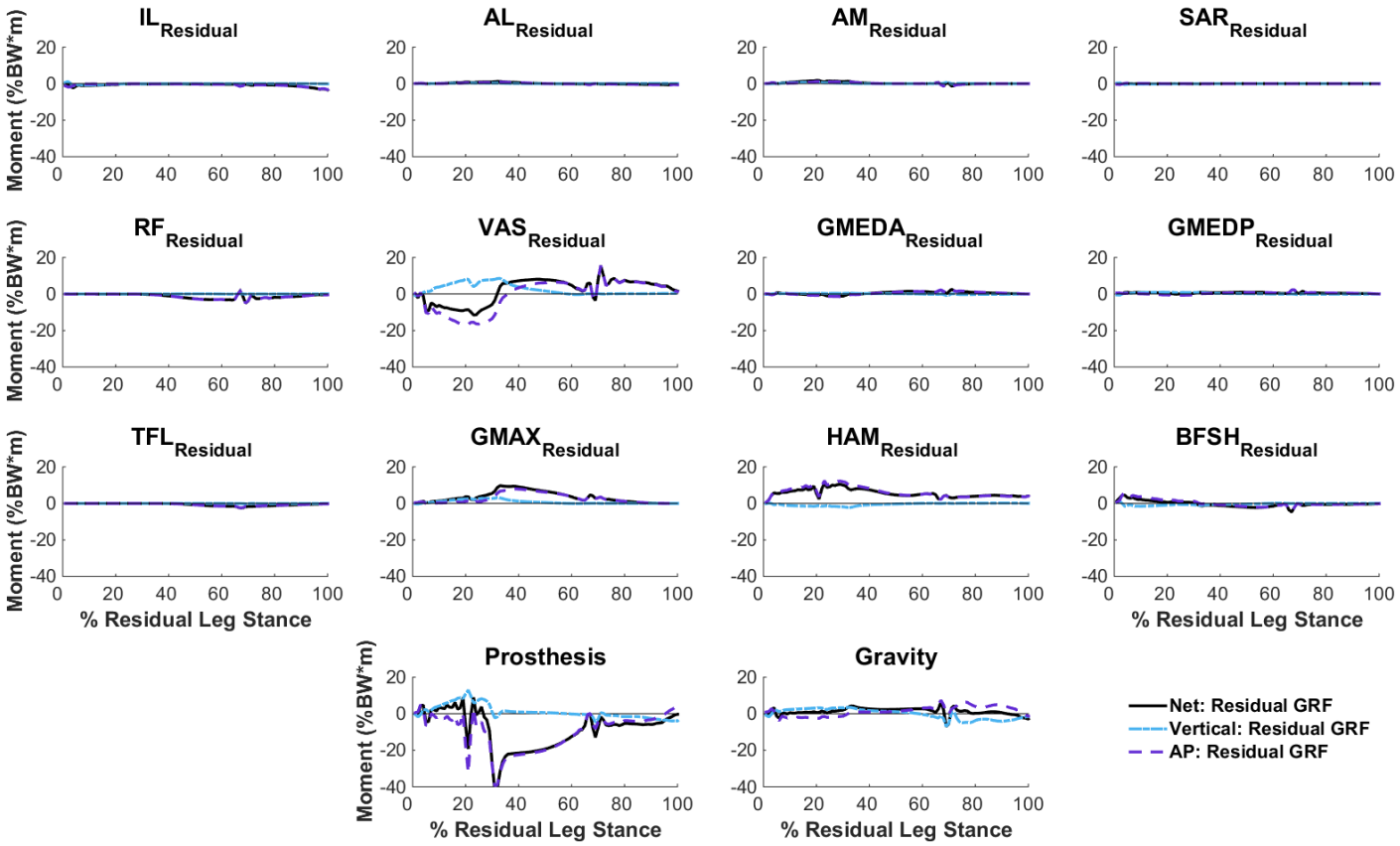

Figure C.7: External sagittal-plane moments about the center-of-mass (time rate of change of angular momentum) during residual stance (left leg of the amputee simulation) generated by the contributions of muscles from the residual leg, the prosthesis and gravity to the residual vertical and anteroposterior (AP) ground reaction forces (GRF). Positive (negative) values indicate angular momentum that acted to rotate the body backward (forward). Contributions to the residual vertical and AP GRFs from the intact leg were small. See Table 4.1 for muscle group abbreviations.

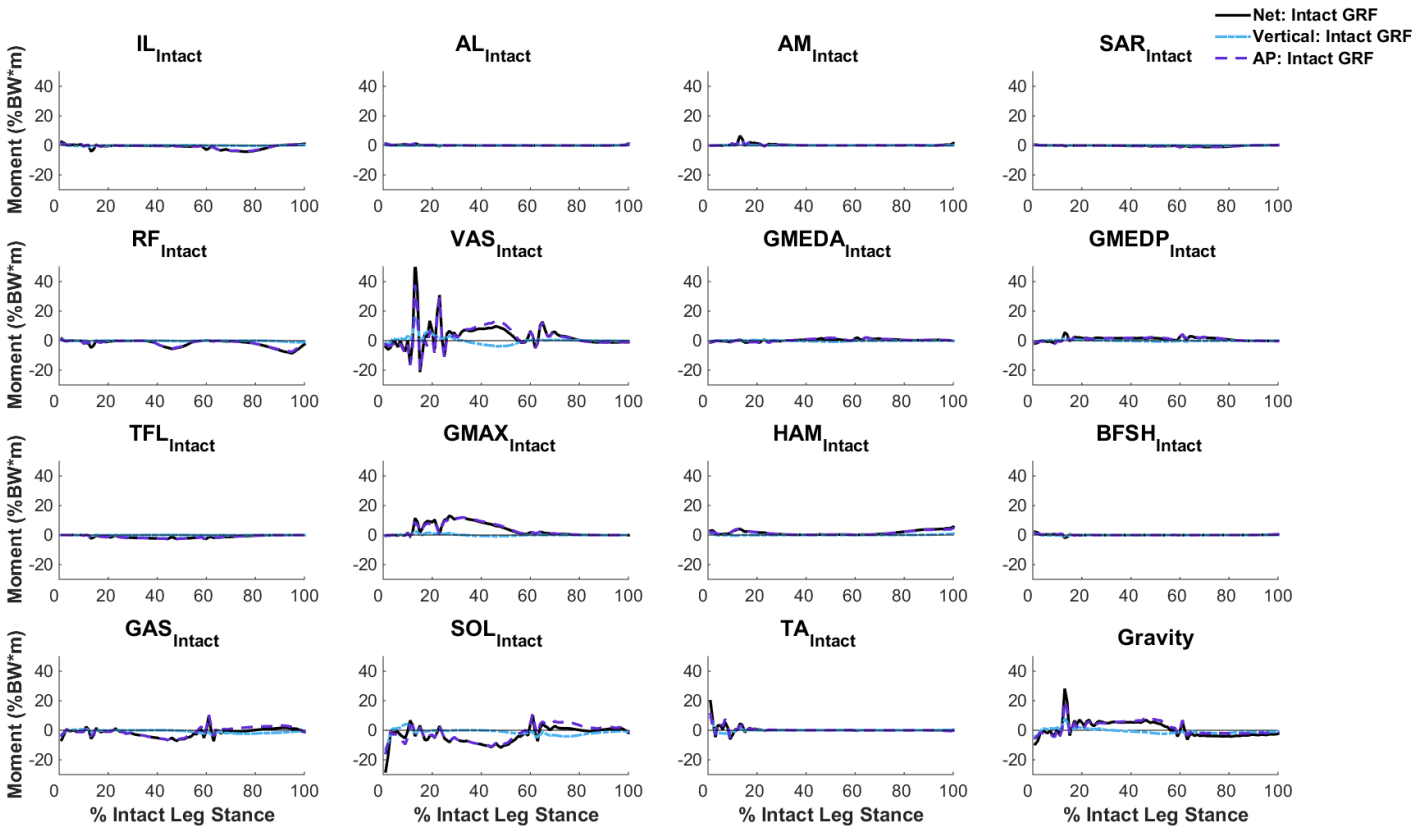

Figure C.8: External sagittal-plane moments about the center-of-mass (time rate of change of angular momentum) during intact stance (right leg of the amputee simulation) generated by the contributions of muscles from the intact leg and gravity to the intact vertical and anteroposterior (AP) ground reaction forces (GRF). Positive (negative) values indicate angular momentum that acted to rotate the body backward (forward). Contributions to the intact vertical and AP GRFs from the residual leg were small. See Table 4.1 for muscle group abbreviations.

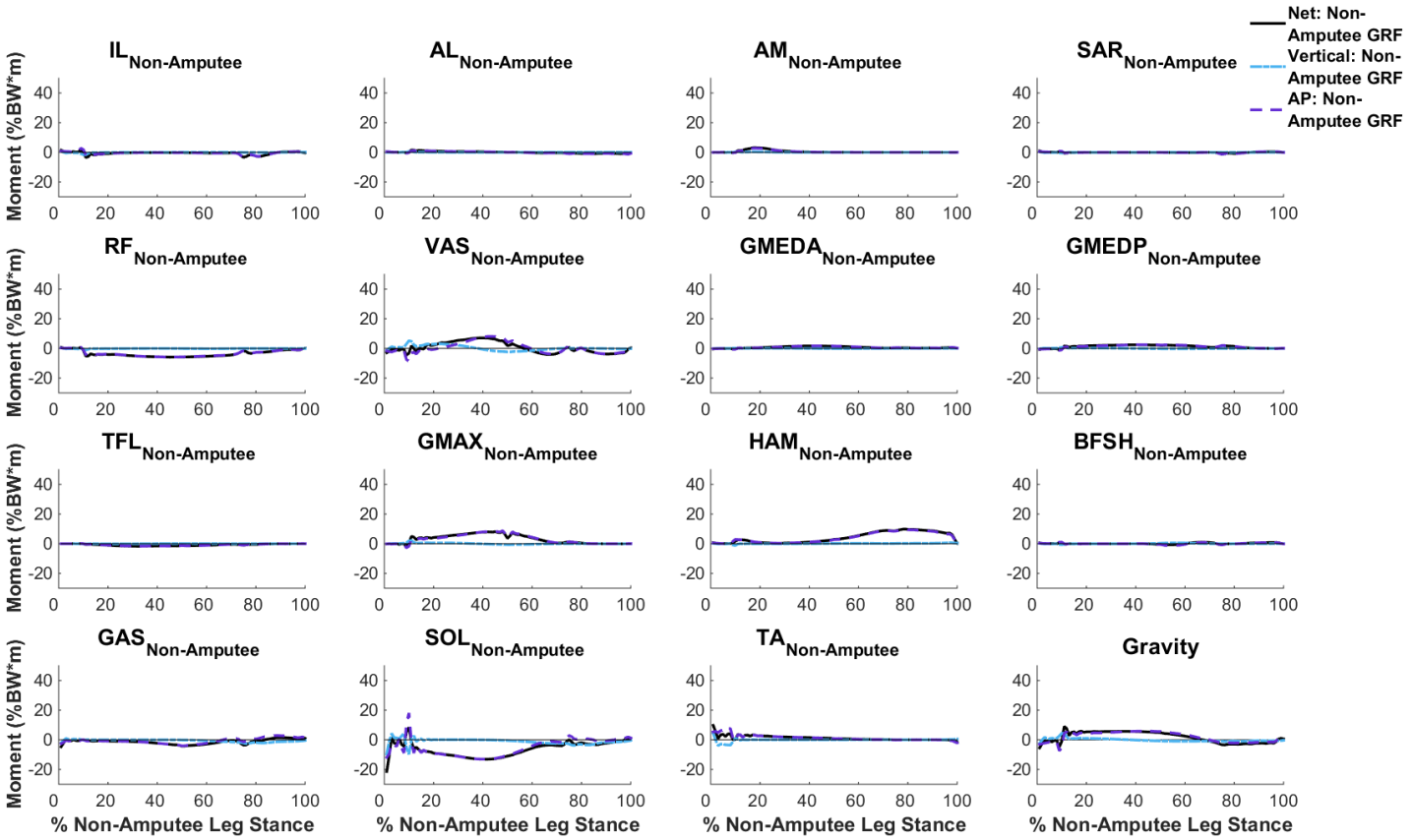

Figure C.9: External sagittal-plane moments about the center-of-mass (time rate of change of angular momentum) during non-amputee stance (right leg of the non-amputee simulation) generated by the contributions of muscles from the non-amputee leg and gravity to the non-amputee vertical and anteroposterior (AP) ground reaction forces (GRF). Positive (negative) values indicate angular momentum that acted to rotate the body backward (forward). Due to model symmetry, the contributions from both non-amputee legs were identical and only one leg is presented. See Table 4.1 for muscle group abbreviations.

References

Agrawal, V., Gailey, R., O'Toole, C., Gaunaurd, I., Finnieston, A., 2013a. Influence of gait training and prosthetic foot category on external work symmetry during unilateral transtibial amputee gait. Prosthet Orthot Int 37, 396-403.

Agrawal, V., Gailey, R.S., Gaunaurd, I.A., O'Toole, C., Finnieston, A., Tolchin, R., 2014. Comparison of four different categories of prosthetic feet during ramp ambulation in unilateral transtibial amputees. Prosthet Orthot Int.

Agrawal, V., Gailey, R.S., Gaunaurd, I.A., O'Toole, C., Finnieston, A.A., 2013b. Comparison between microprocessor-controlled ankle/foot and conventional prosthetic feet during stair negotiation in people with unilateral transtibial amputation. J Rehabil Res Dev 50, 941-950.

Ainsworth, B.E., Haskell, W.L., Whitt, M.C., Irwin, M.L., Swartz, A.M., Strath, S.J., O'Brien, W.L., Bassett, D.R., Jr., Schmitz, K.H., Emplaincourt, P.O., Jacobs, D.R., Jr., Leon, A.S., 2000. Compendium of physical activities: an update of activity codes and MET intensities. Med Sci Sports Exerc 32, S498-504.

Aldridge, J.M., Sturdy, J.T., Wilken, J.M., 2012. Stair ascent kinematics and kinetics with a powered lower leg system following transtibial amputation. Gait Posture 36, 291-295.

Alimusaj, M., Fradet, L., Braatz, F., Gerner, H.J., Wolf, S.I., 2009. Kinematics and kinetics with an adaptive ankle foot system during stair ambulation of transtibial amputees. Gait Posture 30, 356-363.

Allen, J.L., Neptune, R.R., 2012. Three-dimensional modular control of human walking. J Biomech 45, 2157-2163.

Anderson, F.C., Pandy, M.G., 2003. Individual muscle contributions to support in normal walking. Gait Posture 17, 159-169.

Andriacchi, T.P., Andersson, G.B., Fermier, R.W., Stern, D., Galante, J.O., 1980. A study of lower-limb mechanics during stair-climbing. J Bone Joint Surg Am 62, 749-757.

Bae, T.S., Choi, K., Mun, M., 2009. Level walking and stair climbing gait in above-knee amputees. J Med Eng Technol 33, 130-135.

Baker, R., 2001. Pelvic angles: a mathematically rigorous definition which is consistent with a conventional clinical understanding of the terms. Gait Posture 13, 1-6.

Barnett, C.T., Polman, R.C., Vanicek, N., 2013. Longitudinal kinematic and kinetic adaptations to obstacle crossing in recent lower limb amputees. Prosthet Orthot Int.

Bovi, G., Rabuffetti, M., Mazzoleni, P., Ferrarin, M., 2011. A multiple-task gait analysis approach: kinematic, kinetic and EMG reference data for healthy young and adult subjects. Gait Posture 33, 6-13.

Bruijn, S.M., Meyns, P., Jonkers, I., Kaat, D., Duysens, J., 2011. Control of angular momentum during walking in children with cerebral palsy. Res Dev Disabil 32, 2860-2866.

Costigan, P.A., Deluzio, K.J., Wyss, U.P., 2002. Knee and hip kinetics during normal stair climbing. Gait Posture 16, 31-37.
Curtze, C., Hof, A.L., Postema, K., Otten, B., 2012. The relative contributions of the prosthetic and sound limb to balance control in unilateral transtibial amputees. Gait Posture 36, 276-281.
D'Andrea, S., Wilhelm, N., Silverman, A.K., Grabowski, A.M., 2014. Does Use of a Powered Ankle-foot Prosthesis Restore Whole-body Angular Momentum During Walking at Different Speeds? Clin Orthop Relat Res.
Davy, D.T., Audu, M.L., 1987. A dynamic optimization technique for predicting muscle forces in the swing phase of gait. J Biomech 20, 187-201.
Delp, S.L., Loan, J.P., Hoy, M.G., Zajac, F.E., Topp, E.L., Rosen, J.M., 1990. An interactive graphics-based model of the lower extremity to study orthopaedic surgical procedures. IEEE Trans Biomed Eng 37, 757-767.
Delussu, A.S., Brunelli, S., Paradisi, F., Iosa, M., Pellegrini, R., Zenardi, D., Traballesi, M., 2013. Assessment of the effects of carbon fiber and bionic foot during overground and treadmill walking in transtibial amputees. Gait Posture 38, 876-882.
Dempster, W.T., 1955. Space requirements of the seated operator: Geometrical, kinematic, and mechanical aspects of the body with special reference to the limbs, Wright Air Development Center Technical Report. Wright-Patterson Air Force Base, Dayton, OH, pp. 55-159.
DeVita, P., Helseth, J., Hortobagyi, T., 2007. Muscles do more positive than negative work in human locomotion. J Exp Biol 210, 3361-3373.
Dillingham, T.R., Pezzin, L.E., MacKenzie, E.J., 2002. Limb amputation and limb deficiency: epidemiology and recent trends in the United States. South Med J 95, 875-883.
Erdemir, A., McLean, S., Herzog, W., van den Bogert, A.J., 2007. Model-based estimation of muscle forces exerted during movements. Clin Biomech (Bristol, Avon) 22, 131-154.
Fey, N.P., Klute, G.K., Neptune, R.R., 2012. Optimization of prosthetic foot stiffness to reduce metabolic cost and intact knee loading during below-knee amputee walking: a theoretical study. J Biomech Eng 134, 111005.
Fey, N.P., Klute, G.K., Neptune, R.R., 2013. Altering prosthetic foot stiffness influences foot and muscle function during below-knee amputee walking: a modeling and simulation analysis. J Biomech 46, 637-644.
Gailey, R., Allen, K., Castles, J., Kucharik, J., Roeder, M., 2008. Review of secondary physical conditions associated with lower-limb amputation and long-term prosthesis use. J Rehabil Res Dev 45, 15-29.
Gao, B., Cordova, M.L., Zheng, N.N., 2012. Three-dimensional joint kinematics of ACL-deficient and ACL-reconstructed knees during stair ascent and descent. Hum Mov Sci 31, 222-235.

Genin, J.J., Bastien, G.J., Franck, B., Detrembleur, C., Willems, P.A., 2008. Effect of speed on the energy cost of walking in unilateral traumatic lower limb amputees. Eur J Appl Physiol 103, 655-663.

Ghafari, A.S., Meghdari, A., Vossoughi, G.R., 2009. Muscle-driven forward dynamics simulation for the study of differences in muscle function during stair ascent and descent. Proc Inst Mech Eng H 223, 863-874.

Gilbert, S., Chen, T., Hutchinson, I.D., Choi, D., Voigt, C., Warren, R.F., Maher, S.A., 2013. Dynamic contact mechanics on the tibial plateau of the human knee during activities of daily living. J Biomech.

Goffe, W.L., Ferrier, G.D., Rogers, J., 1994. Global Optimization of Statistical Functions with Simulated Annealing. J Econometrics 60, 65-99.

Goswami, A., Kallem, V., 2004. Rate of change of angular momentum and balance maintenance of biped robots. Ieee Int Conf Robot, 3785-3790.

Grabiner, M.D., Koh, T.J., Lundin, T.M., Jahnigen, D.W., 1993. Kinematics of recovery from a stumble. J Gerontol 48, M97-102.

Grood, E.S., Suntay, W.J., 1983. A joint coordinate system for the clinical description of three-dimensional motions: application to the knee. J Biomech Eng 105, 136-144.

Hall, M., Boyer, E.R., Gillette, J.C., Mirka, G.A., 2013. Medial knee joint loading during stair ambulation and walking while carrying loads. Gait Posture 37, 460-462.

Hamner, S.R., Seth, A., Delp, S.L., 2010. Muscle contributions to propulsion and support during running. J Biomech 43, 2709-2716.

Heidenreich, P.A., Trogdon, J.G., Khavjou, O.A., Butler, J., Dracup, K., Ezekowitz, M.D., Finkelstein, E.A., Hong, Y., Johnston, S.C., Khera, A., Lloyd-Jones, D.M., Nelson, S.A., Nichol, G., Orenstein, D., Wilson, P.W., Woo, Y.J., 2011. Forecasting the future of cardiovascular disease in the United States: a policy statement from the American Heart Association. Circulation 123, 933-944.

Herr, H., Popovic, M., 2008. Angular momentum in human walking. J Exp Biol 211, 467-481.

Herr, H.M., Grabowski, A.M., 2012. Bionic ankle-foot prosthesis normalizes walking gait for persons with leg amputation. Proc Biol Sci 279, 457-464.

Hill, S.W., Patla, A.E., Ishac, M.G., Adkin, A.L., Supan, T.J., Barth, D.G., 1999. Altered kinetic strategy for the control of swing limb elevation over obstacles in unilateral below-knee amputee gait. J Biomech 32, 545-549.

Hofmann, A., Popovic, M., Herr, H., 2009. Exploiting Angular Momentum to Enhance Bipedal Center-of-Mass Control. Icra: 2009 Ieee International Conference on Robotics and Automation, Vols 1-7, 2483-2489.

Houdijk, H., Pollmann, E., Groenewold, M., Wiggerts, H., Polomski, W., 2009. The energy cost for the step-to-step transition in amputee walking. Gait Posture 30, 35-40.

Hsue, B.J., Su, F.C., 2009. Gait and kinematics of the trunk and lower extremities in stair ascent using quadricane in healthy subjects. Gait Posture 29, 146-150.

Hsue, B.J., Su, F.C., 2010. The effect of cane use method on center of mass displacement during stair ascent. Gait Posture 32, 530-535.

Jansen, K., De Groote, F., Duysens, J., Jonkers, I., 2014. How gravity and muscle action control mediolateral center of mass excursion during slow walking: a simulation study. Gait Posture 39, 91-97.

Joseph, J., Watson, R., 1967. Telemetering electromyography of muscles used in walking up and down stairs. J Bone Joint Surg Br 49, 774-780.

Kajita, S., Kanehiro, F., Kaneko, K., Fujiwara, K., Harada, K., Yokoi, K., Hirukawa, H., 2003. Resolved momentum control: Humanoid motion planning based on the linear and angular momentum. Iros 2003: Proceedings of the 2003 Ieee/Rsj International Conference on Intelligent Robots and Systems, Vols 1-4, 1644-1650.

Kaufman, K.R., Wyatt, M.P., Sessoms, P.H., Grabiner, M.D., 2014. Task-specific Fall Prevention Training Is Effective for Warfighters With Transtibial Amputations. Clin Orthop Relat Res.

Kendell, C., Lemaire, E.D., Dudek, N.L., Kofman, J., 2010. Indicators of dynamic stability in transtibial prosthesis users. Gait Posture 31, 375-379.

Lee, H.J., Chou, L.S., 2007. Balance control during stair negotiation in older adults. J Biomech 40, 2530-2536.

Lin, H., Lu, T., Hsu, H., 2005. Comparisons of joint kinetics in the lower extremity between stair ascent and descent. J Mech 21, 41-50.

Lin, Y.C., Fok, L.A., Schache, A.G., Pandy, M.G., 2015. Muscle coordination of support, progression and balance during stair ambulation. J Biomech 48, 340-347.

Lin, Y.C., Kim, H.J., Pandy, M.G., 2011. A computationally efficient method for assessing muscle function during human locomotion. Int J Numer Meth Bio 27, 436-449.

Liu, M.Q., Anderson, F.C., Pandy, M.G., Delp, S.L., 2006. Muscles that support the body also modulate forward progression during walking. J Biomech 39, 2623-2630.

Lyons, K., Perry, J., Gronley, J.K., Barnes, L., Antonelli, D., 1983. Timing and relative intensity of hip extensor and abductor muscle action during level and stair ambulation. An EMG study. Phys Ther 63, 1597-1605.

MacKinnon, C.D., Winter, D.A., 1993. Control of whole body balance in the frontal plane during human walking. J Biomech 26, 633-644.

Mancinelli, C., Patritti, B.L., Tropea, P., Greenwald, R.M., Casler, R., Herr, H., Bonato, P., 2011. Comparing a passive-elastic and a powered prosthesis in transtibial amputees. Conf Proc IEEE Eng Med Biol Soc 2011, 8255-8258.

Mandeville, D., Osternig, L.R., Chou, L.S., 2007. The effect of total knee replacement on dynamic support of the body during walking and stair ascent. Clin Biomech (Bristol, Avon) 22, 787-794.

McFadyen, B.J., Winter, D.A., 1988. An integrated biomechanical analysis of normal stair ascent and descent. J Biomech 21, 733-744.

Miller, W.C., Speechley, M., Deathe, B., 2001. The prevalence and risk factors of falling and fear of falling among lower extremity amputees. Arch Phys Med Rehab 82, 1031-1037.

Moffet, H., Richards, C., Malouin, F., Bravo, G., 1993. Load-carrying during stair ascent: a demanding functional test. Gait & Posture 1, 35-44.

Mundermann, A., Dyrby, C.O., D'Lima, D.D., Colwell, C.W., Jr., Andriacchi, T.P., 2008. In vivo knee loading characteristics during activities of daily living as measured by an instrumented total knee replacement. J Orthop Res 26, 1167-1172.

Nadeau, S., McFadyen, B.J., Malouin, F., 2003. Frontal and sagittal plane analyses of the stair climbing task in healthy adults aged over 40 years: what are the challenges compared to level walking? Clin Biomech (Bristol, Avon) 18, 950-959.

Neptune, R.R., Kautz, S.A., Zajac, F.E., 2000a. Muscle contributions to specific biomechanical functions do not change in forward versus backward pedaling. J Biomech 33, 155-164.

Neptune, R.R., Kautz, S.A., Zajac, F.E., 2001. Contributions of the individual ankle plantar flexors to support, forward progression and swing initiation during walking. J Biomech 34, 1387-1398.

Neptune, R.R., McGowan, C.P., 2011. Muscle contributions to whole-body sagittal plane angular momentum during walking. J Biomech 44, 6-12.

Neptune, R.R., McGowan, C.P., Hall, A.L., 2011. Muscle contributions to frontal and transverse plane whole-body angular momentum during walking. Proceedings of the International Society of Biomechanics Conference, vol. 129.

Neptune, R.R., McGowan, C.P., Hall, A.L., 2012. The role of ankle plantarflexors in maintaining dynamic balance during human walking, ASME 2012 Summer Bioengineering Conference, Fajardo, Puerto Rico.

Neptune, R.R., Sasaki, K., Kautz, S.A., 2008. The effect of walking speed on muscle function and mechanical energetics. Gait Posture 28, 135-143.

Neptune, R.R., Wright, I.C., Van Den Bogert, A.J., 2000b. A Method for Numerical Simulation of Single Limb Ground Contact Events: Application to Heel-Toe Running. Comput Methods Biomech Biomed Engin 3, 321-334.

Neptune, R.R., Zajac, F.E., Kautz, S.A., 2004. Muscle force redistributes segmental power for body progression during walking. Gait Posture 19, 194-205.

Nolan, L., 2012. A training programme to improve hip strength in persons with lower limb amputation. J Rehabil Med 44, 241-248.

Nott, C.R., Neptune, R.R., Kautz, S.A., 2014. Relationships between frontal-plane angular momentum and clinical balance measures during post-stroke hemiparetic walking. Gait Posture 39, 129-134.

Novak, A.C., Brouwer, B., 2011. Sagittal and frontal lower limb joint moments during stair ascent and descent in young and older adults. Gait Posture 33, 54-60.

Ozyurek, S., Demirbuken, I., Angin, S., 2013. Altered movement strategies in sit-to-stand task in persons with transtibial amputation. Prosthet Orthot Int 38, 303-309.

Pandy, M.G., Lin, Y.C., Kim, H.J., 2010. Muscle coordination of mediolateral balance in normal walking. J Biomech 43, 2055-2064.

Peterson, C.L., Hall, A.L., Kautz, S.A., Neptune, R.R., 2010. Pre-swing deficits in forward propulsion, swing initiation and power generation by individual muscles during hemiparetic walking. J Biomech 43, 2348-2355.

Pickle, N.T., Wilken, J.M., Aldridge, J.M., Neptune, R.R., Silverman, A.K., 2014. Whole-Body Angular Momentum During Stair Walking Using Passive And Powered Lower-Limb Prostheses. Journal of Biomechanics.

Pijnappels, M., Bobbert, M.F., van Dieen, J.H., 2004. Contribution of the support limb in control of angular momentum after tripping. J Biomech 37, 1811-1818.

Pijnappels, M., Bobbert, M.F., van Dieen, J.H., 2005. How early reactions in the support limb contribute to balance recovery after tripping. J Biomech 38, 627-634.

Pijnappels, M., Bobbert, M.F., van Dieen, J.H., 2005a. How early reactions in the support limb contribute to balance recovery after tripping. J Biomech 38, 627-634.

Pijnappels, M., Bobbert, M.F., van Dieen, J.H., 2005b. Push-off reactions in recovery after tripping discriminate young subjects, older non-fallers and older fallers. Gait Posture 21, 388-394.

Pijnappels, M., van der Burg, P.J., Reeves, N.D., van Dieen, J.H., 2008. Identification of elderly fallers by muscle strength measures. Eur J Appl Physiol 102, 585-592.

Powers, C.M., Boyd, L.A., Torburn, L., Perry, J., 1997. Stair ambulation in persons with transtibial amputation: an analysis of the Seattle LightFoot. J Rehabil Res Dev 34, 9-18.

Prinsen, E.C., Nederhand, M.J., Rietman, J.S., 2011. Adaptation strategies of the lower extremities of patients with a transtibial or transfemoral amputation during level walking: a systematic review. Arch Phys Med Rehabil 92, 1311-1325.

Protopapadaki, A., Drechsler, W.I., Cramp, M.C., Coutts, F.J., Scott, O.M., 2007. Hip, knee, ankle kinematics and kinetics during stair ascent and descent in healthy young individuals. Clin Biomech (Bristol, Avon) 22, 203-210.

Raasch, C.C., Zajac, F.E., Ma, B., Levine, W.S., 1997. Muscle coordination of maximum-speed pedaling. J Biomech 30, 595-602.

Ramstrand, N., Nilsson, K.A., 2009. A comparison of foot placement strategies of transtibial amputees and able-bodied subjects during stair ambulation. Prosthet Orthot Int 33, 348-355.

Rankin, J.W., Richter, W.M., Neptune, R.R., 2011. Individual muscle contributions to push and recovery subtasks during wheelchair propulsion. J Biomech 44, 1246-1252.

Reeves, N.D., Spanjaard, M., Mohagheghi, A.A., Baltzopoulos, V., Maganaris, C.N., 2008. Influence of light handrail use on the biomechanics of stair negotiation in old age. Gait Posture 28, 327-336.

Reeves, N.D., Spanjaard, M., Mohagheghi, A.A., Baltzopoulos, V., Maganaris, C.N., 2009. Older adults employ alternative strategies to operate within their maximum capabilities when ascending stairs. J Electromyogr Kinesiol 19, e57-68.

Reid, S.M., Novak, A.C., Brouwer, B., Costigan, P.A., 2011. Relationship between stair ambulation with and without a handrail and centre of pressure velocities during stair ascent and descent. Gait Posture 34, 529-532.

Sanderson, D.J., Martin, P.E., 1996. Joint kinetics in unilateral below-knee amputee patients during running. Arch Phys Med Rehabil 77, 1279-1285.

Sasaki, K., Neptune, R.R., 2006. Differences in muscle function during walking and running at the same speed. J Biomech 39, 2005-2013.

Schmalz, T., Blumentritt, S., Marx, B., 2007. Biomechanical analysis of stair ambulation in lower limb amputees. Gait Posture 25, 267-278.

Segal, A.D., Zelik, K.E., Klute, G.K., Morgenroth, D.C., Hahn, M.E., Orendurff, M.S., Adamczyk, P.G., Collins, S.H., Kuo, A.D., Czerniecki, J.M., 2012. The effects of a controlled energy storage and return prototype prosthetic foot on transtibial amputee ambulation. Hum Mov Sci 31, 918-931.

Silverman, A.K., Fey, N.P., Portillo, A., Walden, J.G., Bosker, G., Neptune, R.R., 2008. Compensatory mechanisms in below-knee amputee gait in response to increasing steady-state walking speeds. Gait Posture 28, 602-609.

Silverman, A.K., Neptune, R.R., 2011. Differences in whole-body angular momentum between below-knee amputees and non-amputees across walking speeds. J Biomech 44, 379-385.

Silverman, A.K., Neptune, R.R., 2012. Muscle and prosthesis contributions to amputee walking mechanics: a modeling study. J Biomech 45, 2271-2278.

Silverman, A.K., Neptune, R.R., Sinitski, E.H., Wilken, J.M., 2014. Whole-body angular momentum during stair ascent and descent. Gait & Posture.

Simoneau, G.G., Krebs, D.E., 2000. Whole-body momentum during gait: A preliminary study of non-fallers and frequent fallers. Journal of Applied Biomechanics 16, 1-13.

Sinitski, E.H., Hansen, A.H., Wilken, J.M., 2012. Biomechanics of the ankle-foot system during stair ambulation: implications for design of advanced ankle-foot prostheses. J Biomech 45, 588-594.

Startzell, J.K., Owens, D.A., Mulfinger, L.M., Cavanagh, P.R., 2000. Stair negotiation in older people: a review. J Am Geriatr Soc 48, 567-580.

Teh, K.C., Aziz, A.R., 2002. Heart rate, oxygen uptake, and energy cost of ascending and descending the stairs. Med Sci Sports Exerc 34, 695-699.

Torburn, L., Schweiger, G.P., Perry, J., Powers, C.M., 1994. Below-knee amputee gait in stair ambulation. A comparison of stride characteristics using five different prosthetic feet. Clin Orthop Relat Res, 185-192.

van Dieen, J.H., Spanjaard, M., Konemann, R., Bron, L., Pijnappels, M., 2007. Balance control in stepping down expected and unexpected level changes. J Biomech 40, 3641-3649.

Vanicek, N., Strike, S.C., McNaughton, L., Polman, R., 2010. Lower limb kinematic and kinetic differences between transtibial amputee fallers and non-fallers. Prosthet Orthot Int 34, 399-410.

Vrieling, A.H., van Keeken, H.G., Schoppen, T., Hof, A.L., Otten, B., Halbertsma, J.P., Postema, K., 2009. Gait adjustments in obstacle crossing, gait initiation and gait termination after a recent lower limb amputation. Clin Rehabil 23, 659-671.

Vrieling, A.H., van Keeken, H.G., Schoppen, T., Otten, E., Halbertsma, J.P., Hof, A.L., Postema, K., 2007. Obstacle crossing in lower limb amputees. Gait Posture 26, 587-594.

Vrieling, A.H., van Keeken, H.G., Schoppen, T., Otten, E., Halbertsma, J.P., Hof, A.L., Postema, K., 2008a. Uphill and downhill walking in unilateral lower limb amputees. Gait Posture 28, 235-242.

Vrieling, A.H., van Keeken, H.G., Schoppen, T., Otten, E., Hof, A.L., Halbertsma, J.P., Postema, K., 2008b. Balance control on a moving platform in unilateral lower limb amputees. Gait Posture 28, 222-228.

Wild, S., Roglic, G., Green, A., Sicree, R., King, H., 2004. Global prevalence of diabetes: estimates for the year 2000 and projections for 2030. Diabetes Care 27, 1047-1053.

Wilken, J.M., Rodriguez, K.M., Brawner, M., Darter, B.J., 2012. Reliability and minimal detectible change values for gait kinematics and kinetics in healthy adults. Gait Posture 35, 301-307.

Wilken, J.M., Sinitski, E.H., Bagg, E.A., 2011. The role of lower extremity joint powers in successful stair ambulation. Gait Posture 34, 142-144.

Winters, J.M., Stark, L., 1988. Estimated mechanical properties of synergistic muscles involved in movements of a variety of human joints. J Biomech 21, 1027-1041.

Wu, G., Cavanagh, P.R., 1995. ISB recommendations for standardization in the reporting of kinematic data. J Biomech 28, 1257-1261.

Wu, G., Siegler, S., Allard, P., Kirtley, C., Leardini, A., Rosenbaum, D., Whittle, M., D'Lima, D.D., Cristofolini, L., Witte, H., Schmid, O., Stokes, I., 2002. ISB recommendation on definitions of joint coordinate system of various joints for the reporting of human joint motion—part I: ankle, hip, and spine. J Biomech 35, 543-548.

Yack, J.H., Nielsen, D.H., Shurr, D.G., 1999. Kinetic patterns during stair ascent in patients with transtibial amputations using three different prostheses. Journal of Prosthetics and Orthotics 11, 57-62.

Zachazewski, J.E., Riley, P.O., Krebs, D.E., 1993. Biomechanical analysis of body mass transfer during stair ascent and descent of healthy subjects. J Rehabil Res Dev 30, 412-422.

Zajac, F.E., 1989. Muscle and tendon: properties, models, scaling, and application to biomechanics and motor control. Crit Rev Biomed Eng 17, 359-411.

Zajac, F.E., Gordon, M.E., 1989. Determining muscle's force and action in multi-articular movement. Exerc Sport Sci Rev 17, 187-230.

Zajac, F.E., Neptune, R.R., Kautz, S.A., 2002. Biomechanics and muscle coordination of human walking. Part I: introduction to concepts, power transfer, dynamics and simulations. Gait Posture 16, 215-232.

Ziegler-Graham, K., MacKenzie, E.J., Ephraim, P.L., Travison, T.G., Brookmeyer, R., 2008. Estimating the prevalence of limb loss in the United States: 2005 to 2050. Arch Phys Med Rehabil 89, 422-429.

Zmitrewicz, R.J., Neptune, R.R., Sasaki, K., 2007. Mechanical energetic contributions from individual muscles and elastic prosthetic feet during symmetric unilateral transtibial amputee walking: a theoretical study. J Biomech 40, 1824-1831.

Vita

Nicole Guckert Harper attended The University of Texas at Austin where she received her Bachelor of Science in Biomedical Engineering in May, 2010. She subsequently entered the Graduate School at The University of Texas at Austin where she received her Master of Science in Engineering in 2012. The focus of her graduate research has been on the biomechanics of stair ascent with an emphasis on identifying the function roles and coordination of individual muscles during amputee and non-amputee stair ascent. The overall goal of this research is to facilitate the development of refined prosthesis and targeted rehabilitation programs to improve an individual's ability to ascend stairs.

Permanent email address: nicole.harper@utexas.edu

This dissertation was typed by the author.